THE JOURNAL OF APPLIED CHEMISTRY OF THE USSR

Vol. 24 1951

MAY

IN ENGLISH TRANSLATION

CONSULTANTS BUREAU
152 WEST 42ND ST. NEW YORK 18, N. Y.

—An agency for the interpretation of international knowledge—

TABLE OF CONTENTS

		page	Russ. page
1.	The Kinetics of the Reaction between SO_2 and Ferric Sulfate in Aqueous Solution. I. N. Kuzminykh and T. B. Bomshtein	497	453
2.	The Oxidation of Magnesium and of its Alloys at High Temperatures. I. A. Makolkin	505	460
3.	Electrolytic Brassplating in an Oxalic Acid Bath. A. I. Stabrovsky	515	471
4.	The Effect of Strain upon Metal Corrosion. E. M. Zaretsky	521	477
5.	The Copolymerization of Vinyl Acetate with Maleic Anhydride and the Properties of the Resultant Copolymers. S. N. Ushakov, S. P. Mitsengendler and V.A. Chekhovskaya	529	485
6.	The Aging of Triacetate Films. A. A. Freiman	535	490
7.	The Transformations of Acrylonitrile and α-Methylstyrene with Hydrogen Peroxide. M. F. Shostakovsky and A. V. Bogdanova	541	495
8.	The Composition of Fatty Acids Derived from Oxidized Paraffin. A. E. Drabkin and Z. V. Soloveichik	549	502
9.	The Behavior Patterns of the Changes in the Operation of Charcoal Beds under Various Conditions of Dynamic Sorption of some Essential Oils from Aqueous Solutions. L. M. Voitko and A. N. Kharin	557	509
10.	The Reduction of Carbon Dioxide with Coke made from Mined Coal. V. N. Ershov and V. V. Pomerantsev	569	520
11.	The Transition of a Catalyst into a Heterogeneous State and the Underlying Causes of this Phenomenon. V. K. Tsyskovsky and N. A. Kiseleva	577	527
12.	The Synthesis and Investigation of Nopene. B. N. Rutkovsky and L. A. Alferova	583	532

Brief Communications

13.	The Kinetics of Absorption during Intensive Stirring. M. Kh. Kishinevsky	595	542
14.	The Passivity of Stainless Steel. G. P. Maitak and N. N. Gratsiansky	597	545
15.	A Laboratory Apparatus for the Production of Ketene on a Large Scale. D. D. Smolin, F. P. Kravtsov and A. P. Skoldinov	601	547
16.	The Composition of Resinous Deposits in the Manufacture of Cellulose. S. S. Malevskaya and E. I. Evropyeva	607	551
17.	The Production of a Corklike Material from Polyvinyl Chloride Plastics. M. V. Alekseyev	611	554
18.	The Synthesis of Asymmetrical Azo Compounds. B. M. Bogoslovsky and Z. S. Kazakova	613	556
19.	A Highly Dispersed Preparation of Sulfathiazole Silver. K. A. Libman	617	558

THE JOURNAL OF APPLIED CHEMISTRY OF THE U. S. S. R.

VOLUME XXIV, No. 5

May 1951

Publication of the Academy of Sciences of the U. S. S. R.

IN ENGLISH TRANSLATION

Copyright 1951

CONSULTANTS BUREAU
152. West 42 Street
New York 18, N. Y.

Printed in France

Annual Subscription $80.00
Single issue $12.00

THE KINETICS OF THE REACTION BETWEEN SO_2 AND FERRIC SULFATE IN AQUEOUS SOLUTION

I. N. Kuzminykh and T. B. Bomshtein

The reaction of SO_2 with $Fe_2(SO_4)_3$ in aqueous solution may be of practical importance. The literature [1] describes the use of this reaction on an industrial scale for the reduction of iron ($Fe^{\cdot\cdot\cdot} \rightarrow Fe^{\cdot\cdot}$) in the hydrometallurgy of copper, the $CuSO_4$ being treated with sulfur dioxide in towers before its electrolysis. In accordance with the stoichiometric reaction:

$$Fe_2(SO_4)_3 + SO_2 + H_2O = 2FeSO_4 + 2H_2SO_4, \qquad (1)$$

this yields weak sulfuric acid as a by-product, which is immediately used for the wet leaching of more copper out of the oxidized ores. We also have a description of an instance [2] in which the $CuSO_4$ solution is treated with sulfur dioxide produced for this purpose by roasting pyrites in large tanks before the copper is recovered from it by the action of metallic iron.

We have not found any information in the literature on the kinetics of the reaction of SO_2 with $Fe_2(SO_4)_3$; all we have is the terse statement [3], based upon practical experience, that the velocity of this reaction depends upon the acidity of the solution and the temperature.

We concluded that this problem deserved study. We have carried out several laboratory experiments in which we observed the reaction between SO_2 and $Fe_2(SO_4)_3$ in aqueous solution. These experiments had as their purpose the determination of the velocity of this reaction with such factors as the concentration of SO_2, $Fe_2(SO_4)_3$, and H_2SO_4 in the solution. Most of the experiments were run at 50°, some of them being run at 25 and 75°. The experiments involved mixing fixed amounts of an aqueous solution of SO_2 with an acidulated solution of $Fe_2(SO_4)_3$ and then determining the progress of the reaction by analyzing the solution at definite intervals of time.

The experimental apparatus is shown in Fig. 1.

The reaction was carried out in a 0.5-liter flask. A definite amount of ferric sulfate solution of known concentration was placed in the flask before each run. On the outside, Flask 1 was surrounded by a coil of wire for electric heating and a layer of

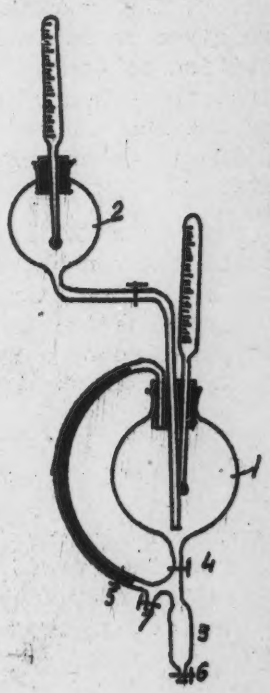

Fig. 1. Layout of experimental apparatus.

1-Reaction flask; 2-flask containing SO_2 solution; 3-calibrated pipet; 4,5,6,7-stopcocks.

insulation, which enabled us to maintain the desired temperature during the run. Through holes in the stopper of Flask 1 there passed a thermometer and a tube for supplying the SO_2 solution from flask 2, where it was preheated to the same temperature. Another hole in the stopper served for an outlet tube to allow the air displaced by this solution to escape from Flask 1 and to let air in when samples of the solution were taken from the flask. Flask 1 was fitted with a 10-ml calibrated pipet 3, used in taking these samples.

At the instant the solutions were mixed, Flask 1 was shaken vigorously and a stop watch was started. The stopcocks 4 and 5 were opened to take samples from Flask 1; the solution entering the pipet 3 was then allowed to flow out (by opening stopcocks 6 and 7) into the container for determining the quantity of unreacted SO_2. This was done by passing CO_2 from a gas tank through the solution to be analyzed. The SO_2 blown off was trapped in three absorbing bottles filled with iodine solution. After the SO_2 had been driven out of the solution, the latter was analyzed for its $Fe^{\cdot\cdot}$, $Fe^{\cdot\cdot\cdot}$, and free H_2SO_4.

The loss of SO_2 and $Fe^{\cdot\cdot\cdot}$ in the solution during the run served as a criterion of the rate of the process under study. The runs lasted 3-4 hours, and as long as 5.5 hours in some instances. A sample of the solution in Flask 1 was taken every half-hour for analysis. The initial concentration of SO_2 in the solution varied from 0.03 to 0.35 mole per liter in different tests, the $Fe_2(SO_4)_3$ concentration ranging from 0.02 to 0.4 mole per liter (the total iron content in the solution being 8-44 grams per liter, including $Fe^{\cdot\cdot}$). The solution contained 2 to 50 grams of sulfuric acid per liter; in working up our experimental results, we allowed for the acid formed during the reaction.

We began with practice runs, which demonstrated the satisfactory reproducibility of the experimental data. We also ran tests in which the iron was in solution only as $FeSO_4$; in these tests the SO_2 underwent no change, all of it being blown out of the solution by the carbon dioxide.

The results of our experiments on the velocity of the reaction at 50° are given in Table 1. The table lists the duration of the run, the initial composition of the solution, the decrease in the SO_2 in the solution during the first three hours and during the entire run, and the decrease in the $Fe^{\cdot\cdot\cdot}$ during the run and per hour (in some runs). The table also shows the consumption of SO_2 in moles per mole of reacted $Fe_2(SO_4)_3$, calculated from the tabulated data.

Calculations showed that our test results did not fit the stoichiometric equation given above: we found that for 1 mole of $Fe_2(SO_4)_3$ entering into reaction much more than 1 mole of SO_2 (1.2-1.7 moles) was consumed in the solution. This was due to the fact that the reaction cited above, which yielded a sulfate, was paralled by a reaction that yielded a dithionate, in which three moles of SO_2 were used per mole of $Fe_2(SO_4)_3$:

$$Fe_2(SO_4)_3 + 3SO_2 + 2H_2O = 2FeS_2O_6 + 2H_2SO_4. \qquad (2)$$

The literature contains several references [4] to the fact that the reaction between SO_2 and $Fe_2(SO_4)_3$ gives rise to a mixture of ferrous sulfate and ferrous dithionate, reducing the temperature and lowering the solution acidity favoring the formation of the dithionate. The reaction proceeds in several stages; it is believed that first $Fe_2(SO_3)_3$ is formed, turning the solution red, it then being converted into the dithionate:

$$Fe_2(SO_4)_3 + 3SO_2 + 3H_2O = Fe_2(SO_3)_3 + 3H_2SO_4;$$

$$Fe_2(SO_3)_3 = FeS_2O_6 + FeSO_3;$$

$$FeSO_3 + H_2SO_4 = FeS_2O_6 + H_2O.$$

The proportion of SO_2 (x) and of $Fe^{\cdot\cdot\cdot}$ (y) converted into the dithionate

can be computed from the equation:

$$x = 1.5(1 - 1/n) \quad \text{and} \quad y = 0.5(n - 1),$$

where n is the consumption of SO_2 in moles per mole of reacted ferric sulfate. Whence:

n	1	1.1	1.2	1.3	1.4	1.5	1.6	1.7	1.8
x·100%	0.0	13.6	25.0	34.6	42.7	50.0	56.1	61.8	66.7
y·100%	0.0	5.0	10	15	20	25	30	35	40

Hence, 25-60% of the SO_2 and 10-25% of the $Fe^{\cdots}$, in terms of the reacted quantities of these substances, were converted into the dithionate in our tests. When we compare these tests, we see that the difference in the yield of the dithionate is a function of the SO_2:$Fe^{\cdots}$ ratio in the solution. We see from Fig. 2, where this function is plotted graphically, that increasing the amount of SO_2 in the initial solution over that of the $Fe_2(SO_4)_3$ results in an increase in the yield of the dithionate.

The experiments in which we analyzed the solution for iron as well as for SO_2 in the course of the reaction showed that the consumption of SO_2 per mole of reacted $Fe_2(SO_4)_3$ differed in different tests, though it remained the same throughout the run in each individual test. Another characteristic fact is that the tests that featured a different SO_2:$Fe^{\cdots}$ ratio and displayed a different dithionate yield proved to be identical kinetically: the reaction rate based on unit concentrations of the reagents was always the same, no matter how the proportion of dithionate formed differed in these tests.

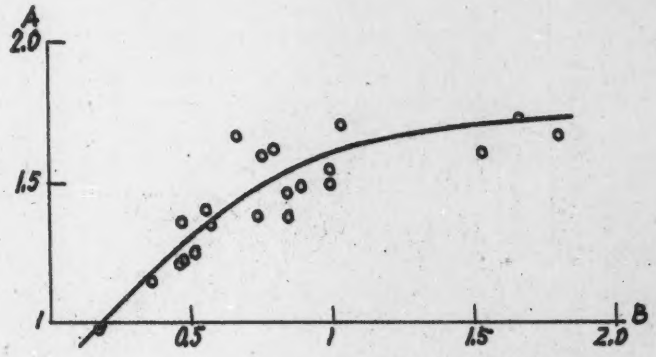

Fig. 2. Dithionate yield as a function of the SO_2:$Fe^{\cdots}$ ratio in the solution.

A-Consumption of SO_2, moles, per mole of $Fe_2(SO_4)_3$; B-molar SO_2:$Fe_2(SO_4)_3$ ratio in the original solution.

To explain these facts we have to admit that the two reactions cited above, one of which results in the formation of ferrous sulfate, and the other in the formation of the dithionate, are not parallel and independent of each other, but occur in the solution one after the other, Equations (1) and (2) merely expressing the stoichiometry of these reactions and not the actual course of the process. It must be assumed that the reaction between SO_2 and $Fe_2(SO_4)_3$ in aqueous solutions does not consist of the two cited complex reactions, but of a series of simpler successive reactions, the slowest one (which one we do not know) governing the overall process velocity. No dithionate is formed when SO_2 reacts in solution with ferrous sulfate: therefore, the process cannot consist of an initial formation of the sulfate, followed by its conversion into the dithionate. On the other hand, we know [4] that dithionates in an acid medium can be decomposed into a sulfate and SO_2 by heating. The conclusion is inescapable that the reaction between SO_2 and $Fe_2(SO_4)_3$ in aqueous solution consists, at first, of a series of intermediate reactions, resulting in the formation of the dithionate, which then breaks down into the sulfate, giving off SO_2.

We endeavored to calculate the reaction kinetics of Equations (1) and (2);

Table 1

The Velocity of the Reaction between SO_2 and $Fe_2(SO_4)_3$ in Aqueous Solution as a Function of the Concentration of SO_2, $Fe_2(SO_4)_3$, and H_2SO_4. Temperature of the Experiment: +50°C.

Test No.	Length of test, hours	Initial composition of solution				Per Cent of substances reacted								Consumption of SO_2, moles/mole of $Fe_2(SO_4)_3$
						After 1 hour		After 2 hours		After 3 hours		By the end of the run		
		Fe (g/l)	$Fe_2(SO_4)_3$ (mole/l)	SO_2 (mole/l)	H_2SO_4 (g/l)	SO_2	Fe^{+++}	SO_2	Fe^{+++}	SO_2	Fe^{+++}	SO_2	Fe^{+++}	
1	4	37.3	0.1615	0.1358	2	76	-	84	-	89	-	91.8	53	1.44
2	5	41.7	0.1792	0.1358	5	73.7	28.5	83.2	35.8	87.3	-	90.3	43.3	1.58
3	5.5	41.4	0.1818	0.120	20	49.1	-	60.7	-	69	-	78.3	35.6	1.45
4	5	39.4	0.1737	0.120	50	21.6	-	33.85	-	45.35	-	51.0	29.3	1.2
5	5	37.8	0.1911	0.1733	25	58.35	-	72.0	-	76.25	-	81.35	51.3	1.44
6	2.5	38.4	0.1982	0.1733	33	29.5	-	41.4	-	-	-	44.7	44.9	0.9
7	3	38.4	0.1982	0.1748	33	34.0	-	42.75	-	50.75	-	50.75	-	-
8	5.5	8.4	0.0233	0.0973	5	16.8	-	19.7	97.9	-	-	34.2	97.9	1.36
9	5	18.0	0.0701	0.117	5	40	-	53.7	-	56.9	-	64.0	62.9	1.7
10	5.5	52.2	0.220	0.1209	5	62.1	-	75.7	-	81.45	-	86.3	34	1.39
11	5.5	61.5	0.2755	0.1209	5	52.7	-	59.6	-	97.9	21.3	97.9	21.9	2
12	5.5	41.7	0.0768	0.1172	5	42.85	-	56.1	53.6	57.3	-	68.9	66.75	1.575
13	5.5	52.3	0.2484	0.1172	5	63.7	-	82.3	-	85.5	30.1	91.6	32.1	1.35
14	5	42.9	0.3366	0.1569	5	87.2	33.4	91.6	34.3	94.0	36.6	95.5	36.6	1.22
15	4	42.9	0.338	0.1569	5	-	-	-	-	95.4	-	95.65	36.8	1.207
16	4	39.2	0.351	0.1172	5	93.0	-	96.9	26.5	98.6	-	98.6	27.3	1.208
17	3	30.6	0.2746	0.0977	5	83.6	26.6	92.5	28.5	95.8	-	95.8	-	1.15
18	3	40.0	0.1943	0.0374	5	90.0	-	93	-	96	18.8	96.0	18.8	0.976
19	4.5	40.25	0.201	0.1472	5	79.75	-	86.9	-	91.7	-	93.2	50.3	1.36
20	2.5	40.7	0.2021	0.2014	5	78	-	82.9	-	-	-	83.8	56.6	1.47
21	4.5	40.3	0.193	0.2014	5	76.9	-	82.75	-	85.3	-	88.1	54.6	1.68
22	2.5	39.9	0.1907	0.3456	5	61.4	-	63.65	-	-	-	65.75	73.2	1.63
23	3.5	39.9	0.1986	0.3456	5	52.3	-	58.9	-	60.9	-	62.2	82.5	1.31
24	5.5	37.0	0.1698	0.1358	5	76.3	-	82.6	-	86.8	-	93.0	46.5	1.6
25	4	41.9	0.1683	0.1121	5	-	-	80.35	-	86.2	-	83.35	33.7	1.6
26	4.5	38.0	0.1903	0.1627	5	81.2	-	88.1	-	91.9	-	95.0	56.0	1.45
27	4.5	38.0	0.1903	0.1627	5	-	-	-	-	-	-	95.1	56.0	1.45
28	4	44.35	0.3965	0.2239	5	92.4	39.55	96.0	41.4	98.0	41.4	98.8	41.6	1.34
29	4.5	41.85	0.3745	0.2239	50	60.1	28.7	67.3	32.9	72.7	34.7	76.3	37.95	1.20
30	4	25.1	0.223	0.2239	5	81.6	52.1	-	-	89.2	58.1	90.7	59.6	1.528
31	4	10.9	0.0962	0.2239	5	59.95	80.6	63.8	84.5	67.7	84.5	66.4	84.5	1.83

but we met with failure, as might have been expected. We proceeded as follows in the kinetic interpretation of our experimental results: to identify the influence of a given factor (solution acidity, SO_2 or $Fe^{\cdots}$ concentration, temperature) upon the velocity of the process in question, we chose those portinns of our experimental curves along which all the other conditions remained the same, so that the difference in the reaction time had to be due solely to a difference in the value of the factor in question. This sort of processing of our experimental data, using graphical plots, enabled us to determine how the reaction time varied with the concentration of H_2SO_4, SO_2, or $Fe_2(SO_4)_3$ in the solution or with the temperature, all the other conditions remaining the same. It was then easy to determine the relationship between these factors and the process rate.

TABLE 2

Duration of the Reaction Between SO_2 and $Fe_2(SO_4)_3$ as a Function of the Concentration of H_2SO_4, SO_2, and $Fe_2(SO_4)_3$ in the Solution

Test No.	Drop in SO_2 concentration, in moles/liter	Solution acidity, g/liter			Time, seconds	Curve No. in Figs. 3 and 4
		Initial	Final	Mean		
1	0.10-0.08	7.2	9.75	8.47	280	1
2		9.25	10.52	9.88	300	
3		22.41	25.29	23.85	1000	
4		53.32	56.61	54.97	4400	
1	0.09-0.07	9.55	10.82	10.18	350	2
2		9.94	11.31	10.62	400	
3		23.88	26.48	25.18	1400	
4		54.9	58.27	56.58	6800	
1	0.08-0.06	9.75	11.91	10.83	500	3
2		10.53	12.29	11.41	600	
3		25.3	27.85	26.57	2400	
4		56.61	59.81	58.21	10600	
1	0.07-0.05	10.83	12.95	11.89	750	4
2		11.32	13.38	12.35	900	
3		26.5	29.28	27.89	3500	
1	0.06-0.04	11.92	14.21	13.06	1300	5
2		12.3	14.75	13.52	1600	
3		27.85	30.75	29.3	5350	
1	0.05-0.03	12.92	15.51	14.22	2700	6
2		13.39	16.63	15.01	3100	
3		29.29	32.09	30.69	9920	

Inasmuch as the acidity of the solution varied during each run, we had to begin our kinetic analysis with an elucidation of the part played by that factor. We employed the test group 1-4 for this purpose, since all the experimental conditions remained the same in this group of tests but the initial acidity of the solution. We read off the time in which the SO_2 concentration in the solution dropped from 0.1 to 0.08, from 0.09 to 0.07, from 0.08 to 0.06, from 0.07 to 0.05, from 0.06 to 0.04, and from 0.05 to 0.03 moles per liter on the curves representing the course of each of these tests. Knowing the initial solution acidity and the decrease of $Fe^{\cdots}$ during the reaction, we calculated the mean acidity (grams of H_2SO_4 per liter), to which the test results were referred.

Our results are given in Table 2 and Fig. 3. Increasing the solution

acidity slows down the process considerably. The same data are plotted on a logarithmic scale in Fig. 4, yielding straight lines that are parallel to one another. The slope of these straight lines indicates that the duration of the reaction between SO_2 and $Fe^{\cdot\cdot\cdot}$ in aqueous solution is proportional to the solution acidity to the 1.7 power.

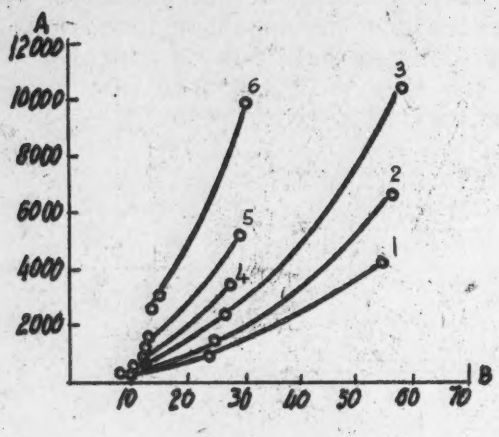

Fig. 3. Reaction time as a function of the solution acidity for various drops in the SO_2 concentration.

A-Reaction time, seconds; B-H_2SO_4 concentration, grams/liter. Drop in SO_2 concentration, moles/liter: 1) 0.10-0.08; 2) 0.09-0.07; 3) 0.08-0.06; 4) 0.07-0.05; 5) 0.06-0.04; 6) 0.05-0.03.

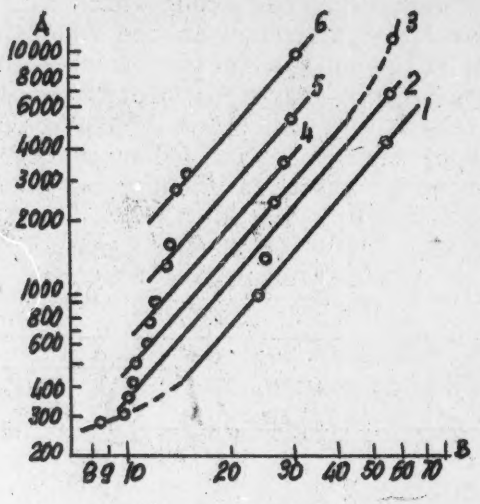

Fig. 4. Reaction time as a function of the solution acidity for various drops in the SO_2 concentration.

A-Reaction time, seconds; B-H_2SO_4 concentration, grams/liter. Drop in SO_2 concentration, moles/liter: 1) 0.10-0.08; 2) 0.09-0.07; 3) 0.08-0.06; 4) 0.07-0.05; 5) 0.06-0.04; 6) 0.05-0.03.

This relationship enabled us to eliminate thenceforth the influence of the acidity. The same procedure was employed to discover the sequence of the reactions as far as $Fe_2(SO_4)_3$ was concerned: we took a series of tests and read off the time required in each test for the reaction to progress by the same change in the concentration of SO_2. Thus, the reaction time in each group of tests was governed solely by the $Fe^{\cdot\cdot\cdot}$ concentration and the solution acidity. To eliminate the influence of the latter factor, the reaction time was recalculated, using the relationship discovered above, for a single standard acidity (10 grams H_2SO_4 per liter). These results were expressed as a straight line on logarithmic cross-section paper for each interval of SO_2 concentration.

Two straight lines are reproduced in Fig. 5 by way of example, representing the following intervals of SO_2 concentration: 0.07-0.05 and 0.05-0.03 moles/liter, respectively. They have the same slope; the magnitude of the latter indicates that the reaction time is inversely proportional to the square of the concentration of $Fe_2(SO_4)_3$ in the solution, all other conditions being the same. It follows that the velocity of the reaction between SO_2 and $Fe_2(SO_4)_3$ is proportional to the cube of the $Fe_2(SO_4)_3$ concentration:

$$-\frac{d[SO_2]}{dt} = K'[Fe_2(SO_4)_3]^3,$$

if the decrease in the SO_2 in the solution is taken as a guide.

Data on the variation of the reaction rate with the concentration of SO_2

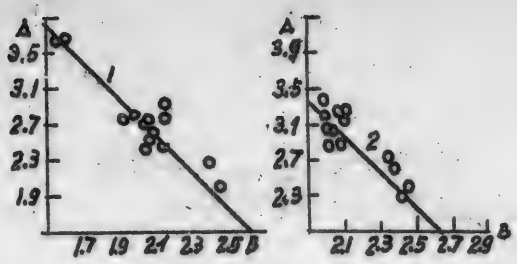

Fig. 5. Reaction time as a function of the $Fe_2(SO_4)$ concentration for various drops in the SO_2 concentration.

A-log t, seconds; B-log [$Fe_2(SO_4)_3$ moles/liter · .1000. Drop in SO_2 concentration, moles/liter: 1) 0.07-0.05; 2) 0.05-0.03.

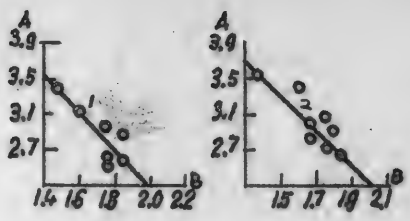

Fig. 6. Reaction time as a function of the SO_2 concentration for various drops in the $Fe_2(SO_4)_3$ concentration.

A-log t, seconds; B-log [SO_2 moles/liter·1000]. Drop in SO_2 concentration, moles/liter: 1) 0.13-0.11; 2) 0.12-0.10.

in the solution were obtained in a similar manner. The foregoing data indicate the powerful influence of this factor. Grouping the logarithmic graphs (Fig. 5) in a single diagram and passing vertical sections through them, we see that, for a given $Fe^{...}$ concentration in the solution the reaction time drops sharply as the concentration of SO_2 in the solution is raised.

Working up a series of tests with the same concentration range of $Fe_2(SO_4)_3$ and recomputing the resultant reaction time in terms of the standard acidity, we secured 8 parallel lines on a logarithmic graph. Figure 6 reproduces two of these lines by way of example [0.13-0.11 and 0.12-0.10 moles of $Fe_2(SO_4)_3$ per liter, respectively]. The slope of these lines is such as to make the reaction time inversely proportional to the square of the SO_2 concentration in the solution, all other conditions being equal. Therefore, the velocity of the reaction between SO_2 and $Fe_2(SO_4)_3$ is proportional to the cube of the SO_2 concentration:

$$-\frac{d[SO_2]}{dt} = K''[SO_2]^3,$$

if the decrease in the SO_2 concentration is taken as a guide.

All these results were obtained at 50°. A few tests run at other temperatures indicated that the rate of this process rises sharply as the temperature is raised. Employing the method of working up the experimental data set forth above, we found that lowering the temperature from 50 to 25° prolongs the reaction time about 20 times, provided all other conditions remain the same. Raising the temperature from 50 to 75° shortens the reaction time by a factor of approximately 5.6. The latter figures must be regarded as merely provisional.

SUMMARY

1. The velocity of the reaction between SO_2 and $Fe_2(SO_4)_3$ in aqueous solutions has been measured. A study has been made of the influence of various concentrations of SO_2, $Fe^{...}$, and free H_2SO_4 (most of the experiments being run at 50°).

2. The decrease in the SO_2 in solution totaled 1.2-1.7 mole per mole of the reacted $Fe_2(SO_4)_3$. The reaction products include ferrous dithionate as well as ferrous sulfate.

3. The reaction time is proportionnal to the 1.7th power of the concentra-

tion of free H_2SO_4.

4. The velocity of the reaction between SO_2 and $Fe_2(SO_4)_3$ in aqueous solution, when judged by the drop in SO_2, is proportional to the cube of the SO_2 and $Fe_2(SO_4)_3$ concentrations.

LITERATURE CITED

[1] G.G.Urazov and L.R.Edelson. Data on the Metallurgy of Non-Ferrous Metals, p. 213. Leningrad, (1932).

[2] Y.H.Taylor, P.F.Whelan, Bull. Inst. Metals, 457, (1942).

[3] T.P.Campbell. Hydrometallurgy of Non-Ferrous Metals (Russ. Ed.), p. 179. Metallurgy Press (1934).

[4] Gmelin, Handbuch anorg. Chemie, I, 1, 594 (1907); 470 (1932).

Received July 14, 1950.

THE OXIDATION OF MAGNESIUM AND OF ITS ALLOYS AT HIGH TEMPERATURES

I. A. Makolkin

Research Institute of Production Technology and Organization

There have been several papers published on the rate at which magnesium and its alloys with various metals are oxidized [1]. But these researches have either been carried out in another temperature range or with alloys of different composition or, lastly, not in the gaseous medium in which we are interested. This has led us to undertake the present investigation, in which we consider the surface oxidation of magnesium, aluminum, zinc, and various alloys of magnesium in air, nitrogen, carbon dioxide, and sulfur dioxide.

EXPERIMENTAL

In our investigations on the oxidation process we employed the adsorption balance described earlier [2], designed on the basis of experimental research performed in the laboratory of Academician Dubinin, where adsorption balances have been in use for a long time in research on adsorption phenomena [3].

Experience has shown that this method of measuring the gain in weight during the oxidation process possesses several advantages over the customary method of weighing on analytical balances or microbalances. Basically, these advantages are as follows: 1) the sample remains in the furnace during weighing, since the gain in weight is determined by observing the displacement of the control sight in the cathetometer field of view with a micrometer eyepiece; 2) the sample can stay in the furnace as long as desired, since the whole corrosion-time curve can be recorded by reading off the gain in weight at equal time intervals; no oxidation products can be lost, thus eliminating the weighing errors that are unavoidable in the usual method of weighing, because the samples have to be taken out of the furnace while hot for weighing.

The adsorption-balance data could not be used in the experiments made in sulfur dioxide, since the molybdenum spring of the balance might be oxidized by the SO_2. The SO_2 tests were therefore run in the apparatus shown in Fig. 1. (See Plate, page 621).

The furnace (E) is used to heat the tube (G) in which the porcelain or quartz boats containing the samples under test are placed. Inasmuch as the temperatures used in the SO_2 tests did not exceed 460° C in this investigation, boats of molybdenum glass could be employed instead of porcelain. This was particularly advantageous whenever samples 200 mm long, intended for mechanical tests, were kept in the furnace, since we had no porcelain boats big enough to take samples that long. The tube (G) was either a porcelain tube 1000 mm long and 35-40 mm in diameter or a molybdenum-glass tube of the same dimensions, both ends of which were taper-ground and fitted with vacuum stopcocks.

The samples were placed in the central section of a rather long furnace,

in which the temperature gradient did not exceed 3-5° C. Two to four such furnaces were in operation at the same time, with one to three test samples heated in the gas current in each furnace.

Oxidation lasted at least 16 hours, with a complete set of measurements of the gain in weight every 2 or 4 hours at the given test temperature and with the samples weighed before and after the run.

The gas was supplied either from a tank (argon, nitrogen) or from a Kipp generator (CO_2), the air being either drawn through by a water-jet pump or forced through by an oil pump.

The gas first passed through a tube filled with glass wool, then through three Drexel bottles containing sulfuric acid (O), calcium chloride (N), and soda lime (M), respectively. Then the gas was passed through glass wool again and entered the preheating furnace (B), from which it passed to the furnace (E) that contained the samples. Upon leaving the furnace, the gas passed through a Drexel bottle containing sulfuric acid (P), which served as a liquid seal, and then through a rheometer (I), which measured the gas flow rate (ordinarily maintained at 40 cc per minute).

The temperature in the furnaces containing the samples was measured by means of Pt - Pt/Rh thermocouples (H) and was regulated to within $\pm$ 5° C by means of the potentiometer (K). The gas temperature in the preheating furnaces was measured by chromel-alumel thermocouples (D) and was regulated to within $\pm$ 10°C by means of contact galvanometers.

In addition, there were control thermocouples (D) in every furnace, connected to the galvanometers (E). The thermoregulators, galvanometers, thermocouples, and rheometers were all calibrated in advance by the Bureau of Weights and Measures.

The carbon dioxide was produced in a Kipp generator by reacting marble with chemically pure hydrochloric acid; it was dried by passing it through concentrated sulfuric acid.

The sulfur dioxide was produced by burning pure lump sulfur in a capacious porcelain boat placed in a separate porcelain tube and was passed through a glass-wool filter to free it of solid particles of sulfur. In some instances the SO_2 was produced by burning lead sulfide in air.

A water-jet pump was used to draw the SO_2 together with air into the furnace containing the samples. Analysis of the furnace gases indicated 8% SO_2 and 92% air. It will be shown below that a mixture of this composition affords good protection to the metal against oxidation by atmospheric oxygen.

The nitrogen was freed of any atmospheric oxygen by passing it through incandescent copper shavings.

The SO_2 in the air was analyzed by oxidizing the sulfur dioxide to sulfuric acid with hydrogen peroxide.

The percentage of CO_2 in the air was determined by absorbing it in a potassium hydroxide solution in a Burrel apparatus, with the measuring buret replaced by a more accurate one, enabling measurements to be made with an accuracy of 0.05 mm. The percentage of CO_2 in the gas was found to vary from 5 to 17%.

The pure metals magnesium, aluminum, and zinc were tested, as well as 2 cast alloys of aluminum, the composition of which are given in Table 1.

Samples of magnesium and aluminum, with areas ranging from 32 to 62 sq. cm. were cut from metal sheets. The zinc samples were made of zinc wire, with a total area of 12.4 sq. cm.

TABLE 1

Composition of Tested Magnesium Alloys

Method of analysis	Alloy No.	Per cent of individual components			
		Al	Zn	Mn	Mg
Chemical	MC-4	6.35	2.48	0.25	Remainder
	MC-5	9.44	0.59	0.33	Remainder
Spectral	MC-4	7.40	3.55	0.20	Remainder
	MC-5	9.45	0.50	0.29	Remainder

The samples of the MC-4 and MC-5 alloys, with areas of 32 or 62 sq. cm. were cut off from round cast bars as flat plinths. The surface of the samples was treated with carbon tetrachloride and then with alcohol and dried with filter paper before use.

No special study was made of the effect of the cleanness of the metal surface upon oxidation, although the cleanness grade probably does affect the oxidation rate. In our research we employed alloy samples with planed surfaces.

Table 1 indicates that the results of chemical and spectral analysis differ somewhat, but both methods give a sufficient idea of the differences in the composition of the two alloys, and in this respect the analysis results are in satisfactory agreement.

Oxidation of the metals and magnesium alloys in the air. The results of our tests are listed in Tables 2, 3, and 4, the gain in weight at intervals of 2 hours being expressed in mg per sq. cm.

Table 2 shows that the oxidation of magnesium is linear at temperatures in the 400-600° C range, so that the mean value of the gain in weight during 2 hours can be calculated. On the other hand, parabolic curves are obtained for the oxidation of aluminum and zinc, so that the mean gain in weight cannot be computed for these metals. (Table 2 appears on page 508).

TABLE 3

Results of the Oxidation of the Alloys MC-4 and MC-5 in Air

Time, hours	Gain in weight of the samples, in mg per sq. cm, during heating at various temperatures							
	400		420		440		460	
	Alloy MC-4	Alloy Mc-5	Alloy MC-4	Alloy MC-5	Alloy MC-4	Alloy MC-5	Alloy MC-4	Alloy MC-5
2	0.0142	0.0408	0.0416	0.0658	0.0687	0.1875	0.1219	0.3656
2	0.0150	0.0344	0.0344	0.0719	0.0812	0.1907	0.1250	0.3594
2	0.0152	0.0375	0.0438	0.0625	0.0781	0.1907	0.1250	0.3625
2	0.0130	0.0314	0.0354	0.0578	0.0719	0.1656	0.1250	0.3469
2	0.0182	0.0348	0.0344	0.0516	0.0844	0.1734	0.1219	0.3719
2	0.0222	0.0422	0.0374	0.0516	0.0813	0.1875	0.1312	0.3625
2	0.0166	0.0390	0.0374	0.0750	0.0844	0.2000	0.1390	0.3687
2	0.0162	0.0390	0.0282	0.0658	0.0875	0.1806	0.1375	0.3875
2	0.0190	0.0390	0.0384	0.0687	0.0875	0.1875	0.1406	0.3531
Average gain after 2 hours	0.0166	0.0376	0.0368	0.0634	0.0806	0.1848	0.1286	0.3642
Total gain throughout run	0.1496	0.3381	0.3310	0.5707	0.7250	1.6635	1.1671	3.2782

Table 2

Results of the Oxidation of Magnesium, Aluminum and Zinc in Air

Time, hours	Gain in weight of the samples, in mg. per sq. cm. during heating at various temperatures										
	magnesium						aluminum				zinc
	400°	440°	460°	500°	550°	600°	400°	460°	500°	600°	390°
2	0.0125	0.0479	0.0666	0.2500	0.2916	0.7875	0.0096	0.0173	0.0288	0.0442	0.1456
2	0.0167	0.0438	0.0625	0.2604	0.4375	0.7583	0.0058	0.0096	0.0154	0.0231	0.0728
2	0.0125	0.0458	0.0604	0.2917	0.4615	0.8521	0	0	0.0077	0.0154	0.0405
2	0.0188	0.0417	0.0771	0.2708	0.5521	0.8167	0	0	0.0096	0.0173	0.0324
2	0.0146	0.0521	0.0688	0.2396	0.6042	0.8333	0	0	0.0058	0.0115	0.0243
2	0.0208	0.0500	0.0625	0.2479	0.5625	0.8063	0	0	0.	0.0211	0
2	0.0104	0.0542	0.0708	0.2542	0.5833	-	0	0	0	0.0096	0
2	0.0146	0.0563	0.0729	0.2792	0.5792	-	0	0	0	0.0192	0
2	0.0229	-	-	0.2833	-	-	0	0	0	0.0135	0
Average gain after 2 hours	0.0160	0.0440	0.0677	0.2641	0.5090	0.8090	-	-	-	-	-
Total gain throughout the run	0.1438	0.3518	0.5416	2.3770	4.0720	4.8542	0.0154	0.0269	0.0673	0.1749	0.3150

Table 4

Oxidation of the MC-4 and MC-5 Alloys in N_2, CO_2 and SO_2

Time, hours	Gain in weight of the samples, in mg. per sq. cm. during heating at various temperatures											
	nitrogen				carbon dioxide				sulfur dioxide			
	Alloy MC-4		Alloy MC-5		Alloy MC-4		Alloy MC-5		Alloy MC-4		Alloy-MC-5	
	440°	460°	440°	460°	420°	460°	420°	460°	420°	460°	420°	460°
2	0.0500	0.0625	0.0562	0.0750	0.0781	0.0875	0.0626	0.0656	0.0148	0.1934	0.0118	0.0059
2	0.0437	0.0656	0.0484	0.0797	0.0282	0.0375	0.0094	0.0782	0.0148	0.0148	0.0328	0.0000
2	0.0360	0.0672	0.0219	0.0390	0.0196	0.0344	0.0188	0.0719	0 .000	0.0268	0.000	0.0536
2	0.0219	0.0425	0.0188	0.0672		0.0188	0	0.0313	0.000	0.000		
2	0.0125	0.0406	0.0469	0.0797	0	0	0	0.0156	0.000	0.000	0.000	0.000
2	0.0484	0.0468	0.0391	0.0407				0.0125				
2	0.0453	0.0328	0.0375	0.0734								
2	0.0244	0.0516	0.0188	0.0390								

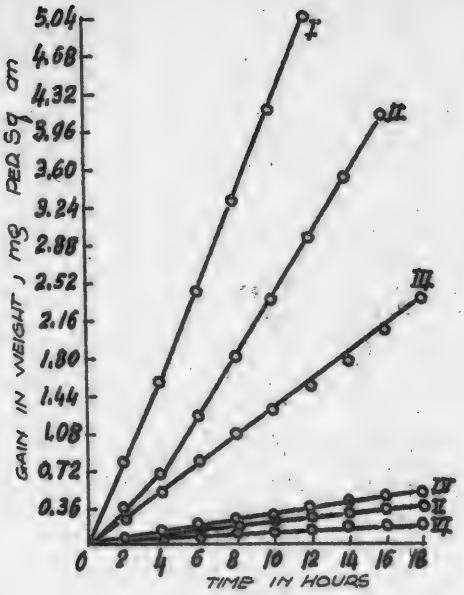

Fig. 2. Oxidation of pure magnesium in air.

Oxidation temperature, °C: I) 600; II) 550; III) 500; IV) 460; V) 420; VI) 400.

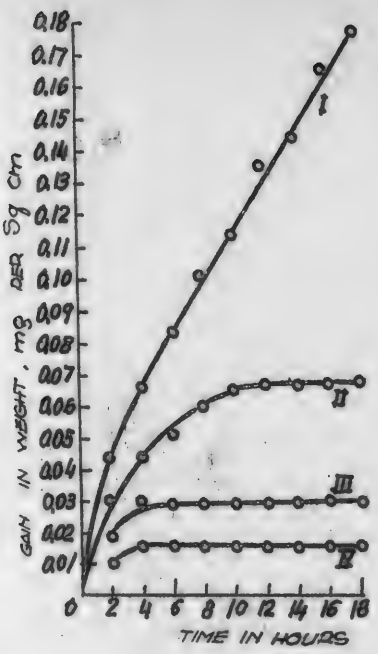

Fig. 3. Oxidation of aluminum in air.

Oxidation temperature, °C: I) 600; II) 500; III) 460; IV) 400.

The oxidation curves for magnesium, aluminum, and zinc in air are given in Figs. 2, 3, and 4, respectively.

We see from the data in Table 3 that the magnesium alloys MC-4 and MC-5 are oxidized in air in the 400-600° range like magnesium itself, i.e., linearly, though much faster than magnesium, as is seen in Tables 2 and 3 and Fig. 5.

The oxidation of these alloys proceeds somewhat differently at 500°, as is seen in Fig. 6.

At this temperature the oxidation process follows a rising curve for the alloy MC-4. The alloy MC-5, which contains more aluminum than the MC-4 alloy, is oxidized even faster, being burned up entirely after a stay of 20 minutes in the furnace.

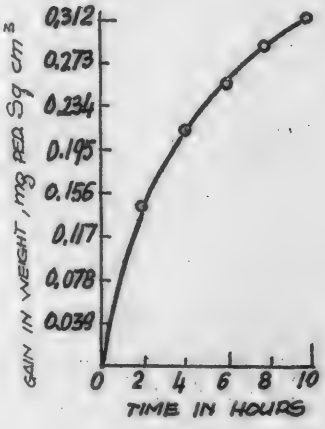

Fig. 4. Oxidation of zinc in air at 390° C.

The MC-4 alloy lasts in the furnace for a longer time. Apparently, increasing the percentage of aluminum in the alloy increases the latter's oxidation rate. This is found to be true at lower temperatures as well, as is readily seen in Table 3 and Fig. 5.

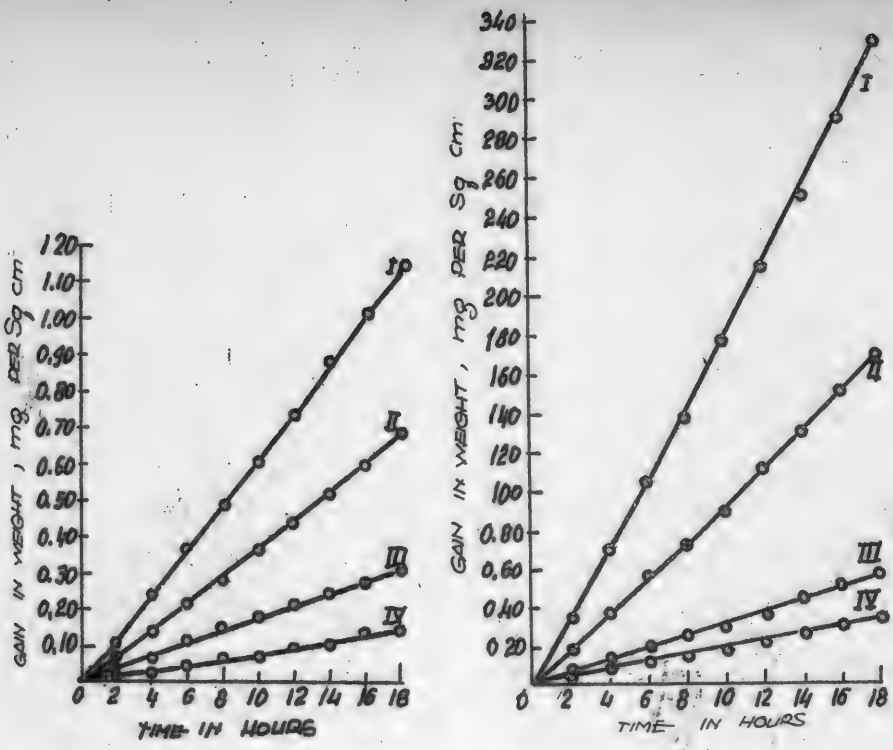

Fig. 5. Oxidation of cast magnesium-aluminum alloys in air: Left – MC-4 alloy; Right – MC-5 alloy. Oxidation temperature (°C): I – 460; II – 440; III – 420; IV – 400.

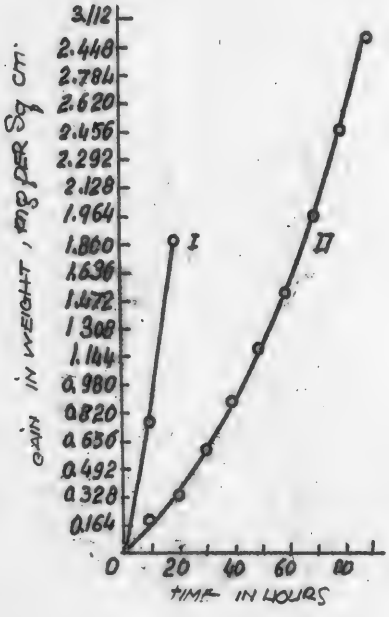

Fig. 6. Oxidation of the MC-4 and MC-5 alloys in air at 500°C. Alloy: I – MC-4. II – MC-5.

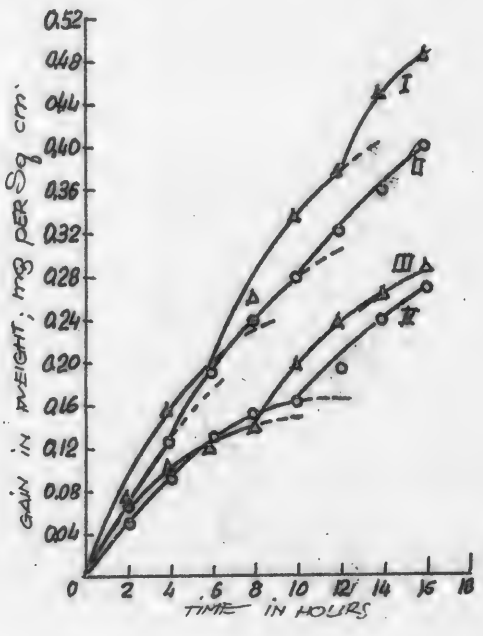

Fig. 7. Oxidation of the MC-4 and MC-5 alloys in nitrogen. Alloys and oxidation temperatures, °C: I – MC-5, 460; II – MC-4, 460; III – MC-5, 440; IV – MC-4, 440.

Oxidation of the MC-4 and MC-5 alloys in N_2, CO_2, and SO_2. The results of our experiments on the oxidation of the alloys MC-4 and MC-5 in N_2, CO_2, and SO_2 are tabulated in Table 4.

Table 4 shows that the oxidation of the alloys MC-4 and MC-5 in nitrogen, carbon dioxide, and sulfur dioxide follows damped curves that look like parabolas.

These curves are reproduced in Figs. 7, 8, and 9.

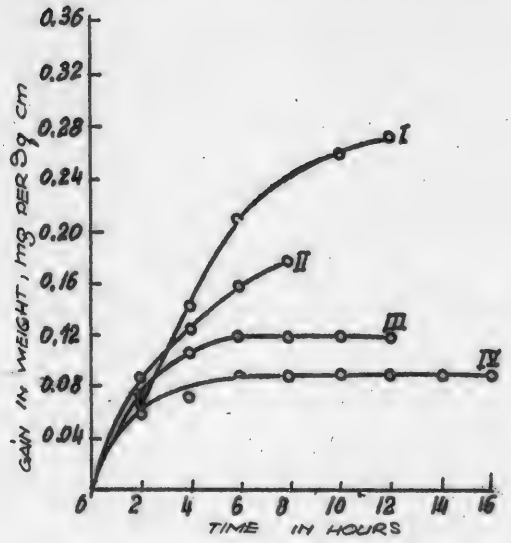

Fig. 8. Oxidation of the MC-4 and MC-5 alloys in CO_2 (5-17%). Alloys and temperature, °C; I – MC-5, 460; II – MC-4, 460; III – MC-4, 420; IV – MC-5, 420.

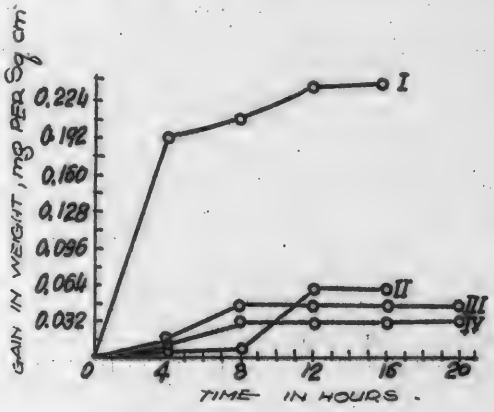

Fig. 9. Oxidation of the MC-4 and MC-5 alloys in sulfur dioxide. Alloys and temperature, °C: I – MC-4, 460; II – MC-5, 460; III – MC-5, 420; IV – MC-4, 420.

Microstructure and mechanical properties of the alloys. The microstructure of the samples of alloys MC-4 and MC-5 in their initial stages is typical for the cast state. Their structure consists of grains of a solid solution, with inclusions of Al_3Mg_4 along the boundaries of these grains. The solid solution is seen to break down near the Al_3Mg_4 inclusions, as is usually the case for samples cast in sand. The fine particles settling out of solution after etching are dark in color.

Figs. 10 and 11 show the microstructure of one of these samples at different magnifications (see Plate, page 621).

After the samples had been heated to 420° for 16 hours nearly all the Al_3Mg_4 entered the solid solution, the structure of the samples consisting of grains of the solid solution, as shown in Fig. 12 (see Plate, page 621), no matter what medium they were heated in (air, nitrogen, carbon dioxide, or sulfur dioxide).

The mechanical properties of these homogenized samples were higher than those of the case samples.

If we take the mean values of σ and δ for each gaseous medium, we get the values for these constants given in Table 5.

The results of metallographic analysis and mechanical tests yield the following conclusions:

1) In their original state the samples have a cast structure.

TABLE 5

Mean Values of σ and δ for Round Samples of MC-4 in Various Media

Gas medium	Temperature, °C	Heating time, hours	Mean values	
			σ, kg/mm²	δ, %
Samples in initial state	–	–	18.3	5.0
After heating in air	420	16	20.3	6.5
After heating in nitrogen	420	16	20.1	6.6
After heating in SO_2	420	16	20.6	8.0

TABLE 6

Mean Values of σ and δ for Flat Samples in Various Media

Temperature, °C	Carbon dioxide		Air		$\sigma_{CO_2} - \sigma_{air}$ (kg/mm²)	$\delta_{CO_2} - \delta_{air}$ (%)
	σ, kg/mm²	δ, %	σ, kg/mm²	δ, %		
450	24.0	13.5	23.0	8.5	1.0	5.0
500	22.5	9.5	19.0	5.5	3.5	4.0
550	20.0	6.5	18.0	5.5	2.0	1.0
600	17.5	6.5	14.0	3.5	3.5	3.0
650	14.5	3.0	Samples burned up			
Average	21.0	9.0	18.5	5.7	2.5	3.3

2) The structure of the samples became homogeneous after 16 hours of heat treatment in the furnace at 420°, which improved their mechanical properties appreciably.

3) The structure and the mechanical properties of the samples are similar after heating in various gaseous media (air, nitrogen, and sulfur dioxide). There is some tendency, however, for the values of σ and δ to be higher after heating in sulfur dioxide, as is seen in Table 5.

These constants increased much more when the tests on the effect of the heat treatment medium upon the mechanical properties of the magnesium alloys were run on flat samples, in which the ratio of the surface to the cross section was half of that for the round samples. This is seen in Table 6.

Thus, the difference between the mean values of σ_{CO_2} and σ_{air} at various temperatures was 2.5 kg/sq. mm (or 12%), the difference between the mean values of δ_{CO_2} and δ_{air} being 3.3%, or 37%.

It follows that the film of carbonates and of sulfates formed on the surface of the magnesium alloys when the latter are heated in CO_2 and SO_2, respectively, protects the alloys against oxidation by atmospheric oxygen and appreciably improves their mechanical properties.

SUMMARY

1. A study has been made of the oxidation of magnesium, aluminum, and zinc, and of magnesium-aluminum alloys in atmospheric oxygen at high temperatures, and of the magnesium alloys in nitrogen, carbon dioxide, and sulfur dioxide.

2. It has been shown that aluminum and zinc are oxidized in accordance with a parabolic law in atmospheric oxygen; a similar law applies to the oxidation of the magnesium alloys in nitrogen, carbon dioxide, and sulfur dioxide.

The oxidation of magnesium and of its alloys in atmospheric oxygen, on the other hand, is linear.

3. It has been shown that increasing the percentage of aluminum in magnesium alloys increases the rate at which these alloys are oxidized in atmospheric oxygen, nitrogen, CO_2, and SO_2.

4. It has been shown that the mechanical properties of magnesium alloys are improved by treating them with CO_2 and SO_2. This is due to the fact that the resulting carbonates and sulfates form a protective film on the surface of the alloy. This makes it obvious that the heat treatment of magnesium alloys should be carried out in an atmosphere of nitrogen, carbon dioxide, or sulfur dioxide.

5. The heat treatment of magnesium alloys in a protective gas prevents the parts from catching fire during treatment.

LITERATURE CITED

[1] Leontis and Rhines, Metals Technol, 13 [4], 1 (1946); Pilling and Bedwort, J. Inst. Metals, 29, 529 (1923).

[2] I.A.Makolkin, Factory Lab., 10, 1209 (1949).

[3] M.M.Dubinin. The Physico-Chemical principles of Sorption Techniques, 193 (1935).

Received April 26, 1950.

ELECTROLYTIC BRASSPLATING IN AN OXALIC ACID BATH

A. I. Stabrovsky

The author has made a study of various solutions of complex non-cyanide salts of copper and zinc with the objective of replacing the cyanides in the brassplating bath by non-cyanide salts. The present paper sets forth the results of an investigation of deposition at the cathode from an oxalic acid solution.

Electrolysis of solutions of mixtures of simple copper and zinc salts does not produce cathodic deposits of brass that are suitable coatings. This is due to the great difference between the standard potentials of copper (+0.34 volt) and zinc (-0.76 volt), amounting to 1.1 volts.

As we shall show later on, the joint deposition of copper and zinc at the cathode is readily effected by the electrolysis of complex copper and zinc oxalates, as is the case in a cyanide bath.

The advantage of oxalic acid solutions over cyanide ones is that they are non-poisonous and are more stable when exposed to the air.

EXPERIMENTAL

Preparation of solutions. When copper and zinc sulfates are reacted with sodium oxalate, we get the respective complex salts:

$$Na_2Cu(C_2O_4)_2 \cdot 2N_2O \quad \text{and} \quad Na_4Zn(C_2O_4)_3 \cdot xH_2O.$$

The solutions of these salts were prepared from pure reagents, boric acid being used as the buffer additive. The solution of copper or zinc sulfate was preheated before the bath was made up. When sodium oxalate was added to the copper or zinc sulfate solution, the solution was stirred until all the precipitate dissolved.

Cathodic deposition of brass. We used the method of measuring the discharge potentials and plotting the polarization curves to determine the feasibility of depositing brass at the cathode from an oxalate solution. With this in mind, we prepared: a 0,01 molar solution of the complex copper salt, a 0.015-molar solution of the complex zinc salt, and a mixture containing 0.01 mol of the complex zinc salt, and a mixture containing 0.01 mole of the complex copper salt and 0.015 mole of the complex zinc salt per liter. The total sodium oxalate content was 25 grams per liter in each of these solutions. The electrode potentials were measured during electrolysis at various C.D.'s.

The measurement results are given in Fig. 1.

We see in Fig. 1 that as the C.D. is raised, the cathodic polarization of copper rises faster than that of zinc, so that the discharge potentials of these metals come closer together. The discharge potentials of copper and zinc are

closest at a C.D. of 0.1 amp/dm^2.

The fact that the cathodic polarization of copper is higher than that of zinc is due chiefly to the fact that in an oxalate solution, as in a cyanide one, the concentration of single copper ions is lower than that of single zinc ions. This follows from the values of the instability constants of the complex copper and zinc oxalate ions. The instability constant is $2.05 \cdot 10^{-10}$ for the complex copper ion and $7.05 \cdot 10^{-9}$ for the complex zinc ion.

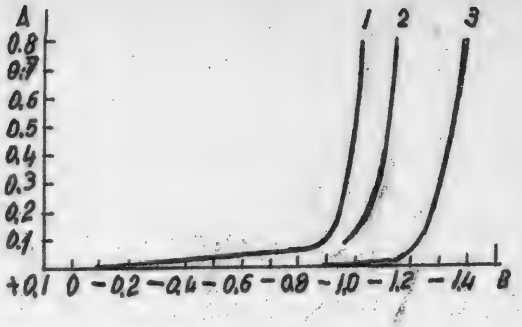

Fig. 1. Curves of the discharge potentials of copper, zinc, and brass from various solutions at various current densities.

A-C.D., amp/dm^2; B-cathode potential, volts.

Solutions: 1) 0.01 molar $Na_2Cu(C_2O_4)_2$, n $Na_2C_2O_4$; 2) 0.0015 molar $Na_4Zn(C_2O_4)_3$, n $Na_2C_2O_4$; 3) [0.001 molar $Na_2Cu(C_2O_4)_2$ + 0.01 molar $Na_4Zn(C_2O_4)_3$], n $Na_2C_2O_4$.

In the electrolysis of an oxalate solution containing complex copper and zinc salts the joint deposition of copper and zinc on the cathode (Fig. 1, Curve 3) takes place at a more highly electronegative potential than the discharge potential of copper, in contrast to what happens in a cyanide bath. This is due to the properties and composition of the resulting cathodic deposit, the static potential of which was much more highly electronegative than the potential of ordinary brass. On the other hand, the marked drop in the cathodic polarization of zinc (Fig. 1, Curves 2 and 3) indicates that a solid solution of brass is formed at the cathode, inasmuch as the depolarizing effect of copper upon zinc when they are deposited together can be exerted only in consequence of the energy of formation of a solid solution.

In order to determine the composition of the platings, the brass was deposited on a platinum cathode. The percentages of copper and zinc in the platings were determined by electroanalysis. The analysis results are listed in Table 1.

TABLE 1

Per cent Copper and Zinc in Cathodic Deposits Produced at 20-22° C as a Function of C.D.

Cathode C.D., amp/dm^2	Electrolysis time, min.	Cathodic current efficiency, %	Per cent composition of deposits		Appearance of cathodic deposits
			Copper	Zinc	
0.1	15	80.5	33.4	66.6	Silver-white, slightly dull
0.2	10	78.7	29.8	70.2	Silver-white, dull
0.3	10	80.5	28.5	71.5	Silver-white, dull

We see from the data in Table 1 that the composition of the cathodic deposits produced at 0.1-0.3 amp/dm^2 depend but little upon the C.D., the percentage of zinc in the coatings being very high, ranging from 66.6 to 71.5%, depending upon the electrolysis conditions.

When an oxalate solution is electrolyzed, silver-white lustrous deposits are formed within a short time (3-5 min.). Prolonging the electrolysis yields dull, friable, and dark deposits, which are quite useless as platings. The densest electrolytic deposits are formed at a solution pH of 5 to 6.

Effect of Colloids Upon the Plating Quality and Upon the Cathodic Polarization of Copper and Zinc

Various colloids were added to the oxalate baths to ascertain the effect of colloids upon the improvement of electrocrystallization in the cathodic deposition of metals and upon the cathodic polarization of copper and zinc. The colloid additives used included gelatin, joiner's glue, peptone, dextrin, and others.

Most of these colloids improved the quality of the coatings. The addition of gelatin to the oxalate bath produced dense, lustrous copper-zinc cathodic deposits of high quality. These deposits were quite satisfactory as platings. The best results are obtained when the bath contains 0.05 to 0.50 g of gelatin per liter. Raising the gelatin percentage above this level causes dull coatings to be deposited on the cathode.

We ran tests of the electrodeposition of brass under various conditions in order to learn the effect of electrolysis time and cathodic C.D. upon the composition and quality of the coatings produced in a bath to which gelatin has been added. The results of these tests are listed in Table 2.

TABLE 2

Composition and External Appearance of Brass Deposits Produced in a Bath Containing 0.1 Gram of Gelatin per Liter, as Functions of the Cathode C.D. Platinum Cathode; Brass Anode; Solution Temperature: 20°C; pH 5.36.

Cathode C.D., amp/dm^2	Electrolysis time, min.	Cathodic current efficiency, %	Per cent composition of deposits		Appearance of cathodic deposits
			Copper	Zinc	
0.1	60	58.5	70.6	29.4	Light pink, lustrous
0.2	50	53.1	63.4	36.6	Bright with a greenish tinge, lustrous
0.3	40	45.3	58.5	41.5	Bright, greenish, lustrous
0.4	30	40.4	56.3	43.7	Bright, lemon-yellowish tinge, lustrous
0.5	20	36.7	56.0	44.0	Ditto
0.6	15	35.3	54.7	45.3	Ditto
0.7	15	35.0	51.3	48.7	Ditto

The table indicates that satisfactory brass coatings are formed at a C.D. ranging from 0.1 to 0.7 amp/dm^2 in a bath to which gelatin has been added, the quality of the brassplating not being impaired by prolonging the electrolysis. This makes it possible to increase the allowable cathode C.D., and to secure cathode deposits of any desired thickness of the brass coating.

It is worthy of note that adding gelatin to the bath greatly increases the percentage of copper in the resultant brass deposits. When 0.1 g of gelatin is added to the solution per liter, the percentage of copper in the cathode deposit rises from 29.8 to 63.4% at a C.D. of 0.2 amp/dm^2 (Tables 1 and 2). The reason for this is that the presence of gelatin causes the cathodic polarization of zinc to rise faster than that of copper.

Figure 2 reproduces the curves of the cathodic polarization of copper and zinc as functions of the C.D. for the deposition of these metals from solutions with and without a gelatin additive. The figure shows that the addition of 0.2 gram of gelatine per liter to the bath raises the cathodic polarization of zinc by 0.255 volt for a cathode C.D. of 0.3 amp/dm^2, while the cathodic polarization

of copper is increased only 0.75 volt. That is why the percentage of zinc in the cathodic deposits does not exceed 48.7% when the cathode C.D. is raised from 0.1 to 0.7 amp/dm^2 in electrolyzing a solution containing gelatin.

Not much research has been done on the way in which colloids improve the electrocrystallization of cathodically deposited metals or how they affect the cathodic polarization of copper and zinc. According to the findings of Izgaryshev and Titov [1], the increase in the cathodic polarization of copper and zinc when colloids are present is caused by the formation of coordination compounds of the ions of these metals with the colloids.

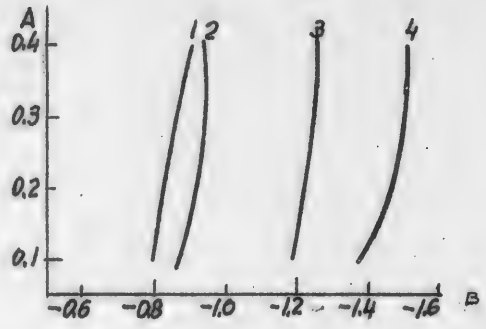

Fig. 2. Curves of the discharge potentials of copper and zinc from oxalate solutions with and without gelatin at various values of C.D.

A-C.D., amp/dm^2; B-cathodic potential, volts. Copper curves: 1) without gelatin; 2) with 0.2 grams of gelatin per liter; Zinc curves: 3) without gelatin; 4) with 0.2 gram of gelatin per liter.

Cathodic and anodic current efficiencies in brassplating. The cathodic current efficiency in the deposition of brass from an oxalate bath to which gelatin has been added differs only slightly from the cathodic current efficiency in a cyanide bath, amounting to 50-60%.

When gelatin is added to the oxalate bath (Tables 1 and 2), the current efficiency of copper-zinc deposition at the cathode drops. Increasing the solution acidity or the C D. causes the evolution of considerable hydrogen at the cathode, this causing the cathodic current efficiency to drop again. Increasing the cathode C.D. from 0.1 to 0.7 amp/dm^2 caused the current efficiency of the deposition of brass at the cathode to drop from 58.5 to 35.0%.

The anodic current efficiency in the deposition of brass depends chiefly upon the composition of the bath, the pH of the solution, and the C.D. used. If the bath contains insufficient sodium oxalate or the solution pH is low, the anode becomes coated with a white deposit of zinc oxalate as electrolysis progresses, the anodic current efficiency in the deposition of brass decreasing. Increasing the C.D. above the allowable limit passivates the anode, causing a decrease in its solubility. Increasing the C.D. from 0.1 to 0.4 amp/dm^2 caused a drop in the anodic current efficiency in brass deposition from 98.4 to 43.7%. At a C.D. of 0.1 to 0.2 amp/dm^2, the anodic current efficiency of brass deposition was much higher than that of the cathode, being 98.4 to 91.0%, respectively.

Composition of the bath and operating regime. The initial constituents of the solution for the oxalate bath were copper and zinc sulfates, sodium oxalate, boric acid, and gelatin.

Optimum Bath Composition

Initial Substances	Grams/liter
Copper sulfate ($CuSO_4 \cdot 5H_2O$)	2.5
Zinc sulfate ($ZnSO_4 \cdot 7H_2O$)	4.5
Sodium oxalate ($Na_2C_2O_4$)	26.0
Boric acid (H_3BO_3)	20.0
Gelatin	0.1

The percentages of copper and zinc in the bath are limited by the solubilities of their complex oxalate salts in the solution, which is saturated with

sodium oxalate. Using an excess of sodium oxalate in the bath improves the operation of the anodes and increases the stability of the solution.

The boric acid acts as a buffer, retarding any change in the solution pH during electrolysis. The addition of gelatin improves the electrocrystallization of the cathodically deposited metals and also affects the composition of the resultant brass coatings, increasing the percentage of copper in them.

There is hardly any change in the concentration of copper and zinc in the solution during the operation of the oxalate bath. The excess of the complex salts of copper and zinc produced in the solution as the result of the dissolution of the anodes is thrown down as a precipitate. The total of oxalate ions in the bath and the solution acidity diminish.

Oxalic acid must be added to the bath at regular intervals, determined by experience, to maintain the solution pH constant. Sodium oxalate must likewise be added as the total of oxalate ions in the bath diminishes.

A rise in the temperature of the solution increases the solubility of the complex salts of copper and zinc; this increases the tendency for contact copper to be deposited on the steel parts, while the dispersibility of the solution is decreased. Stirring the solution likewise diminishes the dispersibility of the bath and eliminates the effect of colloids upon the cathodic process entirely.

In his research on the process of copperizing in oxalate solution, Lainer [2] has shown that contact copper diminishes the strength of the bond between the coatings and the underlying metal. But if the parts to be plated are suspended from a live cathodic busbar, practically no contact copper is deposited.

In electrolyzing an oxalate solution, the most satisfactory brassplating is secured at a bath temperature of 20-30°, a cathode C.D. of 0.2-0.3 amp/dm^2, and a solution pH ranging from 5 to 6. Increasing the cathode C.D. to 0.6-0.7 amp/dm^2 does not impair the quality of the coatings, but the solution acidity and the total content of oxalate ions change rapidly, owing to the drop in the current efficiency.

The concentration of gelatin decreases as an oxalate bath is operated, part of it being carried off with the plated parts, while part is probably thrown down with the cathodic deposit. It is therefore advisable to replenish the gelatin in the bath from time to time.

Dispersibility of the solution and properties of the brass coatings. The Haring and Blum method was used to secure comparative data on the dispersibility of an oxalate and a cyanide bath.

Tests indicated that there is little difference between the dispersibilities of these baths, that of the oxalate bath containing gelatin being +53.4%, while that of the cyanide bath was 65.6%.

In our investigation of the properties of the brass coatings produced in an oxalate bath containing gelatin, we tested their porosity, chemical and corrosion resistance, brittleness, and the strength of their bond to the underlying metal.

We found that satisfactory plasticity and adequate strength of the bond between the coating and the underlying metal are ensured by the correct treatment of the surfaces of the parts to be plated and by immersing them in the bath under load. When this is done, the brassplating does not crack nor spall off from the surface of the underlying metal even after repeated bending of the plated steel plates.

Subjecting the coatings to the ferroxyl test indicated that the porosity of the deposits decreased as the thickness of the layer of brass increased.

When brass coatings containing 50-85% copper are immersed in a dilute (1:1) solution of hydrochloric acid, the zinc is dissolved out of the surface layer of these coatings, accompanied by the evolution of considerable hydrogen. The comparatively high rate at which the zinc is dissolved out of the surface of brass coatings in a hydrochloric acid solution is apparently due to some peculiarity of structure of these coatings, in contrast to those produced in cyanide solutions, inasmuch as no noticeable dezincing occurs in the coatings produced in the latter.

The electrochemical protective properties of the brass coatings were determined by measuring the potentials of the deposits upon a copper base in a molar solution of zinc sulfate, compared to those of pure zinc. Our measurements indicated that the potentials of coatings containing 50-59% copper was much more electronegative than the standard potential of iron, ranging from -0.694 to -0.572 volt. It is therefore quite feasible to provide electrochemical protection of steel parts against corrosion by means of these coatings. Corrosion tests of steel samples indicated that brassplatings 3-4 μ thick protect iron against corrosion satisfactorily, inasmuch as no signs of corrosion were observed when these samples were kept in a moist fresh-water atmosphere for 37 days.

SUMMARY

1. An investigation of the feasibility of brassplating in non-cyanide solutions has shown that copper and zinc are deposited jointly upon a cathode from an oxalate bath at a C.D. ranging from 0.1 to 0.3 amp/dm^2. The percentage of zinc in the deposits ranged from 66.6 to 71.5%. The copper zinc deposits could not be employed as brassplating, however.

2. Adding 0.05 to 0.10 g of gelatin to the oxalate bath per liter improves the electrocrystallization of the cathodically deposited metals, besides affecting the composition of the brass coatings. When 0.1 g of gelatin was added per liter of the bath, the percentage of copper in the cathode deposits rose from 29.8 to 63.4% at a C.D. of 0.2 amp/dm^2. The resultant brass coatings come out of the bath shining and can be used for electroplating.

3. The solution in an oxalate bath possesses the following advantages over a cyanide solution: it contains no poisonous substances and is quite stable when exposed to the air. The dispersibility of an oxalate bath is not much different from that of a cyanide bath, amounting to +53.4% at 16-18°. The dispersibility of a cyanide bath is +65.6% under these conditions.

4. The potential of the brass coatings produced in an oxalate bath and containing 50 to 59% copper are more highly electronegative than the standard potential of iron, ranging from -0.572 to -0.694 volt, depending upon the composition of the brass. These coatings may therefore be employed to protect iron against corrosion electrochemically.

5. An oxalate bath with added gelatin has been employed successfully to brassplate steel parts in order to bond them to rubber. This bath may also be used whenever steel parts must be protected against corrosion, in addition to being brassplated.

LITERATURE CITED

[1] N.A.Izgaryshev and P.S.Titov, J.Russ.Phys.Chem.Soc., 49, 573 (1917).

[2] V.I.Lainer, Bull. All-Union Society of Electrochemistry and Metallurgy, 3, 1, 58-72 (1937).

Received December 20, 1949.

THE EFFECT OF STRAIN UPON METAL CORROSION

E. M. Zaretsky

The problem of the effect of strain upon the corrosion behavior of metals is of extremely great practical significance. Semi-manufactured metal products undergo various kinds of strain in the course of processing, by pressure and cutting. Residual strain may also occur as the result of heat treatment of metal parts. Parts and built-up pieces are under load during operation and are constantly under elastic strain.

Nor is the development of a theory of the effect that strain has upon the corrosion behavior of metals of less practical importance.

The effect of strain upon the corrosion of metals is manifested in two ways. First, strain may change the weight index of corrosion. Second, the picture presented by the metal's failure may change, taking on a local nature, when tensile stresses act together with the corrosion factor [1,2]. Corrosion cracks come under the heading of this group of corrosion processes.

There has been practically no systematic research on the effect of strain upon the rate of corrosion. Isolated experimental findings indicate that strain accelerates metal corrosion as a rule [3]. Evans compared the strain of a metal with the compression of a spring and stated that one of the major causes of this functional relationship was the increase in the stored potential energy as the result of strain [4]. One can hardly accept this point of view.

As we know, the kinetics of corrosion processes are governed, in most instances, not by the stored potential energy, but by secondary processes, which are usually related to the formation and dissolution in an electrolyte of oxide films and to impurities in metals. Starting from the theory of microcells, we can relate the change in the corrosion behavior of metals caused by strain to the following factors.

1. The state of the oxide film on strained metals. Strain involves a rupture of the protective oxide film, thus changing the resistance to corrosion. With the passage of time the oxide film is regenerated to some extent over the exposed areas. In the general case, strained metals are covered with a less perfect oxide film, containing many pores and fissures and readily broken down by the action of the corroding medium.

The failure of the oxide film may turn inert portions of the surface, covered with a fairly thick oxide film, into anodes. A change of this sort may occur wherever the oxide film acted as a cathode. If corrosion is due principally to the predominance of an anodic restriction, the increase in the surface of the anodic regions results in a corresponding increase in the rate of corrosion. The presence of an cathodic restriction will tend to lower the rate of corrosion after strain, owing to the decrease in the surface of the cathodic regions.

2. Decrease in the ohmic resistance of the microcells. Strain involves a crushing of the crystallites. This causes an increase in the number of microcells, a decrease in the size of the microelectrodes, and a corresponding decrease in the ohmic resistance of the microcells.

3. The part played by microanodes and microcathodes in strain. The extent of deformation of the microelectrodes depends upon their plasticity, the distribution and quantitative proportions of the structural components, and the kind of strain involved. Two boundary cases may be cited. Whenever the solid inclusions are distributed throughout a soft continuous phase, it is the continuous constituent that will be chiefly deformed. But if the inclusions are plastic enough, both constituents may be deformed. The regions at the boundaries of the crystalline grains will be less deformed than the interiors. This may result in the formation of new microcells.

4. Microfissures are formed during the process of strain before the metal fails; this increases the surface area of the parts in contact with the corroding medium, and corrosion is increased.

5. The breakdown of a supersaturated solid solution is accelerated by strain. The formation of a new phase gives rise to additional microcells, and the rate of corrosion rises accordingly. The fact that the breakdown occurs chiefly at the crystallite boundaries may promote a tendency toward intercrystallite corrosion [5].

This brief summary of the major factors in the corrosion behavior of deformed metals testifies to its great complexity and the close interlacing of the many variables linking strain to corrosion processes.

EXPERIMENTAL

In this portion of our research we made a study of the effect of residual tensile strain upon the rate of corrosion of the magnesium alloys MA-1, MA-8, and MA-3, zinc, aluminum, copper, and iron.

The chemical composition of these

Material	Chemical Composition per cent															
	Al	Zn	Ce	Mn	S	C	Cr	Si	Ni	Cu	Fe	As	Sb	Bi	Pb	Cd
MA-1	0.15	0.96	0.35	1.68		0.10	Traces	0.16	0.17	0.03	Not found	found	0.02		Not found	0.04
MA-8	5.62		-	1.67	0.15				0.15	Not found	0.03	0.04				
MA-3				0.33					0.09		0.18					
10-20 steel, 1 mm thick				0.32				0.20		<0.05						
Copper, 3 mm thick				<0.20												
Zinc, 3 mm thick																
Aluminum, 2 mm thick																

metals is given in the subjoined table.

All the metals tested were in the rolled state. Corrosion was determined by the loss of weight and of ultimate strength.

In the second stage of our research we examined the effect of strain upon the metal potentials and upon the operation of a model microcell made up of magnesium alloys.

The corrosion tests were made on samples used for testing tensile strength, prepared in the F form (Fig. 1) [6]. The surface of the samples was degreased and pickled in the magnesium alloys, degreasing was followed by removing the artificial oxide film in a chromic anhydride solution. The test pieces were kept in a desiccator above calcined calcium chloride for 20 to 24 hours after being pickled, as well as after being strained.

In the corrosion tests the active surface of the test pieces was 12 sq. cm. The ends of the test pieces and the areas not under stress were protected by a coat of AK-20 cement. When we determined the effect of strain upon total corrosion, all the test pieces made of the same metal were placed in the same solution at one time. At least five test pieces were tested for each value of strain. The volume of electrolyte was 20 liters, and the temperature was 25° C. In order to keep the pH constant, the neutral solutions were buffered with a mixture of 0.01 molar NaH_2PO_4 + 0.05 molar NaOH. The solution pH was 6.8. Unless otherwise stated, the tests lasted 24 hours. Corrosion tests of the magnesium samples were also run for two years in the open air.

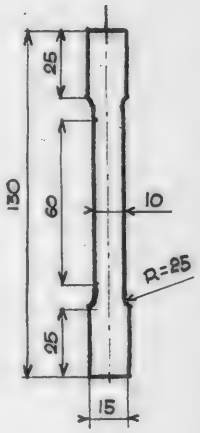

Fig. 1. Test piece for tensile test, prepared in the F form.

Only the loss of weight is given for some tests, owing to the lack of any precise behavior pattern in the change of the ultimate strength after corrosion for various degrees of strain. The preparation of the surface is described in the respective sections of this paper for each metal.

Corrosion Tests

Magnesium alloys. Test pieces 1 mm thick, degreased in a standard triphosphate solution [7], were plunged into a 20% solution of chromic anhydride, heated to 60°, to remove the artificial oxide film. After 3 hours of annealing at 420°, the test pieces were pickled for 0.5 to 1 minute in a 10% nitric acid solution, then strained and weighed.

After the test, the corrosion products were removed in the same chromic anhydride solution. The results of the tests are shown by the curves in Figs. 2, 3, 4, 5, 6, and 7.

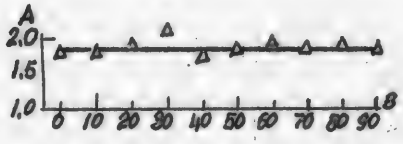

Fig. 2. Effect of strain on the corrosion of the alloy MA-1 in a 0.1-molar NaCl solution.

A-Loss of weight, grams/dm^2; B-load, % of σ_B.

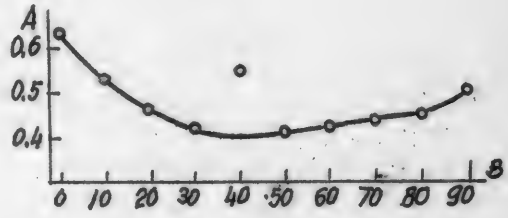

Fig. 3. Corrosion of the alloy MA-1 under atmospheric conditions.

A-Loss of weight, grams/dm^2; B-load, % of σ_B.

Fig. 4. Corrosion of the alloy MA-3 in 0.1-molar NaCl.

A-Loss of weight, grams/dm^2; B-load, % of σ_B; C-σ-$\sigma^1/\sigma \cdot 100$. 1) loss of weight; 2) σ-$\sigma^1/\sigma \cdot 100$.

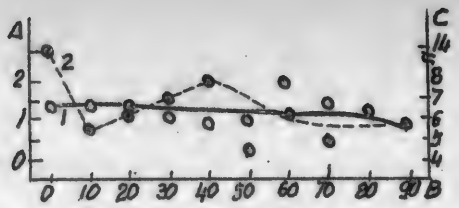

Fig. 5. Corrosion of the alloy MA-3 under atmospheric conditions.

A-Loss of weight, grams/dm^2; B-load, % of σ_B; C-σ-$\sigma^1/\sigma \cdot 100$. 1) loss of weight; 2) σ-$\sigma^1/\sigma \cdot 100$.

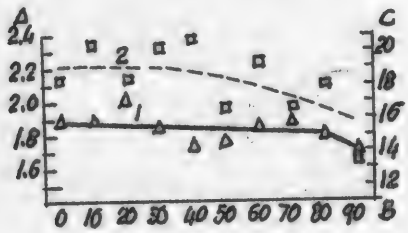

Fig. 6. Corrosion of the alloy MA-8 in 0.1 molar NaCl.

A-Loss of weight, grams/dm^2; B-load, % of σ_B; C-σ-$\sigma^1/\sigma \cdot 100$. 1) loss of weight; 2) σ-$\sigma^1/\sigma \cdot 100$.

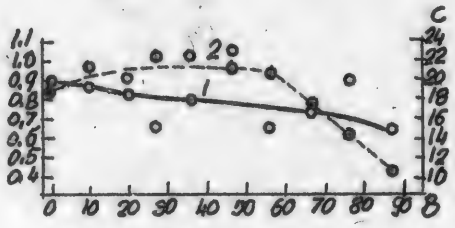

Fig. 7. Corrosion of the alloy MA-8 under atmospheric conditions.

A-Loss of weight, grams/dm^2; B-load, % of σ_B; C-σ-$\sigma^1/\sigma \cdot 100$. 1) loss of weight; 2) σ-$\sigma^1/\sigma \cdot 100$.

The residual tensile strain has no noticeable effect upon the rate of corrosion of the alloy MA-1 in a solution of 0.1-molar NaCl. In the atmospheric test the corrosion rate drops and then rises as the strain is increased (Fig. 3).

The corrosion of the alloy MA-3 in a 0.1-molar solution of NaCl (Fig. 4) increases slightly as the strain is increased up to 80% of σ_B (ultimate strength). At a strain that is 90% of σ_B the corrosion rate is practically the same as that for unstrained test pieces. The variation of the corrosion rate throughout the strain range does not exceed a few per cent.

In the atmospheric test (Fig. 5) the loss of ultimate strength of the alloy MA-3 as the strain is increased rises slightly at first and then drops off. The rate of corrosion at maximum strain is 9% below that in the unstrained state. The corrosion, measured by the loss of weight, drops off slightly with increasing strain.

The corrosion resistance of the alloy MA-8 in a 0.1-molar solution of NaCl rises slightly with increasing strain (Fig. 6). The loss-of-weight curve follows a similar course under atmospheric conditions, as is seen in Fig. 7. The discrepancy between the shape of the loss-of-weight and ultimate-strength curves is attributable to the local nature of the corrosion.

Thus, the residual strain of the tested magnesium alloys has no effect upon their corrosion resistance to a 0.1-molar NaCl solution and to atmospheric conditions or else increases the resistance somewhat. The high anti-corrosion properties of the magnesium alloys tested are worthy of note. After two years of exposure to the open air of an industrial region without any protective coatings, the decrease in the ultimate strength of sheets about 1 mm thick did not exceed 20% for the alloy MA-3, 15% for the alloy MA-8, and 5% for the alloy MA-1.

The effect of strain upon the corrosion resistance of magnesium alloys depends largely upon the nature and extent of the strain, as well as upon the corrosion medium. Bobnovnikov [8] found that reducing the rolling temperature increased the resistance of magnesium alloys to corrosion in a 3% NaCl solution a and in sea-water spray. He adds that the resistance of rolled magnesium to corrosion solutions of sodium chloride and hydrochloric acid does not depend upon the extent of cold working [9]. The same conclusion was reached after tests of the MA-3 alloy, tensile strained, in distilled water [10]. According to other findings, however, rolling lowers the resistance of magnesium to corrosion in a solution of hydrochloric acid [11]. On the other hand, the cold working due to scraping increased the resistance of a Mg-Mn alloy to corrosion in sea water perceptibly [12]. The following tests bear out the conclusion that the nature of the strain and of the corrosion medium affects corrosion resistance in the strained state.

Test pieces cut from sheets of magnesium and from the alloys MA-1 and MA-3 were pickled in nitric acid, polished with No. 00 emery paper, degreased with acetone, and immersed in a 0.1-molar NaCl solution. It was found that polishing increased the corrosion resistance of magnesium and of the MA-1 alloy, while it accelerated the corrosion of the MA-3 alloy. Distilled-water tests indicated a smaller loss of weight for magnesium and for the MA-3 alloy in this state than when unpolished. It may be assumed that the contrary results obtained in various investigations were caused by differences in the initial test conditions, especially in the extent and nature of the strain of the magnesium alloys.

The effect of strain upon the corrosion of magnesium alloys is related to changes in the ratio of the anodic and cathodic restrictions. If we assume that the corrosion of magnesium alloys is due to the predominance of cathodic restriction [13], strain increases the area of the anodic regions at the expense of the surface of the cathodic regions as it breaks the oxide film. The oxide film is rapidly restored on the MA-1 alloy, apparently, which is why the rate of corrosion in 0.1-molar NaCl does not vary with the strain. The appearance of a minimum or a maximum on the corrosion-strain curve for the atmospheric test is probably due to the protective properties of the corrosion products formed on the strained surface.

Aluminum

The aluminum test pieces were annealed for 40 minutes in molten saltpeter at 450° and air cooled; then they were pickled for 1 minute at 60° in 5% NaOH and processed in concentrated nitric acid. The corrosion products were removed by immersing the pieces for 5 minutes in a hot solution containing 35 ml of phosphoric acid and 20 g of chromic anhydride per liter.

The corrosion tests were made in two solutions: 0.3-molar HCl and 0.5-molar NaCl. In the first solution the aluminum corrodes, with the evolution of gaseous hydrogen for the most part. In the second solution, for the most part processes involving oxygen depolarization take place at the cathodic regions of the aluminum's surface. The test in the sodium chloride solution lasted 120 days.

The shape of the curve reproduced in Fig. 8 indicates that the rate of aluminum corrosion increases as the load is raised from 25% of σ_B. Any further increase in strain has practically no effect upon the corrosion rate. In the 0.5-molar NaCl (Fig.9), the aluminum corrosion rate does not change as the load is raised up to 70% of σ_B. Corrosion rises at a load that is 90% of σ_B. It is not impossible that it is here that the oxide film is ruptured and corrosion begins to be accompanied by the evolution of gaseous hydrogen. The acceleration of aluminum corrosion as the result of strain has been observed in other investigations, performed in solutions of nitric, sulfuric, and hydrochloric acids,

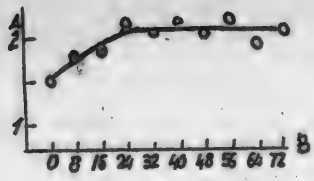

Fig. 8. The effect of strain upon the corrosion of aluminum in 0.3-molar HCl.

A-Loss of weight, grams/dm^2; B-load, % of σ_B.

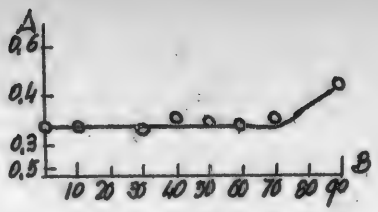

Fig. 9. The corrosion of aluminum in 0.5-molar NaCl.

A-Loss of weight, grams/dm^2; B-load, % of σ_B.

sodium hydroxide, cupric chloride, and sodium chloride [14, 11, 15].

Zinc

The zinc samples were annealed at 150° for two hours and then pickled in 10% nitric acid for 1-2 minutes. A 0.0125-molar solution of sulfuric acid served as the electrolyte. The solution pH was 2.3. The corrosion products were removed in a saturated solution of ammonium acetate.

As is seen in Fig. 10, despite the considerable scattering of the experimental values, the zinc corrosion rate does not rise with increasing strain. As in the case of aluminum, this may be attributed to an increase in the surface of the anodic regions due to strain. The less plastic cathode regions, chiefly the $FeZn_7$ compounds, and are not deformed, so that their effectiveness is not diminished.

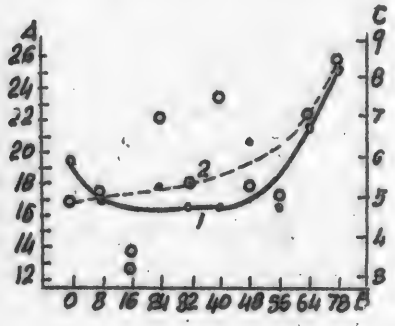

Fig. 10. Effect of strain upon the corrosion of zinc in 0.0125-molar H_2SO_4.

A-Value of σ-σ'/σ; B-load, % of σ_B; C-loss of weight, grams/dm^2. 1)loss of ultimate strength; 2) loss of weight, grams/dm^2.

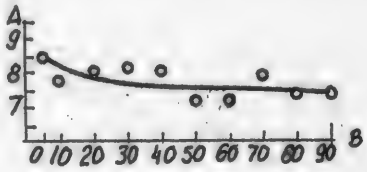

Fig. 11. Effect of strain upon the corrosion of copper in 0.1-molar $(NH_4)_2S_2O_8$.

A-Loss of weight, grams/dm^2; B-load, % of σ_B.

Copper

The copper test pieces were annealed at 750° for two hours, allowed to cool in the furnace, and pickled in 10% nitric acid for 5-8 minutes until their surfaces were bright. Two solutions were employed as corrosion media: 0.1-molar $(NH_4)_2S_2O_8$ and 0.005 molar H_2SO_4. We know that copper does not drive hydrogen out of acid solutions. In these solutions the corrosion of copper is limited by the access of oxygen to the cathodic regions. In the presence of an oxidizing agent, such as ammonium persulfate, corrosion will be governed by a double control, the rate of corrosion then reflecting the changes in the surfaces of both the anodic and the cathodic regions.

The solution was buffered by a mixture that contained 0.01 mol of H_3PO_4 and 0.0033 NaH_2PO_4. The pH of the solution was 2, as measured with a glass electrode. The results of these tests, represented by the curve in Fig. 11, show that the rate of corrosion of copper drops as the strain is increased, as has been reported previously [14]. Since copper has a comparatively high potential, the traces of other metals present in the copper will not act as cathodes; apparently the cathodic processes take place in the regions covered with an oxide film. When the oxidizing agent is present in excess and the cathodic control predominates, any rupturing of the oxide film due to strain diminishes the surface area of the cathode regions and thus lowers the rate of corrosion.

In the 0.005-molar solution of H_2SO_4, the rate of corrosion is limited by the access of oxygen to the cathode regions. As might have been expected, strain does not affect the rate of corrosion of copper (Fig. 12).

Steel

Test pieces of 10-20 low-carbon steel were anealed at 850° for two hours and then allowed to cool in the furnace. Not all the scale was removed by pickling in sulfuric acid. We therefore milled the test pieces after they had been annealed, degreased them in a standard triphosphate solution [7], and pickled them slightly in a 10% sulfuric acid solution. After the tests were over the corrosion products were removed in a 10% sulfuric acid solution to which 0.2% of stannous chloride had been added. The tests were run in a 1.5-molar solution of sulfuric

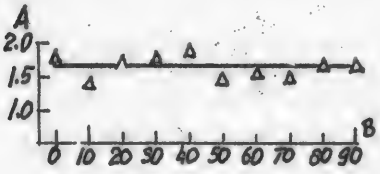

Fig. 12. Corrosion of copper in 0.005-molar H_2SO_4.

A-Loss in weight, grams/dm^2; B-load, % of σ_B.

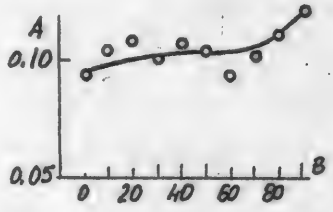

Fig. 13. Effect of strain upon the corrosion of steel in 1.5-molar H_2SO_4.

A-Loss in weight, grams/dm^2; B-load, % of σ_B.

acid. As we see in Fig. 13, the rate of corrosion of steel rises with increasing strain. The acceleration of corrosion is more apparent in the load range of 70-90% of σ_B than at smaller strains. In the corrosion of low-carbon steel, with the evolution of hydrogen, it is chiefly the solid particles of cementite, which are only slightly strained, that are the cathode regions. Deformation of the solid solution of carbon increases the effective area of the anode and thus raises the rate of corroison.

SUMMARY

1. The factors linking strain to the corrosion behavior of metals have been considered.

2. It has been found that residual tensile strain has practically no effect upon the rate of corrosion of the magnesium alloy MA-1 in a 0.1-molar solution of NaCl throughout the range from 0 to 90% of ultimate strength. In the open air, the rate of corrosion of the alloy MA-1 drops somewhat at first as the strain is increased, and then rises, without ever reaching its initial value.

3. The rate of corrosion of the alloy MA-3 in a 0.1-molar solution of NaCl rises slightly as the strain is increased and then drops off. In the open air,

the rate of corrosion is somewhat lower at maximum strain than in the unstrained state.

4. The rate of corrosion of the alloy MA-8 in 0.1-molar NaCl drops somewhat as the strain is increased. Its pattern of behavior is the same in the open air.

5. The rate of corrosion of aluminum rises with increasing strain in solutions of 0.5-molar NaCl and 0.3-molar HCl.

6. The corrosion of zinc in a 0.0125-molar solution of H_2SO_4 rises with increasing strain.

7. In a 0.1-molar solution of $(NH_4)_2S_2O_8$ the rate of corrosion of copper drops somewhat with increasing strain. Strain has practically no effect upon the corrosion of copper in a 0.005-molar solution of H_2SO_4.

8. The rate of corrosion of 10-20 steel in a 1.5-molar solution of H_2SO_4 rises with increasing strain.

LITERATURE CITED

[1] E.M.Zaretsky, Proc. Acad.Sci. USSR, 58, 4, 607 (1947).

[2] E.M.Zaretsky, J.Appl.Chem., 9, 823 (1947).

[3] G.V.Akimov. Theory and Research Methods of Metal Corrosion, p. 175. USSR Acad. Sci. Press, (1945).

[4] U.R.Evans, Metallic Corrosion, Passivity, and Protection (Trans. from the English), p. 587 (1941).

[5] S.E.Pavlov. The Corrosion of Clad Duraluminum. (1940).

[6] Standard Methods of Testing Materials. Pub. by the All-Union Institute of Corrosion Protection (VIAM).

[7] Handbook of Instructions of the All-Union Institute of Corrosion Protection. State Defense Press (1942).

[8] N.N.Bobovnikov, Trans. All-Union Institute of Corrosion Protection, 31, 1935.

[9] L.Witby, Trans. Faraday Soc., 29, 11, 15 (1933).

[10] L.Graf, Luftwiss, 5, 160 (1940).

[11] G.Tamman and F.Neubert, Z. anorg. Chem., 207, 87 (1940).

[12] O. Kornke and G.Masing. Die korrosion v. Nichteisenmetallen u. deren Legierungen, Leipzig, 2, 447 (1938).

[13] G.B.Clark and G.V.Akimov, Trans. 2nd Conference on Metallic Corrosion, 2. USSR Acad. Sci. Press (1940).

[14] J.Gochralski and E.Schmidt, Z. Metallkunde, I, (1928).

[15] V.O.Krenig, Information Handbook, All-Union Institute of Corrosion Protection. 15, 3 (1938).

Received August 6, 1949.

THE COPOLYMERIZATION OF VINYL ACETATE WITH MALEIC ANHYDRIDE AND THE PROPERTIES OF THE RESULTANT COPOLYMERS*

S. N. Ushakov, S. P. Mitsengendler and V. A. Chekhovskaya

Chair of Plastics, Leningrad Institute of Technology

The data in the literature on the behavior of maleic anhydride in copolymerization with other monomers are contradictory.

The earlier papers, prior to 1930, state that maleic anhydride by itself cannot be polymerized, but that it readily enters into a compound with many unsaturated compounds, such as stilbene and other ethylene derivatives [1].

Similar behavior of maleic anhydride and of its esters in the copolymerization of these monomers with styrene is described in the literature [2,3].

The percentage of maleic anhydride in the copolymer does not exceed 50% no matter what the excess of the anhydride in the original mixture.

The findings of Alfrey and Levine [2] on the copolymerization of maleic anhydride with styrene in the presence of air are given in Table 1. Their results lead these authors to believe that maleic anhydride and its esters are not polymerized themselves. The polymer radical, which is terminated by a maleic component (M·), cannot add its own monomer (M), so that in these systems the macromolecule chain does not grow as $-M-M(K_{M \cdot M} = 0)$; this is why the systems they investigated had the single constant $\alpha = 1/\sigma = 24$, computed from the constitutional equation [4] for the case when one of the constants is zero:

TABLE 1

Experimental Data on the Copolymerization of Styrene with Maleic Anhydride [2]

Molar per cent maleic anhydride		Copolymer yield (%)	$\alpha = \frac{1}{\sigma}$
In original mixture	In copolymer		
5.0	38.9	2.9	37.5
5.0	34.3	1.9	22.2
9.1	42.4	1.7	28.8
16.7	45.0	1.9	23.0
50.0	48.9	–	21.7
95	49.9	2.8	11.5

The mean value of $\alpha = 1/\sigma = 24 \pm 5$, $\mu = \beta = 0$.

$$\mu = \beta = \frac{K_{M \cdot M}}{K_{M \cdot S}} = 0; \qquad \frac{1}{\alpha} = \sigma = \frac{K_{S \cdot S}}{K_{S \cdot M}} = 0.041.$$

Another paper on the copolymerization of maleic anhydride with allyl acetate cites results that are just the opposite of those mentioned above [5]. An investigation of this latter system indicated that maleic anhydride can be polymerized itself when no air is present.** The inhibiting action of the air is less prominent

*Report V of a series on the copolymerization of complex vinyl esterd with maleates.

**29 Molecules of maleic anhydride was polymerized for every decomposed molecule of benzoyl peroxide.

when the anhydride is copolymerized with allyl acetate, the percentage of the anhydride in the copolymer even exceeding 50% when there is an excess of it present in the original mixture.

We have observed similar behavior of maleic anhydride in its copolymerization with vinyl acetate. Investigation of this pair of monomers indicates that maleic anhydride is an even more active constituent when paired with vinyl acetate than in the presence of allyl acetate.

As the active constituent, it predominates in the initial copolymers even when there is an excess of vinyl acetate in the original mixture (Tests 1 and 5, Table 2). When there is an excess of maleic anhydride in the original mixture, its percentage of the copolymer exceeds 60% (in the presence of air, which inhibits the formation of the -M-M- bond, as has been said) (Tests 9, 10, and 11, Table 2).

TABLE 2

Copolymerization of Vinyl and Maleic Anhydride at 65° C in the Presence of Benzoyl Peroxide

Test No.	Molar ratio of constituents VA/MA	Reaction time, hours	Peroxide (%)	Reaction temperature, °C	Molar percentage of maleic anhydride		M'/M_0 ratio	Copolymer as % by weight of original mixture	Medium
					In original mixture M_0	In copolymer (M')			
1	10	15.0	0.1	65	9.0	51.6	5.7	10.0	Benzene
2	10	3.0	0.5	65	9.0	45.6	5.0	20.9	Benzene
3	10	12.0	0.2	65	9.0	45.5	5.0	19.0	Acetone
4	10	12.0	0.2	78	9.0	9.4	1.0	85.0	
5	2	1.0	0.5	65	33.0	52.1	1.6	48.0	Benzene
6	2	18.0	0.2	65	33.0	45.0	1.5	75.0	
7	2	14.0	0.5	56	33.0	45.0	1.5	70.0	
8	1	12.0	0.5	65	50.0	49.7	0.99	44.0	Acetone
9	0.3	4.5	0.1	65	75.0	52.8	0.70	25.6	Acetone
10	0.1	7.0	2.0	65	90.9	61.4	0.67	22.4	
11	0.1	9.5	1.0	90	90.9	61.5	0.67	-	

Thus the experimental data show that the growth of the macromolecule in the copolymerization of maleic anhydride with the active monomer styrene is due to three elementary reactions that give rise to the bonds S-S, S-M, and M-S, inasmuch as the proportion of reactions involving the formation of a -M-M- bond is practically zero.

When maleic anhydride is copolymerized with such inactive monomers as allyl acetate and vinyl acetate, however, the macromolecule's growth is due to four elementary reactions: V-V, V-M, M-V, and M-M, for the equilibrium constant of the addition reaction of maleic anhydride (M) to "its own" radical ($M^{\cdot}$) is not zero ($K_{M^{\cdot}M} \neq 0$). These systems are therefore characterized by two constants, μ and σ.

In the case of maleates, the addition of the maleic constituent to a similar radical takes place when vinyl acetate and styrene are present. But comparison of the constants for these systems indicates that $\mu = K_{M^{\cdot}M}/K_{M^{\cdot}S}$ is much lower for the more active monomer styrene than it is for the inactive vinyl acetate (Table 3).

TABLE 3

Activities of the Monomers Styrene and Vinyl Acetate in Copolymerization with Maleates [2]

Monomer M_1	g_1 (σ)	Monomer M_2	g_2 (μ)
Styrene	0.30 ± 0.02	Diethyl fumarate	0.070 ± 0.007
Styrene	6.52 ± 0.5	Diethyl maleate	< 0.01
Vinyl acetate	0.011 ± 0.001	Diethyl fumarate	0.044 ± 0.003
Vinyl acetate	0.17 ± 0.01	Diethyl maleate	0.043 ± 0.005

Copolymerization of maleic anhydride with vinyl acetate. The reaction of maleic anhydride with vinyl acetate is much more vigorous than that of its acid ester. The reaction takes place with explosive rapidity at 65° C when even a slight excess of vinyl acetate is present.* The reaction must therefore be carried out with a diluent (benzene, acetone).

A study of this reaction has shown that maleic anhydride exhibits the same behavior pattern as a maleate, their behavior conforming fully with the contemporary theory of copolymerization [7,8,9].

Like its acid ester, maleic anhydride behaves as the more active constituent: the percentage of maleic anhydride predominates in the initial copolymer (provided the transformation is not far-reaching) even when there is a tenfold excess of the vinyl acetate in the original mixture. As a result, the initial mixture is progressively enriched with the vinyl acetate, so that as the percentage of polymerization increases the copolymer begins to contain a higher percentage of this latter constituent. At 80-85% conversion, for instance, the average composition of the copolymer is nearly the same as that of the original mixture (Tests 1, 2, 3, and 4, Table 2). The activity of the maleic anhydride decreases as the percentage of vinyl acetate in the original mixture drops (the concentration of the V· radicals decreases), and the consumption of the two constituents becomes more nearly even (Tests 5, 6, and 7, Table 2). When the maleic anhydride is present in excess in the original mixture, polymerization is slow until all the vinyl acetate has been used up, after which it comes to a stop, even when a large excess of benzoyl peroxide is present and heating is continued for a long time. The yield of the copolymer is 22-26% of the original mixture (or 240% of the original vinyl acetate).

What is noteworthy and basically new in the behavior of maleic anhydride and of its acid ester when they are copolymerized with vinyl esters is, as we have mentioned above, that maleic anhydride and its derivatives can polymerize with themselves as -M-M-M when such inactive constituents and vinyl and allyl acetates are present.

All the initial copolymers thus contain more than 50% of maleic anhydride. Only at higher conversion, when all the maleic anhydride has been used up, and practically only the vinyl acetate is being polymerized, does the percentage of the latter begin to predominate in the copolymer (Tests 2, 3, and 4, in Table 2). When the initial mixture contained an excess of maleic anhydride, the copolymers we secured contained more than 60% of maleic anhydride.

The structure of a copolymer containing an excess of the anhydride may be represented schematically as follows: -V-M-M-V-M-V-M-M-M-V-M-V-M-M-.

The enrichment of the copolymer with maleic anhydride (M'/M_0) is shown in the figure as a function of the composition of the original mixture. The consumption of the active constituent (M) is extremely high with a tenfold excess of vinyl acetate and low conversion (10%). But as the concentration of maleic

*The value of $\sigma < 0.02$ [8], for maleic anhydride, while $\sigma = 0.0345$ [7], for its acid ester.

anhydride in the original mixture rises (the percentage of the V· radicals drops), the consumption of the two components levels off. When the original mixture contains an excess of maleic anhydride, the copolymer contains less of this constituent ($M'/M_0 < 1$), as follows from the copolymerization equations.

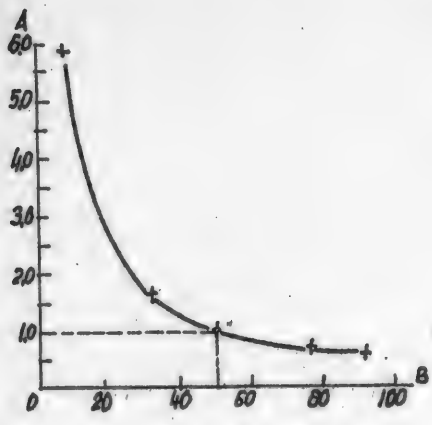

Effect of the composition of the original mixture upon the composition of the copolymer.

A-Ratio of the molar percentages of maleic anhydride in the copolymer and in the original mixture (M'/M_0); B-molar percentage of maleic anhydride in the original mixture M_0.

As the figure indicates, the azeotropic mixture in this system is located at a point close to the equimolar ratio of the constituents. Change in temperature has practically no effect upon the composition of the copolymer (cf Tests 6 and 7, 10 and 11, Table 2).

Properties of the copolymers produced. The copolymers of vinyl acetate and maleic anhydride are insoluble in benzene, gasoline, or ether, but they are readily soluble in water, in contrast to the copolymers of vinyl acetate and monomethyl maleate. Water readily saponifies the acetate groups in the macromolecule, evolving free acetic acid and forming a copolymer of the "Povimal" type. The data of the analysis of the copolymers indicate that saponification is paralleled by a reaction between the COOH and OH groups that are formed, yielding polylactones * as follows:

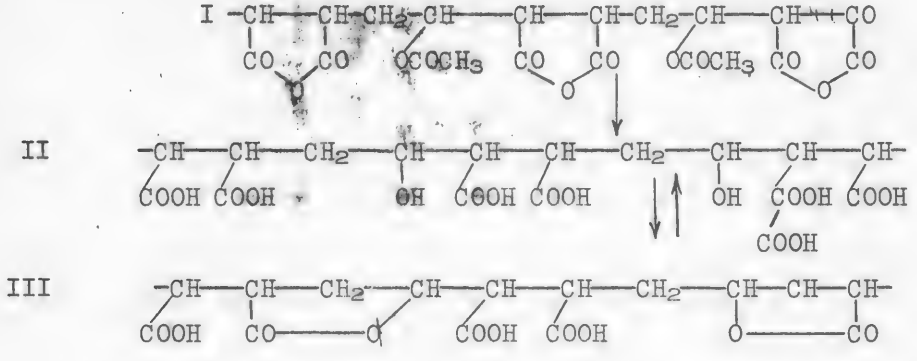

An analysis of the copolymer of vinyl acetate and maleic anhydride after its saponification with water is given in Table 4. We note that saponification of 53.9 links of maleic anhydride in the copolymer yielded 46.8 links of maleic acid with free COOH groups and 7.1 links with COOH groups combined into lactones (after saponification with an alkali); of 46.1 links of vinyl acetate, 29.5 were saponified, 22.4 links being found as vinyl alcohol with a free OH group and 7.1 links being combined into lactones with the 7.1 links of maleic acid.**

SUMMARY

1. The copolymerization of vinyl acetate and maleic anhydride exhibits the same behavior patterns as the copolymerization of the former with monomethyl maleate, which are in accordance with the contemporary theory of copolymerization.

2. Maleic anhydride, like its ester, can combine with itself in the presence

---

* As we know, γ-hydroxy acids readily form lactones in aqueous solutions.

** The number of COOH groups was determined by potentiometric titration.

TABLE 4

Analysis of the Saponified Copolymer. Composition Before Saponification: 53.9% Maleic Anhydride; 46.1% Vinyl Acetate

Name of link	Molar %	Total acid and alcohol content, moles	Total vinylic derivatives
Free maleic acid	46.8	53.9 (acid)	
Combined maleic acid ...	7.1		
Vinyl acetate	16.6		
Vinyl alcohol	22.4	29.5 (alcohol)	46.1
Combined vinyl alcohol .	7.1		
	100.0	100.0	

of vinylic esters, yielding copolymers containing more than 50% of the maleic constituent.

3. The resultant copolymers are readily saponified by water, yielding high-molecular compounds with side rings and chains (lactones).

LITERATURE CITED

[1] Wagner-Yaurig, Ber., 63, 3213 (1930).

[2] F.Alfrey and E.Lavin, J.Am.Chem.Soc., 67, 11, 2044 (1945).

[3] F.Alfrey, E.Merz, H.Mark, J.Polymer Res., 1, 37 (1946).

[4] F.Lewis and F.Mayo, J.Am.Chem.Soc., 66, 9, 1594 (1944).

[5] Bartlett and Nozaki, J.Am.Chem.Soc., 68, 1495 (1946).

[6] F.Mayo, F.Lewis, and C. Walling, J.Am.Chem.Soc., 70, 4, 1529, 1533 (1948).

[7] S.N.Ushakov, S.P.Mitsengendler, and B.M.Polyatskina, J.Appl.Chem. 23, 5, 512 (1950).*

[8] S.N.Ushakov, S.P.Mitsengendler, and B.M.Polyatskina, J.Appl. Chem. 23, 5, 521 (1950).**

[9] S.N.Ushakov, S.P.Mitsengendler, and G.A.Shtraikhman, Prog. Chem., 1950, 3, 267.

June 29, 1950.

---

*See CB translation p. 535 ff.

**See CB translation p. 545 ff.

THE AGING OF TRIACETATE FILMS

A. A. Freiman

Laboratory of the Technology of Motion-Picture Film Bases,
Leningrad Institute of Motion-Picture Engineers

The literature sheds no light on the problems involved in the aging of films made of cellulose triacetate.

Considerable research has been done up to the present time on the analogous aging process of films made of celulose nitrate and acetone-soluble acetylcellulose. Research papers by Prof. Kozlov and his associates [1,2,3,4], Drinberg [5], Goldman [6], Karfunkel and Fedorov [7], and others have dealt with these problems. Summarizing considerable experimental and reference data on the aging of films, Kozlov [8] views this process as the result of a change in the properties of films with time, governed by the following factors: 1) physical processes, i.e., evaporation of the volatile constituents of the films; 2) structural changes, i.e, relaxation phenomena that take place in anisotropic and plane-oriented films, particularly at high temperature and moisture content; and 3) chemical processes, i.e., the phenomena involved in the decomposition of the cellulose esters that do not possess sufficient chemical stability, and in the oxidative-reduction processes due to atmospheric oxygen or to impurities in the films. External factors: rise in temperature, moisture content of the surrounding air, ultraviolet light, etc., affect these processes greatly.

These processes result in the progressive destruction of the cellulose ester in the film, the extent of this destruction determining the changes in the mechanical and other properties of the film (increased brittleness, yellowing, cloudiness).

The clouding over of the film is an internal layering phenomenon, due to a loss in the compatibility of the cellulose ester with the plasticizers and other solvents, i.e., it signifies that the film has been transformed into a colloidal system. When this occurs, further aging of the film may occur spontaneously, owing to the thermodynamic instability of colloidal systems.

Thus, in the colloid-chemistry sense of the term, films may be said to "age" only when external factors turn the films into colloidal systems. In all other cases, the term "aging" of film must be taken to mean a complex of changes in the properties of film with time, caused by the various factors mentioned above.

The present research had as its objective an investigation of the properties of triacetate film caused by a rise in temperature. Cellulose triacetate is widely used at the present time as a film-forming substance for the manufacture of electric-insulation films, a base for motion-picture film, an organic glass, and other purposes, so that the question of its stability is of considerable interest.

EXPERIMENTAL

To obtain a general picture of the process of artificial aging, we ran tests with commercial samples of film. We then went somewhat more deeply into the subject to ascertain the part played by plasticizers; samples of film were prepared in the laboratory for this purpose. These films were produced in laboratory casting apparatus, on glass, from solutions of the following composition: 22 parts by weight of plasticizer and 865 parts by weight of the solvent mixture, consisting of a 9:1 mixture of methylene chloride and methanol, to 100 parts by weight of the cellulose triacetate.

The general description of the samples of commercial film tested is given in Table 1.

TABLE 1

Characteristics of Samples of Commercial Films

Film sample No.	% of combined acetic acid in acetylcellulose	Plasticizer	Film thickness, mm
1	62.1	Triphenyl phosphate	0.09
2	61.8	Methylenecyclohexyl stearate...	0.07
3	61.8	Ditto	0.03
4	61.8	None	0.05

We investigated the following changes in the properties of the films during artificial aging: loss of weight, viscosity of solutions, vapor penetration, and mechanical properties.

Research method. The films were exposed to a temperature of 160° C, all the samples being hung in a thermostat. In addition, one of the film samples, No. 4, which contained no plasticizer, was exposed to high temperature in a sealed glass tube from which the air had been exhausted to protect it against the influence of air.

The loss of weight of all the samples was determined by weighing them.

The viscosity of solutions of the films was determined in an Ostwald viscosimeter; the film solutions were 0.2% solutions in methylene chloride. The specific gravities of these solutions (at 20° C) were determined in a 10-cc pyknometer for the viscosity calculations. The methylene chloride used was the fraction with a specific gravity of 1.3138, boiling at 40-42° C.

The mechanical properties were measured on a dynamometer.

The vapor penetration was determined as follows, for water vapor: a standard amount of phosphoric anhydride was placed in a brass cup witha screwed-on ring, the top of the cup being closed by a cover of standard size, cut out of the film to be tested, which was pressed tightly on the cup by the hermetically-sealing ring. The cup was placed in a desiccator at room temperature with a saturated solution of ammonium chloride and kept there until it reached constant weight in moist air.

Evaluation of Results

The results of our determinations of the films's loss of weight when exposed to air at 160°C are given by the curves in Fig. 1.

We see from these curves that the maximum loss of weight was suffered by Sample 1, containing triphenyl phosphate, which is attributable to the fact that triphenyl phosphate is more volatile than methylcyclohexyl stearate. None of the films lost any more weight after the volatile components had been driven off, as is shown by the curves in Fig. 1.

The viscosity of solutions of the films is a highly characteristic indication of the changes in their properties. The data on the change in viscosity during aging are shown by the curves in Fig. 2.

Inspection of these curves indicates that the viscosity of solutions of these films drops considerably when they are aged in air at 160°C. The drop in viscosity is greatest when they are aged for 100 hours or more. After exposure to high temperature for 600 hours the viscosity had dropped to 60-75% of its initial value.

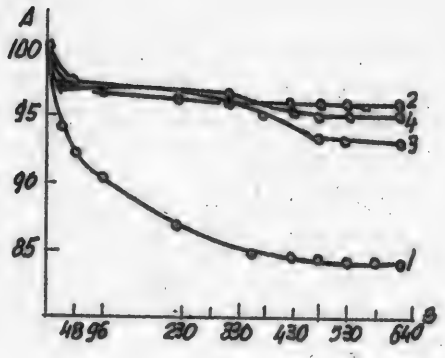

Fig. 1. Loss of weight of various film samples at 160° C, with air admitted during the aging process.

A-Loss of weight,%; B-aging time, hours. 1,2,3,4 - film sample numbers.

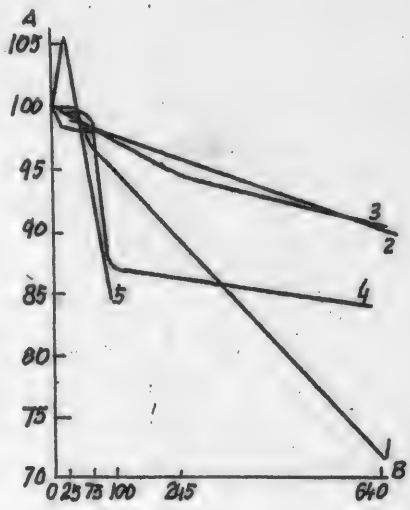

Fig. 2. Change in the viscosity of 0.2% solutions of films in methylene chloride at 160° C with air admitted during the aging process.

A-Viscosity,%; B-aging time, hours. 1,2,3,4-film sample numbers; 5-sample in sealed tube.

The drop in viscosity is especially pronounced in the film sample exposed to high temperature in sealed glass tubes, (Curve 5). In this sample, the viscosity rose slightly during the first 25 hours of heating, probably owing to the volatile components being driven off, but after that the viscosity dropped much faster than in the aging in air. The decomposition of the cellulose esters was obviously accelerated by autocatalysis. The vapors of the volatile components and the acid products of decomposition of the acetylcellulose in the sealed tube evidently promote further decomposition.

It is evident from the foregoing that the acetylcellulose in the films is depolymerized at 160°C, the process going farther in the closed container than in the open air, where the decomposition products of the cellulose ester do not accelerate its decomposition, notwithstanding the oxidizing effect produced by the atmospheric oxygen.

The results of our tests of the changes in the mechanical properties of the films during aging are given in Table 2.

As we see in Table 2, the breaking load increases, while the elongation drops off, in most of the film samples during the aging process. The brittleness of the films increases during the first 25 to 50 hours of aging, especially in

TABLE 2

Results of Tests of the Mechanical Properties of Films During Aging

Film sample No.	Film thickness, mm	Aging time, hours	Average load, kg/mm²	Average elongation, %
1	0.09	0	7.87	11.5
	0.09	25	7.80	10.83
	0.09	50	9.13	10.53
2	0.07	0	5.30	4.5
	0.07	25	5.65	4.6
	0.07	50	7.07	-
	0.07	75	8.41	5
	0.07	100	8.80	5
3*	0.03	25	2.5	2.6
4	0.05	0	5.65	11
	0.05	25	5.01	11
	0.05	50	7.73	11
	0.05	75	7.84	9.15
5**	0.05	25	6.55	10.7
	0.05	50	9.46	9.7
	0.05	75	7.16	10.4
	0.05	100	9.87	10.1

the thin film (3) and in the film that contained no plasticizer (4), while after 100 hours none of the films could be tested in the dynamometer because of their brittleness.

The determination of the vapor penetrability of the films, tested with water vapor, for several samples (Table 3), showed that the penetrability of the films for water vapor increased after prolonged exposure to high temperature.

In order to be able to compare the aging process in films containing various plasticizers, we prepared triacetate films in our laboratory with tricresyl phosphate, triphenyl phosphate, and dibutyl phthalate, as well as without any plasticizer; these films were then exposed to temperatures of 160 and 140° C in the air. The findings on the changes in the viscosity of solutions of these films are shown by the curves in Figs. 3 and 4.

As we see by these curves, the overall pattern of viscosity changes is the

*The film was so brittle that it could not be tested.

**Samples heated in sealed tubes.

TABLE 3

Vapor Penetrability of Films as a Function of the Aging Time

Film sample No.	Aging time, hours	Grams of water vapor penetrating the film
1	0	0.7432
	245	0.9324
2	0	0.7746
	245	1.2284

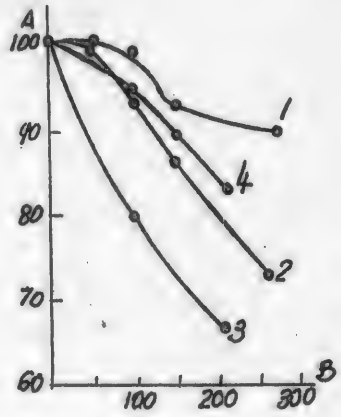

Fig. 3. Change in the viscosity of 0.2% solutions of films containing various plasticizers during aging at 160° C.

A-Viscosity,%; B-aging time, hours. Plasticizers: 1) triphenylphosphate; 2) tricresyl phosphate; 3) dibutyl phthalate; 4) without any plasticizer.

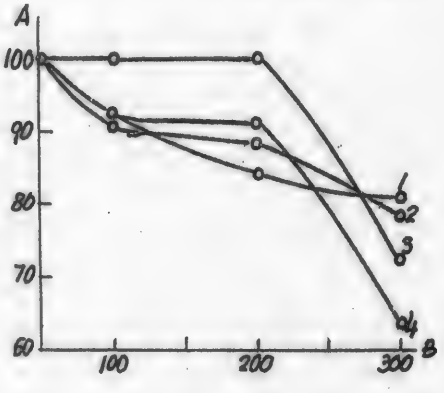

Fig. 4. Change in viscosity of 0.2% solutions of films containing various plasticizers during aging at 140° C.

A-Viscosity, %; B-aging time, hours. Plasticizers: 1) triphenyl phosphate; 2) tricresyl phosphate; 3) dibutyl phthalate; 4) without any plasticizer.

same in the laboratory samples of film as in the commercial samples. The films containing triphenyl phosphate that were prepared in the laboratory had a higher thermal stability than the corresponding commercial sample, possibly because of the impurities that commercial (crude) triphenyl phosphate may contain (such as phenol). Films containing dibutyl phthalate proved to be least resistant to the action of heat, though they possessed the best mechanical properties.

The feasibility of using stabilizers to ensure a higher degree of thermal stability of triacetate films, which is of special importance when they are used for electrical insulation, demands further study; this is the topic of our next paper.

SUMMARY

1. A study has been made of the effect of prolonged exposure to high temperature upon films made of highly acetylated acetylcellulose, with and without plasticizers.

2. The mechanical properties of the films undergo changes during artificial aging in air at 160° C: they become more brittle, their breaking load rises, and their elongation decreases. At the same time the viscosity of solutions of the films drops markedly, which is characteristic of the depolymerization of acetylcellulose.

3. The aging of films containing no plasticizer in sealed tubes with air excluded gives reason to believe that the products of the decomposition of the film during aging exert an autocatalytic effect upon the film.

4. The loss of weight of the films during aging depends upon the properties of the film constituents, especially the plasticizers.

5. The poor resistance of the tested films of highly acetylated acetylcellulose to prolonged exposure to high temperature makes it necessary to explore the possibility of employing special stabilizers.

In conclusion, I wish to express my profound gratitude to Prof. Kozlov, occupying the chair of the technology of motion-picture film bases at the Leningrad Institute of Motion-Picture Engineers, for his invaluable advice and his interest in the present research.

LITERATURE CITED

[1] P.V.Kozlov, Cinema and Photographic Chemical Industry 1 (2), 35 (1933).

[2] P.V.Kozlov and R.V.Zueva, Ibid., 3 (5), 16 (1935); Ibid. 4 (2), 67 (1936).

[3] P.V.Kozlov and I.L.Druyan, Ibid. 5, (5), 23 (1939).

[4] P.V.Kozlov and I.L.Druyan, Ibid. 5 (7), 44 (1939).

[5] A.Ya.Drinberg and E.B.Vvedenskaya, Ibid, 1, (1), 22 (1933).

[6] I.O.Goldman, Ibid. 3, (1935).

[7] Karfunkel and Fedorov, _____ 13, 1940.*

[8] P.V.Kozlov, Ibid 6,(9), 36 (1940).

Received January 30, 1950.

*No source given in original Russian (C.B.).

THE TRANSFORMATIONS OF ACRYLONITRILE AND α-METHYLSTYRENE WITH HYDROGEN PEROXIDE

M. F. Shostakovsky and A. V. Bogdanova

Laboratory of Vinylic Compounds of the Institute of Organic Chemistry,

USSR Academy of Sciences

In research on polymerization products the activation of the initial compounds with peroxides is of considerable interest, as is the ratio of the activated molecules to the unactivated molecules of the initial monomer as well as the possibility of their reacting with molecules of other compounds often present in the reaction medium (water, alcohol, and the like).

The transformations of vinylic esters under the action of peroxides and the ensuing decomposition of the peroxides themselves have been studied in our laboratory, using vinyl acetate and benzoyl peroxide as examples [1]. This example has been used to demonstrate that activated molecules sometimes react more readily with water or alcohol than they do with unactivated molecules of the original monomer.

In this connection we undertook an investigation of the transformations of acrylonitrile and α-methylstyrene in a concentrated solution of hydrogen peroxide. The chemical activity of the double bond in the acrylonitrile molecule results in this compound readily reacting, when an alkali is present, with substances whose molecules contain active hydrogen atoms. The latter are thereby replaced by β-cyanoethyl radicals, so that under these conditions acrylonitrile becomes an active cyanoethylating reagent, able to replace all the active hydrogen atoms successively in the compound.

This substitution follows the pattern of this equation:

$$Ar{-}CO{-}CH_3 + 3CH_2{=}CH{-}CN \longrightarrow Ar{-}CO{-}(CH_2{-}CH_2{-}CN)_3.$$

A condensation of this sort was investigated by Bruson and Riencer [2], who secured products of the mono- and polycyanoethylation of aliphatic-aromatic ketones in a 40% aqueous solution of trimethylbenzylammonium hydroxide, known as "triton-B." These authors also secured cyanoethylation products of substituted derivatives of thiophene and sulfones [3]. We also know of patents describing the reaction of acrylonitrile with phenols in the presence of zinc chloride and anhydrous chloride [4], with amines [5], with halogen acids [6], and with halogens [7].

Gershbein and Hurd [8] investigated the reaction of acrylonitrile with hydrogen sulfide and found that this reaction is exothermic in the presence of "triton B".

Bruson [9] made a study of the reaction of acrylonitrile with various compounds containing active methylene and methenyl groups, namely: fluorene, indene, cyclopentadiene, and the like. They employed chilling to prevent polymerization of the acrylonitrile, as well as solvents that were inert under these conditions

(dioxanes and tertiary butyl alcohol).

The saponification of acrylonitrile has been investigated by Rivkin [10], who found that this compound is not hydrolyzed in neutral or slightly acid aqueous solutions. Acrylonitrile is saponified only to an amide in slightly alkaline media (up to 0.1 N), while in stronger alkalies (0.3 N)the acrylonitrile is completely saponified to an ammonium salt of acrylic acid.

We also know [11] that acrylonitrile polymerizes at 60° without any catalyst, being polymerized at temperatures above 30° with such catalysts as hydrogen peroxide and benzoyl peroxide. The polymerization of acrylonitrile by benzoyl peroxide involves the partial evolution of hydrogen cyanide. As the authors point out, this is a specific reaction of acrylonitrile alone.

What is characteristic of the polyacrylonitriles is their thermal stability; they soften only at very high temperatures, a further rise in temperature entailing the liberation of decomposition products but no depolymerization, as is the case with polymethyl methacrylate and polystyrene.

Another subject of our research was a close homolog of styrene, α-methylstyrene.

We know that the double bond in the styrene molecule is highly active and is responsible for its tendency to polymerize. Styrene is readily polymerized when allowed to stand, even in the cold [12], as well as when various triggers and catalysts are employed. We also know from the patent literature [13] that styrene can enter into simultaneous polymerization with aliphatic nitriles (acrylonitrile and methacrylonitrile), forming solid thermoplastic polymers.

α-Methylstyrene, on the other hand, behaves differently in polymerization reactions. This may be attributed to the effect of the positive methyl group:

$$CH_2=\underset{\displaystyle CH_3}{\overset{\displaystyle |}{C}}-C_6H_5$$

We relate this effect of the CH_3-group to the fact that compounds of this kind do not exhibit activation by peroxides nor is the reaction a free-radical one.

Thus, α-methylstyrene is not polymerized when exposed to light [12], all that happens is its slow oxidation, yielding formaldehyde and acetophenone [14]. α-Methylstyrene is partially polymerized only when heated in an autoclave with concentrated sulfuric or hydrochloric acid [15]. It exhibits a very slight tendency toward thermopolymerization; heating it to 250° in a nitrogen atmosphere within a bomb for 10 hours resulted in the recovery of 60% of the original α-methylstyrene unchanged. An unsaturated dimer of α-methylstyrene, totalling only 25% of the product used for the reaction, was also recovered [12].

Learning how acrylonitrile and α-methylstyrene behave with peroxides in aqueous and alcoholic media was of interest for our further investigation of the properties of these two compounds. The α-methylstyrene may be converted by copolymerization with other unsaturated compounds that are easily activated by peroxides via a free-radical mechanism.

The experiments demonstrated that neither water nor alcohol is added to acrylonitrile or α-methylstyrene when hydrogen peroxide is present in excess. When we attempted to hydrate acrylonitrile with hydrogen peroxide, most of our experiments ended with polymerization of the initial product. This indicates that in the process of activating the acrylonitrile molecules with hydrogen peroxide, polymerization sets in under milder conditions than those required for the addition of water. The polymerization reaction is therefore an obstacle

to other transformations of acrylonitrile. In view of this, we thought it advisable to endeavor to hydrate acrylonitrile in the presence of a different kind of stabilizer. It was found that prolonged heating to 60° likewise caused the process to end with partial or total polymerization whenever the stabilizer amounted to from 2 to 50% of the acrylonitrile used.

As we know, the outlines of the effect of stabilizers upon the polymerization process suggested by Cohen [18] boils down to the binding of the primary free radicals by the stabilizer molecules.

Our experiments have shown that these suggestions have failed of confirmation even under the most severe of polymerization conditions.

Our experiments have likewise shown that the polymerization of acrylonitrile in an aqueous medium with an excess of hydrogen peroxide present sets in at various rates, depending on the temperature (40-60°). Introducing a stabilizer (phenol) into the reaction mixture retarded polymerization perceptibly, at the beginning, but notwithstanding this, when the mixture was heated to 60°, it set in or was completed within intervals of time ranging from 12 to 60 hours, depending upon the amount of stabilizer used. The residueal monomer of acrylonitrile was recovered from the reaction mixture unchanged, as was the phenol.

When an equivalent quantity of phenol was used at 60° in an attempt to hydrate acrylonitrile, polymerization was not observed in the course of 120 hours, the initial products – phenol and acrylonitrile – being again recovered unchanged.

In no run was hydrogen cyanide evolved.

In our attempts to add water and alcohol to α-methylstyrene in the presence of hydrogen peroxide, we recovered the initial α-methylstyrene and a small amount of its oxidation product – acetophenone. The recovery of the latter is in conformity with the statements in the literature [14] that α-methylstyrene may be partially oxidized by oxygen. In none of these tests was the α-methylstyrene polymerized.

As we see it, the ready oxidizability of unsaturated compounds suppresses the polymerization process. When acrylonitrile and α-methylstyrene are copolymerized in the presence of hydrogen peroxide, the α-methylstyrene is involved in the reaction. By heating to 60° for 39 hours we secured a polymer product whose ultimate analysis was that of a copolymer containing one molecule of α-methylstyrene for every two molecules of acrylonitrile.

In an experiment in which identical quantities of acrylonitrile and α-methylstyrene were used, both of the copolymer fractions recovered (the one that was soluble in boiling benzene and the one that was not) had the same ultimate analysis. In this test, apparently, copolymers of different degrees of polymerization were produced. The percentage of nitrogen in the copolymer fractions secured from an acetone solution indicates that acetone cannot be used as a selective solvent to fractionate the copolymer produced.

The test in which an excess of α-methylstyrene was used yielded a copolymer that was divided into two fractions: soluble and insoluble in boiling benzene. The percentage of nitrogen was very different in the two fractions. In the fraction that was insoluble in benzene the percentage of nitrogen corresponded to that for a copolymer containing two molecules of acrylonitrile per molecule of the α-methylstyrene.

The copolymer fraction that was soluble in benzene contained half as much nitrogen as the insoluble fraction, so that we may assume it contained a larger number of molecules of α-methylstyrene per molecule of acrylonitrile.

It is more convenient to investigate copolymerization by synthesizing and

identifying low-molecular products, i.e., readily separable polymers.

EXPERIMENTAL

We used the following reagents in this research: acrylonitrile, α-methylstyrene, hydrogen peroxide, and methanol. The acrylonitrile was first refined by distillation in vacuum, the distillate having the following constants: B.p. 76.5-77.5°; n_D^{20} 1.3910; d_4^{20} 0.8074.

The α-methylstyrene was also vacuum-distilled; its constants were: B.p. 67-68° (20 mm); n_D^{24} 1.5310; d_4^{24} 0.9045.

The hydrogen peroxide used was the commercial perhydrol, containing 34.3% H_2O_2. The H_2O_2 percentage was determined by titrating a solution of the perhydrol in sulfuric acid with a 0.1 N hyposulfite solution containing potassium iodide [17]. The methanol was purified in the usual manner and had the following constants after purification: B.p. 64-65°; n_D^{20} 1.3200; d_4^{20} 0.7930.

Reaction of acrylonitrile with water at 60° in the presence of hydrogen peroxide. 68 g of perhydrol and 68 g of distilled water were placed in a three-necked flask fitted with a reflux condenser, a dropping funnel, a thermometer, and a stirrer. Then 53 g of acrylonitrile, saturated with 3 g of water, was added drop by drop during the course of 1.5 hours at 60°. The outlet end of the condenser was connected via a glass tube to an absorption bottle that contained a 20% aqueous solution of sodium hydroxide. The reaction flask was placed in a water bath. The mixture was heated to the specified temperature with effective stirring.

Four hours after the acrylonitrile began to be added it was observed to polymerize. Filtration yielded 23 g of an air-dry polymer of acrylonitrile, which was insoluble in organic solvents.

The filtrate, which displayed an intense reaction for hydrogen peroxide,* was extracted with ether; the extract was desiccated with sodium sulfate and fractionated in vacuum after the ether had been driven off. Fractionation yielded the following products:

18-20° (78 mm) fraction	20.0 g
Residue	1.0 g.

The constants of the product were: b.p. 76.0-77.0°; n_D^{20} 1.3900; d_4^{20} 0.8072. It was the original acrylonitrile.

The alkali solution in the wash bottle was transferred quantitatively to a measuring flask. A Liebig-Denige titration [18] of this solution showed no traces of hydrogen cyanide.

In another version of this experiment, in which the reagents were mixed together at room temperature, after which the mixture was heated, the polymer was formed 3 hours after heating had begun. This yielded 15 g of an air-dry polymer of acrylonitrile. The wash bottles contained no hydrogen cyanide in either case.

Reaction of acrylonitrile and water in the presence of hydrogen peroxide containing stabilizers. The reaction took place with phenol added. 52 g of acrylonitrile, 1 g of phenol, and 4 g of water were mixed together and allowed to stand for 12 hours. Then this mixture, heated to 60-62°, was added drop by drop to a reaction flask containing 100 g of perhydrol and 100 g of water. A white precipitate was thrown down 12 hours after heating had begun. The test lasted 48 hours, after which filtration and drying yielded 47 g of an air-dry polymer of acrylonitrile. Extraction of the filtrate yielded 4 g of the monomer of acrylonitrile, with the following constants: b.p. 76.5-77.5°; n_D^{20} 1.3910; d_4^{20} 0.8070.

The results of tests in which various amounts of phenol were used are listed

*Hydrogen peroxide turns a solution of ammonium thiocyanate containing Mohr's salt bright red.

in the subjoined table.

Test No.	Phenol (% of acrylonitrile)	Time elapsing before start of polymerization, hours	Total heating time, hours	Resulting products, g	
				Polymer	Other products
1	2	12	36	47	Monomer of acrylonitrile: 4
2	10	30	48	51	Phenol: 2
3	50	48	60	40.5	Phenol: 16
4	100	-	120	None	Acrylonitrile: 48 Phenol: 48

We see in this table that increasing the percentage of phenol merely affects the period elapsing before the acrylonitrile starts to polymerize; the ensuing period of time, required for the more complete formation of the polymer, does not depend upon the amount of stabilizer present. 20 to 50% of the phenol taken for the reaction was recovered.

Reaction of α-methylstyrene with water in the presence of hydrogen peroxide. 59 g of α-methylstyrene, 50 g of perhydrol, and 50 g of water were placed in the reaction flask of the apparatus described above. The mixture was heated, with efficient stirring, to 40° over a water bath. The outlet tube of the condenser was connected to a wash bottle containing distilled water. 28 hours of heating to 40° caused no change in the reaction mixture. Then the mixture was heated to 60° for 66 hours, the heating time thus totalling 94 hours. The recovered product had two layers. The upper layer was washed with water, desiccated with potash, and distilled in vacuum:

Fraction I, 64-65° (17 mm) ..... 50.8 g,
Fraction II, 65-94° (17 mm) ..... 0.3 g,
Fraction III, 94-96° (17 mm) ..... 3.5 g,
Residue ..... 1.8 g.

The constants of Fraction I were: $n_D^{16.5}$ 1.5360; $d_4^{16.5}$ 0.9128; this fraction was the initial α-methylstyrene.

Fraction III was acetophenone, the constants of which were: b.p. 202-203°; n_D^{24} 1.5335; d_4^{24} 1.0025.

Another 3 g of acetophenone was recovered from the aqueous layer by extraction with ether.

Reaction of α-methylstyrene with methanol in the presence of hydrogen peroxide. A mixture of 59 g of α-methylstyrene, 50 g of methanol, and 50 g of perhydrol was placed in the reaction flask and heated to 40°, with stirring, for 115 hours. At the end of this time the reaction mixture consisted of two layers. The upper layer was desiccated with potash and distilled in vacuum, the following products being recovered:

Fraction I, 65-66° (16 mm) ..... 42.5 g,
Residue ..... 13.0 g.

The constants of Fraction I were: n_D^{24} 1.5320; d_4^{24} 0.90040; this fraction was the initial α-methylstyrene.

The residue yielded 10 g of acetophenone and about 1 g of a tarry product.

The lower layer was an aqueous solution of methanol.

Reaction of a mixture of equal parts of acrylonitrile and α-methylstyrene

in the presence of hydrogen peroxide. A mixture of 25 g of acrylonitrile, 25 g of α-methylstyrene, and 150 g of perhydrol was heated to 60° over a water bath while stirred efficiently. After 21 hours of heating the reaction mixture turned cloudy, and after 39 hours of heating a polymer settled out as a white, rubbery mass. It weighed 46.3 g. When the polymer was heated, it could be drawn out in fine threads, which grew brittle upon cooling. The polymer was insoluble in methanol or ether. It was partly soluble in boiling benzene and wholly insoluble in acetone.

Investigation of the synthesized polymer. a) 7.6 g of the polymer was dissolved in 200 ml of boiling benzene. The portion of the polymer that did not dissolve was dried in a cabinet at 110° for 12 hours. This yielded 3.7 g of a brittle white product.

Ultimate analysis of the portion of the polymer that was insoluble in benzene:

3.315 mg substance: 9.73 mg CO_2; 2.15 mg H_2O.
3.134 mg substance: 9.22 mg CO_2; 2.03 mg H_2O.
Found %: C 80.10, 80.29; H 7.26, 7.26.
$C_{15}H_{16}N_2$. Computed %: C 80.32; H 7.19.

The ultimate analysis indicates that the polymer contains two molecules of acrylonitrile per molecule of α-methylstyrene.

We were unable to recover any substances from benzene solution by reprecipitation with ether. We therefore drove off most of the benzene and precipitated 0.4 g (dry) of a solid product from the concentrated solution with ether.

Ultimate analysis of the portion of the polymer that was soluble in benzene:

2.866 mg substance: 8.46 mg CO_2; 1.905 mg H_2O.
4.050 mg substance: 11.915 mg CO_2; 2.65 mg H_2O.
Found %: C 80.53, 80.29; H 7.44, 7.32.
$C_{15}H_{16}N_2$. Computed %: C 80.32; H 7.19.

Determination of the molecular weight of the portion of the polymer that was soluble in benzene:

0.0964 g substance: 12.48 g dioxane; $\Delta t = 0.08°$.
Found: M 482.7.
$(C_{15}H_{16}N_2)_2$. Computed: M 448.6.

Except for the polymer, no other products were isolated in processing the reaction mixture.

b) 7.1 g of the crude polymer was dissolved in 75 ml of acetone. Fraction I of the polymer was precipitated with methanol. It weighed 3.2 g after having been dried in a cabinet at 110° for 12 hours.

Determination of nitrogen in Fraction I of the polymer:

4.100 mg substance: 0.372 ml N_2 (750 mm, 23°).
4.025 mg substance: 0.370 ml N_2 (749 mm, 23°).
Found %: N 10.33, 10.45.

The acetone -methanol solution was then treated with ether; after it had stood for a long time, Fraction II of the polymer was filtered out of it (0.5 g in the dry state).

Determination of nitrogen in Fraction II of the polymer:

6.495 mg substance: 0.736 ml N_2 (757 mm, 22°).
6.995 mg substance: 0.794 ml N_2 (759 mm, 22°).
Found %: N 13.06, 13.12.
$C_{15}H_{16}N_2$. Computed %: N 12.49.

Reaction of acrylonitrile with an excess of α-methylstyrene in the presence of hydrogen peroxide. A mixture of 20 g of acrylonitrile, 70 g of α-methylstyrene, and 150 g of perhydrol was heated to 60°, the conditions being those of the previous test.

After 27 hours of heating a slight cloudiness appeared in the upper layer, which turned into a thick white emulsion after a total of 70 hours of heating. The emulsion was separated from the aqueous layer and treated with ether. This yielded 34.8 g of a soft polymer. The crude polymer was washed with water to remove the hydrogen peroxide and then washed with ether. Then it was dried at 110° for 12 hours in a drying cabinet. It was a solid white product that could be easily rubbed to powder.

Investigation of the polymer product. 11.3 g of the polymer product was dissolved in 100 ml of boiling benzene; the part of the polymer that did not dissolve was dried at 110° for 12 hours in a drying cabinet. This yielded 1 g of a brittle white product.

Determination of nitrogen in the portion of the polymer that was insoluble in benzene:

5.558 mg substance: 0.589 ml N_2 (759 mm, 21°)
6.530 mg substance: 0.702 ml N_2 (758 mm, 21°).
Found %: N 12.29, 12.45.
$C_{15}H_{16}N_2$. Computed %: N 12.49.

Ether precipitated a viscous liquid product from the benzene solution; it was washed with ether and dried in a cabinet at 110°. The dried polymer was a brittle white product; it weighed 7.0 g.

Determination of nitrogen in the portion of the polymer that was soluble in benzene:

5.560 mg substance: 0.319 ml N_2 (761 mm, 22°).
5.085 mg substance: 0.300 ml N_2 (759 mm, 21°).
Found %: N 6.65; 6.84.

Determination of the molecular weight of the portion of the polymer that was soluble in benzene:

0.2078 g substance: 13.9 g dioxane; Δt 0.18°.
Found: M 415.6.
$(C_{15}H_{16}N_2)_2$. Computed: M 448.6.

The aqueous layer was extracted with ether. The ether extract was desiccated with potash, the ether was driven off, and the residue fractionated in vacuum. Fractionation yielded the following fractions:

Fraction I, 73-75° (18 mm) ..... 14.1 g,
Fraction II, 75-110° (18 mm) .... 5.7 g,
Residue ..... 13.5 g.

The constants of Fraction I were: b.p. 162-162.5°; n_D^{22} 1.5320; d_4^{22} 0.9064; it was the original α-methylstyrene.

Fraction II yielded 4.3 g of acetophenone, the constants of which were: b.p. 201-201°; n_D^{24} 0.5340; d_4^{24} 1.0190.

SUMMARY

1. A study has been made of the transformations of acrylonitrile and α-methylstyrene in reactions involving the addition of water, alcohols, and phenols in the presence of hydrogen peroxide. It has been found that a) acrylonitrile

polymerizes readily and does not react with water, alcohols, or phenols; and b) α-methylstyrene is not polymerized, but enters into addition reactions and is oxidized under these conditions.

2. It has been found that acrylonitrile and α-methylstyrene form a copolymer in the presence of hydrogen peroxide, which bears out the assertion that a free-radical mechanism of transformation of α-methylstyrene is possible, as follows:

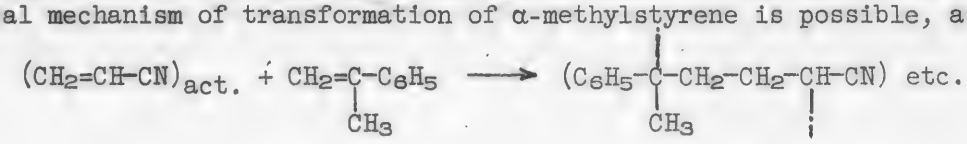

LITERATURE CITED

[1] M.F.Shostakovsky, Bull. USSR Acad. Sci. 12 (1948).

[2] H.A.Bruson and T.W.Reiner, J.Am.Chem.Soc., 64, 2852 (1942).

[3] H.A.Bruson and T.W.Reiner, J.Am.Chem.Soc., 70, 214 (1948).

[4] W.D.Langley, R.Adams, J.Am.Chem.Soc. 44, 2320 (1922).

[5] British Patent 404,744 (1934); 457,621 (1936), I.G.Farbenindustrie.

[6] Mouren, Bull. soc. chim. France, 27, 901 (1920).

[7] U.S.Patent 2,231, 262 (1941); 2,231,838 (1941); 2,231,360 (1941).

[8] L.L.Gershbein and Ch.D.Hurd, J.Am.Chem.Soc., 64, 241 (1947).

[9] H.A.Bruson, J.Am.Chem.Soc., 64, 2457 (1942).

[10] S.M.Rivkin, Trans. All-Union Inst. Synthetic Rubber Research, 2, 87 (1948).

[11] W.Kern and H.Fernon, Rubber Chem. and Technol., XVII, 2, 356 (1944).

[12] H.Staudinger and F. Breusch, Ber, LXII, 1, 442 (1929).

[13] French Patent 807,951 (1937), I.G.Farbenindustrie; C.A., 31, 6378 (1937).

[14] Tiffeneau, A. Chem. (8), 10, 162 (1907).

[15] V.Grignard, C, 11, 624 (1901).

[16] S.G.Cohen, J.Polymer Sci., 11, 5 (1947); S.G.Cohen, J.Am.Chem.Soc., 67, 17 (1945).

[17] F.P.Treadwell, Treatise of Analytical Chemistry, Vol. II; Volumetric Analysis, p. 143 (Russ. ed.).

[18] Soborovsky and Yakubovich. Synthesis of Poison Gases, p. 118.

Received June 3, 1950.

THE COMPOSITION OF FATTY ACIDS DERIVED FROM OXIDIZED PARAFFIN

A. E. Drabkin and Z. V. Soloveichik

Lensoviet Institute of Technology, Leningrad

A complex mixture of products is formed in the catalytic oxidation of petroleum hydrocarbons, especially paraffin, the monobasic fatty acids being the most important from the practical standpoint. Isolating these acids from the mixture by simple saponification with alkali is unsatisfactory, inasmuch as the hydroxy acids and ester derivatives are saponified together with the fatty acids. That is why we still do not know enough about the composition of the fatty acids secured from oxidized paraffin.

Bergmann [1], for example, oxidized Galician paraffin and secured acetic, butyric, and lignoceric acids, plus two acids of unknown structure: $C_{16}H_{32}O_2$ and $C_{11}H_{22}O_2$.

Velikovsky [2] oxidized Grozny paraffin and secured a small quantity of fatty acids, the composition of which was not investigated, however.

Various researchers have isolated many more individual acids [3] from the oxidation products of brown-coal and, more especially, synthetic paraffin. This difference in the behavior of petroleum and synthetic paraffin is evidently due to the high percentage of iso compounds in the former; according to Tsyskovsky [4] these form condensation products of high molecular weight.

In the present research we have recovered more than 25% of acids from oxidized Grozny paraffin after carefully eliminating the hydroxy acids; these fatty acids included a series of individual monobasic acids of normal structure with 7 to 24 carbon atoms in the molecule.

EXPERIMENTAL

Isolation of the acids. The initial oxidized Grozny paraffin had an acid number of 86.5 and contained a large quantity of unsaponified compounds, hydroxy acids and ester derivatives.

The hydroxy acids were eliminated, as usual, by precipitation from a tenfold volume of gasoline, but with the gascline subsequently processed with zinc chloride. 12 g of $ZnCl_2$ in 4 g of water were used for 100 g of the oxidized paraffin.

The hydroxy acids* precipitated with gasoline totaled 15% of the paraffin by weight and had an acid number of 130 and a saponification number of 340; the acids precipitated by zinc chloride totaled 17% of the paraffin by weight. They had an acid number of 123 and a saponification number of 312.

* In addition to the true hydroxy acids, various derivatives of these acids were evidently thrown down, but we shall call the whole precipitate hydroxy acids as is customary in the literature, in view of the absence of research on the composition of the precipitate.

After the hydroxy acids had been eliminated from the gasoline solution, it was washed with distilled water until its reaction for Cl' was negative and then it was treated with a 5% aqueous solution of sodium hydroxide.

The soaps were washed repeatedly with gasoline to remove the unsaponified substances, and then they were decomposed with 10% HCl. The fatty acids were extracted with ether, and the solution was washed with water until its reaction was neutral (Congo red as an indicator) and desiccated with freshly calcined sodium sulfate. Then the ether was driven off.

Six kg of oxidized paraffin were used in the test.

Yield: 1.50 kg or 25% of fatty acids; 1.92 kg or 32% of hydroxy acids; 2.40 kg or 40% of unsaponified substances; and 0.18 kg or 3% losses.

Characteristics of the fatty acids: acid number – 130 mg KOH per gram; saponification number – 167 mg KOH per gram; iodine number – 8.

Since not all the unsaponified substances were extracted by the gasoline from the aqueous solution of the soaps, the crude acids were resaponified with 2 N alcoholic alkali. Saponification was performed for 3 hours over a water bath, using a reflux condenser. After saponification, the alcohol was driven off, and the salts were dried at 110° to constant weight. The dry salts were then finely powdered and extracted with petroleum ether until all the unsaponified substances were extracted. The extraction process lasted some 30 hours.

1050 g of the crude acids were taken for refining. This yielded 840 g or 81.9% of refined acids and 87.6 g or 8.4% of unsaponified substances; the losses were 122.4 g or 9.7%.

Esterification of the acids and fractionation of the esters. The acids were separated by preparing their methyl esters, which boiled 30 to 70° below the respective acids. Esterification was carried out with small batches, 100 g at a time. The batch of acids was dissolved in 5 times its volume of absolute methanol, after which the solution was saturated with anhydrous hydrogen chloride. Then the reaction mixture was heated with a reflux condenser for 4 hours over a water bath.

This procedure gave us high yields of the esters. Esterification in the cold requires more than 10 days [5].

After the reaction was completed, the excess alcohol was driven off at a slight vacuum over a water bath. The methyl esters left in the flask were dissolved in ether and washed with a 5% soda solution to remove the unreacted acids (which were later re-esterified). Then the solution was washed with water until its reaction was neutral and desiccated with sodium sulfate, after which the solvent was driven off.

TABLE 1

Fractionation of Methyl Esters. Residual Pressure: 3.5 mm Mercury Column. Quantity used for Distillation: 780 g.

Fraction No.	Temperature range, °C	Quantity	
		Grams	Per cent
1	Up to 100	60.3	7.73
2	100 - 130	72.8	9.33
3	130 - 160	97.2	12.46
4	160 - 190	117.9	15.01
5	190 - 220	104.0	13.33
6	220 - 250	69.5	8.91
	Residue	238.0	30.51
	Losses	20.3	2.72
		–	100 %

800 g of acids were used for esterification. We secured 780 g of esters, or 93% of the theoretical yield. The esters were fractionated in vacuum from an ordinary Claisen flask, first into 30 ° fractions (Table 1) and then into narrower fractions with a herringbone condenser 200 mm high. The fractional distillation

data are listed in Table 2.

TABLE 2

Fractional Distillation of Thirty-Degree Fractions of Methyl Esters
Residual Pressure: 3 mm Mercury Column

Fraction No.	Boiling range, °C	Quantity (g)	Quantity (%)	Fraction No.	Boiling range, °C	Quantity (g)	Quantity (%)
1	38-50	1.1	0.14	15	133-139	33.1	4.25
2	50-58	5.5	0.70	16	139-145	33.1	4.25
3	58-63	8.4	1.08	17	145-152	49.5	6.35
4	63-68	10.2	1.31	18	152-158	28.9	3.70
5	68-73	9.1	1.17	19	158-164	24.6	3.16
6	73-83	20.9	2.64	20	164-170	30.2	3.87
7	83-88	12.7	1.63	21	170-176	21.7	2.79
8	88-93	16.7	2.14	22	176-182	39.5	5.05
9	93-98	11.5	1.48	23	182-188	21.1	2.70
10	98-106	12.7	1.63	24	188-195	20.5	2.63
11	106-115	20.2	2.60	25	195-201	5.0	0.64
12	115-121	11.6	1.49	26	201-207	9.1	1.17
13	121-127	16.2	2.08		Residue	25.2	32.20
14	127-133	34.1	4.37		Losses	22.8	2.78

Examination of the individual ester fractions. The principal fractions investigated were Nos. 1, 4, 8, 11, 14, 17, 20, 22, 24, and 26 (Table 2). Each ester fraction was saponified by heating it with a 0.5 N solution of alcoholic alkali over a water bath, with a reflux condenser. After the alcohol had been driven off, the soaps were decomposed with 10% HCl, and the resultant acids were extracted with ether. Then the ether extracts were washed with water and dessiccated. The acids recovered after the solvent had been driven off were subjected to further investigation.

1) Fraction 1. Boiling range of the esters: 38-50° C (p = 3 mm). This first fraction totaled 1 g. Its analysis was therefore confined to its acid number, which was found to be 420. This number corresponds to a molecular weight of 133.0, or a monobasic acid with the fomula of $C_7H_{14}O_2$.

2) Fraction 4. Weight: 10.2 g. Boiling range of the esters: 63-68° (p = 3 mm). Ester saponification number: 350.2. Acid number: 367.2.

The acids were slightly yellowish liquids. The acid number of 367.2 is the equivalent of a $C_8H_{16}O_2$ acid.

0.2096 g substance: 0.5190 g CO_2; 0.2150 g H_2O.
Found %: C 67.57; H 11.47.
$C_7H_{14}O_2$. Computed %: C 64.61; H 10.75.
$C_8H_{16}O_2$. C 66.66; H 11.11.
$C_9H_{18}O_2$. C 68.35; H 11.39.

Thus, the product is evidently the acid $C_8H_{16}O_2$ with a trace of the acid $C_9H_{18}O_2$.

3) Fraction 8. Weight: 16.7 g. Ester boiling range: 88-93° (p = 3 mm). Ester saponification number: 305.2. Acid number: 298.3. Molecular weight, calculated from the acid number: 187.7.

The barium salts of the acids in this fraction were prepared, and the molecular weight was calculated from the Ba content.

The salts were prepared as follows: A weighed sample of the acids was dissolved in ethyl alcohol, and the salts were thrown down with barium acetate from the solution, heated over a water bath. The precipitated barium salts were washed on a Buchner funnel with 70% alcohol to remove the $Ba(C_2H_3O_2)_2$ and then dried at 105° to constant weight. Then the precipitate was slowly burned over a gas flame and roasted in a muffle furnace until BaO was produced. In view of the tendency of BaO to absorb moisture and carbon dioxide from the air, it was analyzed as barium sulfate.

The salts were found to contain 27.4% Ba, equivalent to a mean molecular weight of 183.7 for the acids.

Comparison of the molecular weights calculated by the acid number and by the percentage of barium in the salts shows that the acids were fairly pure.

0.1821 g substance:	0.4664 g CO_2;	0.1910 g H_2O.
Found %:	C 69.89;	H 11.74.
$C_{10}H_{20}O_2$. Computed %:	C 69.76;	H 11.63.
$C_{11}H_{22}O_2$.	C 70.96;	H 11.83.
$C_{12}H_{24}O_2$.	C 72.00;	H 12.00.

These figures indicate that Fraction 8 consisted of a mixture of the acids $C_{10}H_{20}O_2$ and $C_{11}H_{22}O_2$, with the former predominating.

4) Fraction 11. Weight: 20.2 g. Ester boiling range: 106-115° C (p = 3 mm). Ester saponification number: 297.

The acids recovered from this fraction were solids. Analysis of the barium salts, carried out as in the preceding fraction, showed a barium content of 25.66%. This is equivalent to a molecular weight of 200. The acids contained a slight trace of unsaturated compounds (iodine number: 2.4), so that they were purified by recrystallization of their potassium salts from acetone.

5 g of the acids were heated in acetone until they dissolved, and then precipitated with a 1 N aqueous solution of KOH. The potassium salts thrown down as the solution cooled were filtered out, washed with acetone, and desiccated. Then the salts were decomposed with 10% HCl, and the acids were extracted with ether. Driving off the ether yielded white crystals with an acid number of 273.2 and an iodine number of 0.

0.1603 g substance:	0.4268 g CO_2;	0.1755 g H_2O.
Found %:	C 72.66;	H 12.25.
$C_{11}H_{22}O_2$. Computed %:	C 70.96;	H 11.83.
$C_{12}H_{24}O_2$.	C 72.00;	H 12.00
$C_{13}H_{26}O_2$.	C 72.90;	H 12.10.

Acid number

Found:	273.
$C_{11}H_{22}O_2$. Computed:	300.
$C_{12}H_{24}O_2$.	280.
$C_{13}H_{26}O_2$.	262.

These figures indicate that the fraction consisted chiefly of the acid $C_{12}H_{24}O_2$, with a trace of the acid $C_{13}H_{26}O_2$.

5) Fraction 14. Weight: 34.1 g. Ester boiling range: 127-133° (p = 3 mm). Ester saponification number: 247.

The acids recovered from the esters were light-yellow, with an acid number

of 247.5 and an iodine number of 4.9. The acid number was 244 after the potassium salts had been recrystallized from acetone. The acids contained no unsaturated compounds. They fused at 37°C. The melting point was raised to 50.5°C by repeated recrystallization from 85% ethyl alcohol. By way of comparison, here are the melting points of some acids: $C_{13}H_{26}O_2$, 42.5°; $C_{14}H_{28}O_2$, 53.8°; and $C_{15}H_{30}O_2$ 51.0°C.

0.1133 g substance: 0.3067 g CO_2; 0.1268 g H_2O.
Found %: C 73.87; H 12.5.
$C_{13}H_{26}O_2$. Computed %: C 72.9; H 12.1.
$C_{14}H_{28}O_2$. C 73.68; H 12.28.
$C_{15}H_{30}O_2$. C 74.38; H 12.39.

Acid number:

Found: 244.
$C_{13}H_{26}O_2$. Computed: 262.
$C_{14}H_{28}O_2$. 246.
$C_{15}H_{30}O_2$. 232.

The ultimate analysis and the acid number indicate that the acid $C_{14}H_{28}O_2$ predominates in this substance. The somewhat low melting point is evidently due to the presence of slight impurities.

6) Fraction 17. Weight: 49.5 g. Ester boiling range: 145-152° C (p = 3 mm). Ester saponification number: 225. Data on the acids recovered: acid number 218.6; iodine number 6.4; per cent barium in the salts 21.03%.

Recrystallization of the potassium salts from acetone yielded the acids as white crystals with a melting point of 48° C. The acid number was 217.1, while the iodine number was zero.

0.1623 g substance: 0.4436 g CO_2; 0.1858 g H_2O.
Found %: C 75.45; H 12.8.
$C_{15}H_{30}O_2$. Computed %: C 74.38; H 12.39.
$C_{16}H_{32}O_2$. C 75.00; H 12.50.
$C_{17}H_{34}O_2$. C 75.55; H 12.60.

Triple recrystallization from 85% alcohol raised the melting point to 57°C, this melting point not being raised by further recrystallization.

The acid melting points are given in the literature as follows:

$C_{16}H_{32}O_2$, 62° C; $C_{17}H_{34}O_2$, 60° C; $C_{15}H_{30}O_2$, 51° C.

The ultimate analysis and the melting point indicate that the fraction consisted of the acid $C_{17}H_{34}O_2$. The acid number is closer to that of $C_{16}H_{32}O_2$, however. The molecular weight, as calculated from the percentage of barium in the salts, is likewise that of the acid $C_{16}H_{32}O_2$.

In order to identify the acids better, they were separated by the method of fractional precipitation with barium acetate, based upon the circumstance that the solubility of alkali-earth salts of fatty acids decreases as the molecular weight rises in the homologous series.

A weighed sample of the acids was dissolved in enough hot alcohol to keep the acids from settling out when the solution cooled. Then an aqueous solution of barium acetate was added to the hot solution, its amount being 1/6 of what was theoretically needed to bind all the acids. This precipitated part of the salts. The precipitated salts were filtered out and decomposed with 10% HCl. The acids were extracted with ether, washed with water, and desiccated. The filtrate was again processed with an insufficient quantity of barium acetate. This precipitation was repeated 5 times; the data on this processing are listed in Table 3.

TABLE 3

Fractional Precipitation of Acids

Acid characteristics	Precipitation No.					
	1	2	3	4	5	Residue
Acid melting point, ° C	46-47.5	46-48	45-48	46-48.5	46.5-49	–
Acid number	207.6	209.5	209.0	207.5	214	224

As we see from the figures in Table 3, the acids of the first four precipitates are identical. They were therefore combined and recrystallized from alcohol. The acids fused at 60° C after the recrystallization, which is the melting point given in the literature for the acid $C_{17}H_{34}O_2$ (60° C).

0.1506 g substance: 0.4183 g CO_2; 0.1722 g H_2O.
Found %: C 75.80; H 12.8.
$C_{17}H_{34}O_2$. Computed %: C 75.55; H 12.6.

Acid number:

Found: 206.5.
$C_{16}H_{32}O_2$. Computed: 219.
$C_{17}H_{34}O_2$. 209.
$C_{18}H_{36}O_2$. 197.

Fraction 17 therefore consisted of the acid $C_{17}H_{34}O_2$ with a trace of acids of lower molecular weight.

7) Fraction 20. Weight: 30.2 g. Ester boiling range: 164-170° C (p = 3 mm). Ester saponification number: 214. Acid iodine number: 7.9. Barium content in barium salts: 20.65%.

The esters of this fraction were solids, in contrast to the preceding esters.

The acids fused at 62-63° C after recrystallization of their potassium salts from acetone and repeated recrystallization of the acids from alcohol.

0.1430 g substance: 0.4025 g CO_2; 0.1616 g H_2O.
Found %: C 76.30; H 12.65.
$C_{17}H_{34}O_2$. Computed %: C 75.55; H 12.6.
$C_{18}H_{36}O_2$. C 76.05; H 12.67.
$C_{19}H_{38}O_2$. C 76.51; H 12.75.

Acid number:

Found: 196.
$C_{17}H_{34}O_2$. Computed: 209.
$C_{18}H_{36}O_2$. 197.
$C_{19}H_{38}O_2$. 188.

Judging by the acid number and the ultimate analysis, we had isolated the acid $C_{18}H_{36}O_2$. The slight drop in the melting point indicated the presence of a trace of the acid $C_{17}H_{34}O_2$.

8) Fraction 22. Weight: 39.5 g. Ester boiling range: 176-182° C (P = 3 mm). Saponification number: 195. Characteristics of the acids recovered: acid number: 187.3; iodine number: 9.0; barium content of salts: 18.58.

The acid number remained practically unchanged (186.7) after recrystallization of the potassium salts from acetone. The values of the molecular weight, calculated from the acid number and from the percentage of barium in the salts (300 and 302, respectively) also agreed satisfactorily. This indicated that the

acid was fairly pure; it had a melting point of 66° C after repeated recrystallization from alcohol.

The figures given in the literature for the acid melting points are:

$C_{18}H_{36}O_2$ 69°C; $C_{19}H_{38}O_2$ 65°C; and $C_{20}H_{40}O_2$ 77.0°C.

Ultimate analysis

0.1449 g substance:	0.4083 g CO_2;	0.1635 g H_2O.
Found %:	C 76.89;	H 12.71.
$C_{18}H_{36}O_2$. Computed %:	C 76.05;	H 12.67.
$C_{19}H_{38}O_2$.	C 76.51;	H 12.75.
$C_{20}H_{40}O_2$.	C 76.92;	H 12.82.

Acid number:

Found:	186.9.
$C_{18}H_{36}O_2$. Computed:	197.
$C_{19}H_{38}O_2$.	188.
$C_{20}H_{40}O_2$.	179.

These findings leave no room for doubt that Fraction 22 consisted of the acid $C_{19}H_{38}O_2$.

9) Fraction 24. Weight: 20.5 g. Ester boiling range: 188-195°C (p = 3 mm). Ester saponification number: 172.

Before purification the acids were yellow, with an acid number of 166.4 and an iodine number of 9.7.

Precipitation of the potassium salts from acetone changed the acid number to 170.8, while the iodine number became zero.

Repeated recrystallization from alcohol yielded white crystals with a melting point of 71°C.

Ultimate analysis

0.1613 g substance:	0.4543 g CO_2;	0.1847 g H_2O.
Found %:	C 76.9;	H 12.82.
$C_{20}H_{40}O_2$. Computed %:	C 76.96;	H 12.82.
$C_{21}H_{42}O_2$.	C 77.30;	H 12.88.
$C_{22}H_{44}O_2$.	C 77.65;	H 12.94.

Acid number:

Found:	170.8.
$C_{20}H_{40}O_2$. Computed:	179.
$C_{21}H_{42}O_2$.	172.
$C_{22}H_{44}O_2$.	164.7.

Both the melting point and the acid number are in good agreement with figures for the acid $C_{21}H_{42}O_2$, while the ultimate analysis yields figures that are closer to those for $C_{20}H_{40}O_2$.

Fraction 24 is apparently a mixture of these two acids.

10) Fraction 26. Weight: 9.1 g. Ester boiling range: 201-207° C (p = 3 mm). Ester saponification number 165. Acid characteristics: acid number 156; analysis of barium salts - 16.4% Ba; melting point 59-62°C.

Recrystallization from alcohol raised the melting point to 73° C. This agrees with the figure in the literature for the acid $C_{23}H_{46}O_2$.

Ultimate Analysis:

0.1114 g substance: 0.3154 g CO_2; 0.1285 g H_2O.
Found %: C 77.55; H 12.91.
$C_{22}H_{44}O_2$. Computed %: C 77.65; H 12.94.
$C_{23}H_{46}O_2$. C 77.96; H 13.00.
$C_{24}H_{48}O_2$. C 78.26; H 13.04.

Hence, Fraction 26 consisted of the acid $C_{23}H_{46}O_2$.

The findings of our examination of the 10 selected acid fractions indicate that they are monobasic fatty acids of normal structure.

There is, therefore, every reason to believe that the intervening fractions which were not investigated, are also monobasic acids, and that oxidized Grozny paraffin contains an unbroken series of acids from $C_7H_{14}O_2$ to $C_{23}H_{46}O_2$.

SUMMARY

1. The carboxylic acids recovered from oxidized Grozny paraffin are monobasic and possess a normal structure.

2. The following individual acids have been isolated from the fractions examined: $C_7H_{14}O_2$, $C_8H_{16}O_2$, $C_{10}H_{20}O_2$, $C_{12}H_{24}O_2$, $C_{14}H_{28}O_2$, $C_{17}H_{34}O_2$, $C_{18}H_{36}O_2$, $C_{19}H_{38}O_2$, $C_{21}H_{42}O_2$, and $C_{23}H_{46}O_2$.

LITERATURE CITED

[1] Bergmann, Z. angew. Chem., 31, 69 (1918).

[2] Velikovsky, Trans. Gubkin Petroleum Institute of Moscow, State Fuel Tech. Press (1947).

[3] G.S.Petrov. Synthetic Fatty Acids. Food Industry Press (1944).

[4] V.K.Tsyskovsky, J.Appl. Chem. 19, 428 (1946).

[5] C. Kelber, Ber., 53, 66, 1567 (1920).

Received June 28, 1950.

THE BEHAVIOR PATTERNS OF THE CHANGES IN THE OPERATION OF CHARCOAL BEDS UNDER VARIOUS CONDITIONS OF DYNAMIC SORPTION OF SOME ESSENTIAL OILS FROM AQUEOUS SOLUTIONS

L. M. Voitko and A. N. Kharin

In our previous researches [1,2,3] we explored the patterns of dynamic sorption of certain essential oils from aqueous solutions by granulated activated charcoals. We explored the sorption of coriander oil and the essential oil of eugenolic basil as typical representatives of the oils whose aqueous solutions contain, by and large, only one substance.

The predominant substance in aqueous solutions of coriander oil is d-linalool (at least 90% of the water-soluble portion of the oil) [2], while the predominant constituent in solutions of eugenolic basil oil is eugenol (up to 97%) [2].

We found that the time of protective action and of the distribution of the sorbed oil along the charcoal bed until it "gets through" varies regularly with the length of the bed and conforms satisfactorily with the requirements of the Zhukhovitsky, Zabezhinsky, and Tikhonov theory [4,5], provided the parameters for the conditions of the dynamic tests do not exceed a certain value.

EXPERIMENTAL

The principal parameters governing dynamic absorption are the specific rate of flow of the solution (α) and the mean diameter of the charcoal grains (d) * (cf diagram).

The diagram gives the values of the parameters α and d, at which the applicability of the theory of Zhukhovitsky and his associates is fairly satisfactory.

In this diagram, the solid line marks the boundary of the region in which the theory holds good for sorption on any of the grades of charcoal tested (Birch Nos. 2 and 4, Kernal No. 6, and Anthracite No. 3 (Table 1). This region is somewhat wider for the most porous of these - the birch charcoal. Its conventional boundaries are denoted by the dashed line in the diagram.

The departures from the theory increase as the values of α and d rise, due to a change in the sorption kinetics, the limiting role being transferred from external diffusion to the internal [2,3]. To the extent that internal diffusion plays a part in the rate of sorption of dissolved substances by charcoal grains, we observe departures from the theory of Zhukhovitsky and his associates, the premise of which is the assumption of the limiting role of external diffusion [4,5]. Insofar as the deviations from this theory are due to internal diffusion, their extent will depend on the grade of charcoal [3]. At low values of α and d,

* The notation and the dimensions are the same as in our previous papers [1,2,3].

Diagram Showing the Values of α and d to Which the Zhukhovitsky Theory Applies

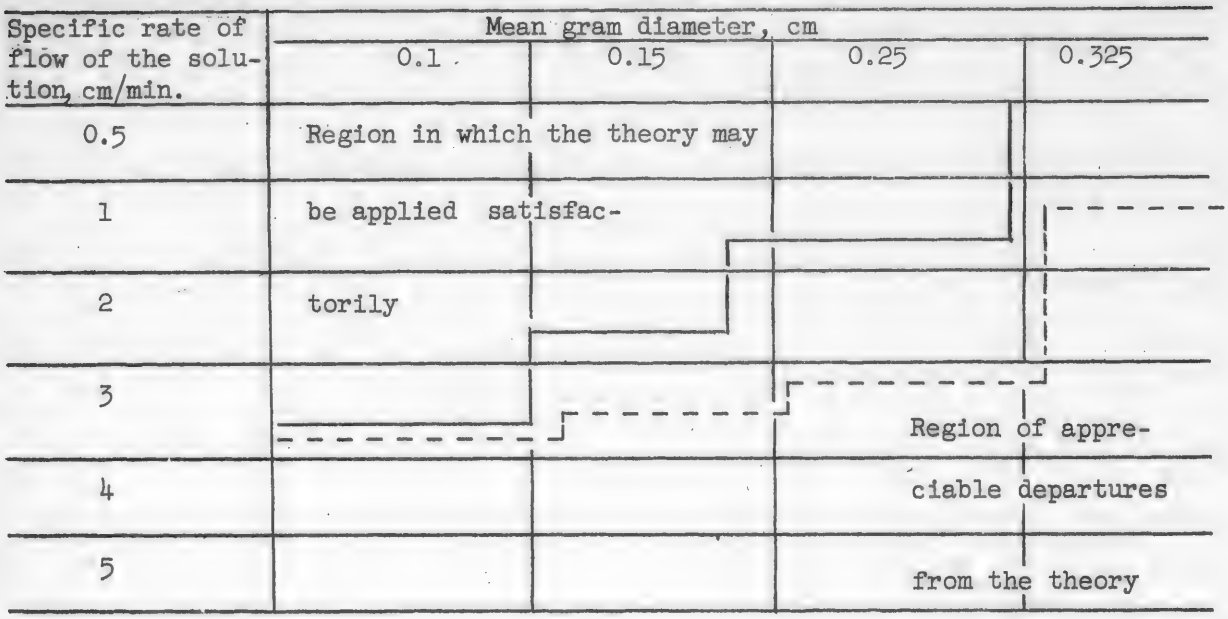

TABLE 1

Characteristics of the Charcoals Tested and Sorption Isotherms of the Essential Oils

Charcoal	Gravimetric density Δ in g/cc	Apparent density δ (g/cc)	True density ρ (g/cc)	Porosity (%)	Ash, (%)	Moisture (%)	Sorption isotherms at 18-20° $a = z\,(y/y_1 + y)$	
							Coriander oil	Eugenolic basil oil
Birch No. 2.	0.178	0.38	1.85	79.5	0.7	0.2	$a = 0.26 \frac{y}{0.13+y}$	
Birch No. 4.	0.170	0.34	1.83	81.6	0.7	0.2	$a = 0.23 \frac{y}{0.13+y}$	$a = 0.41 \frac{y}{0.19+y}$
Anthracite No. 3.	0.424	0.72	1.98	64.0	3.4	0.8	$a = 0.405 \frac{y}{0.15+y}$	
Kernel No.6.	0.320*	0.55*	1.75*	68.6*	6.2*	20.0	$a = 0.249 \frac{y}{0.05+y}$	

when the dynamic process takes place chiefly as an external-diffusion operation, the behavior patterns of dynamic sorption do not depend upon the grade of charcoal.

We ran seven supplementary series of dynamic tests with coriander oil: (I d‴, I f‴, I d', I f' on Charcoal No. 4 and III d", III f", and III f‴ on charcoal No. 6; cf Table 2), in addition to those described in our previous papers [1,2,3], in order to define more accurately the extent of the deviations from the theory of Zhukovitsky and his associates at high α and d.

*All these values are for a charcoal containing no moisture.

TABLE 2

Results of Dynamic Tests

Series designation	Series characteristics C_o g/liter	α cm/min	$\frac{d}{}$ cm	Charcoal No.	Bed length, cm	Duration of protective action θ_{exper}, minutes	θ_{asympt}, minutes*	θ_{calc}, minutes**
				Coriander oil				
					19	836	123	886
					29	1687	1097	1685
I a"	0.85	0.5	0.25	2	49	3532	3045	3443
					69	5402	4993	5301
					89	7248	6941	7179
					29	403	194	404
					49	1292	1162	1212
I b"	0.85	1	0.25	2	69	2138	2130	2110
					89	3097	3098	3018
					109	4057	4066	3956
					29	179	-158	(196)
					49	539	+328	530
I c"	0.85	2	0.25	2	69	900	815	910
					89	1376	1402	1337
					109	1876	1789	1774
					49	246	98	234
					69	428	368	405
I d"	0.85	3	0.25	4	89	622	638	624
					109	840	908	840
					49	148	-12	146
					69	263	+191	240
I e"	0.85	4	0.25	4	89	366	394	352
					109	474	596	479
					89	225	279	(250)
I f"	0.85	5	0.25	4	109	331	441	343
					129	492	603	(435)
					49	714	715	(485)
					69	1174	1525	1135
I b'	0.85	1	0.325	4	89	1717	2335	1785
					109	2250	3145	(2500)
					89	220	524	200
					109	370	694	380
I d'	0.85	3	0.325	4	129	538	964	540
					89	85	126	90
					109	121	288	129
I f'	0.85	5	0.325	4	129	220	450	213
					19	425	215	425
					29	806	702	830
I g"'	0.85	1	0.15	2	49	1593	1676	(1731)
					69	2542	2650	2647
					89	950	852	944
					109	1100	1122	1115
I d"'	0.85	3	0.15	4	129	1400	1392	1372
					89	430	453	430
					109	563	615	561
I f"'	0.85	5	0.15	4	129	680	777	697

* From Equation (I).

** From Equation (III).

(Continuation)

Series designation	Series characteristics: C_o g/liter	α cm/min.	$\frac{d}{}$ cm	Charcoal No.	Bed length, cm	Duration of protective action: θ exper., minutes	θ asympt., minutes *	θ calc., minutes**
				Coriander oil				
III b"	0.65	1	0.25	2	29	600	379	613
					49	1540	1568	1611
					69	2694	2755	2709
					89	3946	3943	3847
					109	5082	5132	5000
III b"	0.34	1	0.25	2	19	385	-47	368***
					29	1037	959	1117***
					49	2702	2957	2895***
					69	4630	4955	4793***
					89	6736	6953	6736***
III c"	0.34	2	0.25	2	29	427	65	(489)****
					49	1056	1063	(1218)****
					69	1928	2062	2047 ****
					89	2919	3061	2946 ****
					109	3996	4060	3865 ****
I b""	0.81	1	0.1	3	14	1465	684	(1232)
					24	2783	2464	2832
					34	4462	4244	4512
					44	6297	6024	6252
I c""	0.81	2	0.1	3	14	614	-9	616
					24	1265	881	1346
					34	2139	1771	2136
					44	2976	2661	2966
I d""	0.81	3	0.1	3	14	333	-197	327
					24	572	123	572
					34	1258	983	1241
					44	1760	1582	1759
I e""	0.81	4	0.1	3	24	307	145	(280)
					34	516	574	484
					44	729	1003	729
					54	968	1432	977
III b"	0.35	1	0.25	6	20	1998	442	1920
					30	3152	2452	3130
					40	4151	4462	4360
					50	5881	6472	5900
III b"'	0.35	1	0.16	6	20	2427	1629	2360
					30	3826	3639	3930
					36	4677	4845	(4856)
					50	7422	7659	7420
III b"'	0.35	1	0.1	6	20	2730	2589	2700
					30	4718	4599	4610
					40	6458	6609	6540
					50	8382	8619	8500

* From Equation (I).

** From Equation (III).

*** Computed for N - 1.25 and L_1 - 11.

**** Computed for N - 1.5 and L_1 - 35.

(Continuation)

Series designation	Series characteristics C_0 g/liter	α cm/min	$\frac{d}{}$ cm	Charcoal No.	Bed length, cm	Duration of protective action $\theta_{exper.}$, minutes	$\theta_{asympt.}$, minutes *	$\theta_{calc.}$ minutes**
				Coriander oil				
III f"	0.35	5	0.25	6	40	240	-22	258
					50	347	380	350
					70	710	1164	684
III f"'	0.35	5	0.16	6	20	200	-216	204
					40	555	588	543
					60	950	1392	962
III d"	0.35	3	0.25	6	20	100	-645	100
					40	469	699	470
					60	1010	2035	1020
				Eugenolic basil oil				
I b"	0.73	1	0.25	4	29	923	737	985
					49	1246	2237	2290
					69	3704	3737	3695
					89	5182	5237	5135
I c"	0.73	2	0.25	4	49	1095	811	1048
					69	1634	1561	1648
					89	2227	2311	2338
					109	2916	3061	3028
I d"	0.73	3	0.25	4	49	622	427	618
					69	977	927	995
					89	1418	1427	1405
					109	1871	1927	1835
I e"	0.73	4	0.25	4	29	122	-175	(144)
					49	287	+200	294
					69	485	575	504
					89	741	950	744
					109	1084	1325	1004
I b"'	0.73	1	0.15	4	39	2217	2079	2215
					49	2945	2829	2935
					59	3668	3579	3655
					69	4395	4329	4365
I b'	0.73	1	0.325	4	29	534	378	(475)
					49	1580	1878	1565
					69	2960	3378	2825
					89	4174	4878	4125

On the basis of this experimental material, we show in the present paper how to compute the operating time of a charcoal adsorber designed to pick up a dissolved*** essential oil from distillation water under various specified conditions.

It is as yet premature to apply the calculatinns given here to essential oils that we have not investigated, although it is not impossible that they may

* From Equation (I).

** From Equation (III).

*** It should be stated that we have investigated the sorption of essential oils dissolved in water, so that our calculations hold good only for those cases in which the distillation water contains no emulsified oil, the absorption of which may exert an effect that we have ignored entirely.

be useful in the designing of adsorbers for the collection of various other essential oils. Ascertaining whether this is feasible or not requires a continuation of the researches under way.

The recovering of essential oils from distillation water by the adsorption method is an interesting problem, of importance for the essential-oil industry of the USSR. That is why a search for methods of calculation as well as the design and construction of the most advanced adsorbers intended for the collecting of essential oils from distillation water requires persistent attention.

Our calculations of the operational time of charcoal beds in the collecting of a given type of essential oil from distillation water is an approach to this problem on the basis of considerable experimental data, analyzed from the standpoint of modern concepts of the phenomenon of the dynamic sorption of substances by porous sorbents.* Moreover, our experimental data on the dynamics of the sorption of two essential oils from aqueous solutions under laboratory conditions enable us to make certain general recommendations concerning the design of adsorbers and the use of charcoal in them.

Table 1 gives the necessary information on the charcoals used in this research, as well as the isotherms for the sorption of the essential oils on these charcoals, calculated from the experimental data [1,2,3]:

$$a = \frac{zy}{y_1 + y},$$

where a is the quantity of substance adsorbed, expressed in grams per gram; y is the equilibrium concentration, expressed in grams per liter; z is the limiting saturation; and y_1 is the concentration in equilibrium with $a = z/2$. z and y_1 were computed by the method of least squares.

The grains of all the coals were irregular in form. We shall not go into the other details of the coals at this point [1,2,3].

All the series of dynamic tests run by us give the concentration of the test solutions of the essential oils, C_0, in grams/liter; the specific rate of the solution, α, expressed in cc/sq.cm./min or in cm/min** ; and the mean diameter of the charcoal grains, d, in cm. Each series consisted of 3-5 tests, in which the duration of the period of protective action, θ minutes, was determined for various lengths of the coal bed, L, in cm. The time θ was read off when the concentration C of the essential oil in grams/liter appeared behind the bed of charcoal ("the passage").

In all the tests with coriander oil and charcoals 2, 3, and 4, $C = 0.04$ gram/liter; $C = 0.03$ gram/liter in the tests using charcoal 6; and $C = 0.07$ gram/liter in the tests with eugenolic basil oil.

Table 2 summarizes the results of our dynamic tests. The value of $\theta_{asympt.}$

---

*The specialized literature contains endeavors to generalize computations of adsorbers for essential oils, but they are based upon extremely limited experimental data and are based upon the recommendations made in the works of Voznesensky [6], which cannot be regarded as satisfactory, inasmuch as they, in turn, are based upon the theory of Mecklenburg and Kubelk, which was criticized justifiably long ago [7]. In some of the papers in which an effort is made to obtain a generalized computation for adsorbers of essential oils not only are the underlying premises known to be false, but even the calculations prove to be full of errors. This is true of the paper by Markov [8], for instance, which is recommended, unfortunately, in several manuals on the processing of crude essential oils [9].

**For calculation of the true mean linear velocity of solution α, it is necessary to divide by the average percentage of free cross section between the charcoal grains, K.

was calculated from the asymptotic formula of Zhukhovitsky, Zabezhinsky, and Tikhonov:

$$\theta_{as} = KL - \tau_{as} \text{ ; where}$$

$$\tau_{as} = \frac{G}{\beta}\left[-0.308 + \frac{\sigma}{\sigma - 1}\left[\frac{1}{\sigma} 2.3 \log 2\left(1 - \frac{C}{C_0}\right) - 2.3 \log 2 \frac{C}{C_0}\right]\right], \qquad (I)$$

$K = \frac{G}{\alpha} + \frac{\varkappa}{\alpha}$ is the protective action factor, in minutes per cm; $\varkappa$ is the percentage of free cross section between the charcoal grains. $\varkappa$ was taken as 0.5 in calculating θ_{as} for the charcoals 2 and 4, while we neglected the $\varkappa/\alpha$ term for the denser charcoals 3 and 6, and assumed that $\underline{K} = G/\alpha$;

$G = \frac{a_0 \cdot \Delta \cdot 1000}{C_0}$ is the Henry coefficient, a dimensionless quantity; $\underline{a}_0$ is the adsorption, in grams per gram, in equilibrium with C_0, in grams per liter, computed from the equations for the sorption isotherms; $\sigma = 1 + \underline{p}$, where $p = C_0/\underline{y}_1$, a dimensionless quantity; β is a kinetic coefficient, computed from the equation we have derived, applying to both of the essential oils:

$$\beta = 0.0252 \cdot \frac{\alpha^{0.5}}{d} \text{ per minute.} \qquad (II)$$

The values of $\theta_{calc.}$ were computed from the semiempirical equation tried out by us:

$$\theta_{calc} = KL - \tau_{as} \frac{NL}{L_1 + L}, \qquad (III)$$

where $\underline{K}$, $\underline{L}$, and τ_{as} have the same significance as in Equation (I), while $\underline{N}$ and L_1, constants for the series, are functions of α and $\underline{d}$.

We derived Equation (III) by introducing empirical corrections into Equation (I), inasmuch as the latter did not give a true picture of the shape of the function θL in the region of marked deviations from the theory of Zhukhovitsky and associates (cf the diagram), and indicated the changes in $\theta(L)$ only for the asymptotic region in the area where this theory can be used satisfactorily, i.e., at large values of θ and $\underline{L}$ [approximately at $L \geqslant 7\alpha/\beta$ (when $C/C_0 \sim 0.05$ and $\underline{p} \sim 3$) and at $L \geqslant 3\alpha/\beta$ (when $C/C_0 \sim 0.1$ and $\underline{p} \sim 3$)].

In our search for a form of the $\theta(L)$ function that would be fairly satisfactory for all values of α and $\underline{d}$, our prinicpal objective was to cover both the asymptotic and the pre-asymptotic regions of changes in $\theta(L)$; this is particularly important at large values of α and $\underline{d}$, at which the asymptotic region is not reached even when $\underline{L}$ exceeds 100 cm (as in the series I f' and I f").

In the pre-asymptotic region of changes in $\theta(L)$, the difference between $\underline{KL}$ and $\theta_{exper.}$ increases with increasing $\underline{L}$. At low values of α and $\underline{d}$, (when the theory may be employed satisfactorily; cf the diagram), the limit of the increase in this difference nearly coincides with $\tau_{as.}$ as computed by the theory of Zhukhovitsky and associates (I); when α and $\underline{d}$ as well as $\underline{L}$, are large, the difference $\underline{KL} - \theta_{exper.}$ becomes greater than $\tau_{as.}$. The factor $\underline{N}$ we have introduced into Equation (I) denotes the extent to which the ultimate value of $\tau = KL - \theta_{exper.}$ deviates from the value called for by the theory of Zhukhovitsky and and associates, due to the effect of internal diffusion upon the progress of the dynamic sorption of dissolved substances, which is ignored by the theory. When $\underline{N}$ is equal or close to 1, Equation (III) coincides with (I) as $\underline{L} \rightarrow \infty$. In the limit (as $L \rightarrow \infty$) the factor $L/(L_1 + L)$ equals 1 at any given value of L_1. This latter quantity may be so chosen for each series of tests at a given $\underline{N}$ in such a manner as to make the period of protective action, computed from Equation (III), vary throughout the range of tested bed lengths in fairly satisfactory conformity with the experimental findings.

The values of $\underline{N}$ and L_1 for all the series of tests are listed in Tables 3, 4, and 5.

Consideration of the data in Tables 3 and 4 leads us to conclude that the values of $\underline{N}$ and L_1 agree for the test series with coriander oil and the eugenolic oil, respectively (with the exception of L_1 in in the series Ie"). In the case of the charcoals 2 and 4 (Tables 3 and 4) $\underline{N}$ and L_1 rise rather regularly with the rise in α and $\underline{d}$, which can be represented by the curves $N(d)$ and $L_1(d)$ at α = constant, and $N(\alpha)$ and $L_1(\alpha)$ at $\underline{d}$ = constant. These curves enable us to determine the values of $\underline{N}$ and L_1, for any values of α and d within the limits indicated in the diagram (some values of $\underline{N}$ and L_1, as found from the curves described above, are given in Table 3 in parentheses).

TABLE 3

Values of N and L_1 for Coriander Oil Charcoals 2 and 4

Specific rate of flow of solution, cm/min	Mean diameter of charcoal grains (cm)							
	0.1		0.15		0.25		0.325	
	$\underline{N}$	L_1	$\underline{N}$	L_1	$\underline{N}$	L_1	$\underline{N}$	L_1
0.5	–	–	–	–	1.0	15	–	–
1	(1.0)	5	1.15	12	1.25	15	1.9	30
2	–	–	–	–	1.4	40	–	–
3	(1.1)	(15)	1.3	30	1.9	75	3.1	130
4	–	–	–	–	3.5	200	–	–
5	(1.7)	40	2.3	100	4.0	250	5.2	350

N and L_1 change more rapidly with a rise in α and $\underline{d}$ for the denser charcoals 3 and 6 (Table 5) than for the charcoals 2 and 4. Inasmuch as the magnitude of the deviations from the theory of Zhukovitsky and associates, represented in the values of $\underline{N}$ and L_1, are related to the internal structure of the charcoals, they will be different for different grades of charcoal. We obtained the values of $\theta_{calc.}$ (Table 2) by inserting the values for $\underline{N}$ and L_1 from Tables 3, 4, and 5 in Equation (III). A comparison of the values of $\theta_{exper.}$ and $\theta_{calc.}$ for all the series of tests indicates that the discrepancies between these quantities does not exceed 5% as a rule, rising to large values only in isolated cases (these values of $\theta_{calc.}$ are given in parentheses).

TABLE 4

Values of N and L_1 for Eugenolic Basil Oil Charcoal No. 4

Specific rate of flow of solution, cm/min	Mean diameter of charcoal grains (cm)					
	0.15		0.25		0.325	
	N	L_1	N	L_1	N	L_1
1	1.1	12	1.25	15	1.9	30
2	–	–	1.4	40	–	–
3	–	–	1.9	75	–	–
4	–	–	3.5	150	–	–

Hence, throughout the range of values of α and $\underline{d}$ shown in the diagram Equation (III) satisfactorily represents the experimental function $\theta(L)$, which opens the way for the use of this equation, with the values of $\underline{N}$ and L_1 given in Tables 3, 4, and 5, for computing the length of the period of protective action of the beds in both the pre-asymptotic and the asymptotic regions of changes in the function $\theta(L)$. At the values of α and $\underline{d}$ at which the tests agree with the theory, Equation (I) may also be employed for this calculation for periods that lie in the asymptotic region.

Now let us consider the conclusions as to the utilization of charcoal in adsorbers that follow from an analysis of the data listed in Table 6, on the saturation of the charcoal beds with the essential oil at various dynamic test conditions. The saturation of the first and second halves of the beds was determined from the curve showing the distribution of the oil along the bed of charcoal [1,2,3].

As we see, at various conditions governing the dynamic tests, the mean saturation of the first half of the bed of charcoal is much greater than that of the second half. This leads us to think that the type of adsorber suggested by Kondratsky [10] is best and most convenient for efficient utilization of charcoal beds, i.e., an adsorber consisting of three identical columns in series. With a setup of this sort, whenever the oil is observed to pass through the charcoal beds of two operating columns, the charcoal in the first column is sent off for extraction. The second column and the third one, now connected in series with it, continue to operate until another "break-through" occurs. In this manner, only the most highly saturated charcoal is sent off for extraction.

Inspection of the magnitude of saturation of charcoal beds of identical length at constant $\underline{d}$ and varying α (series Ia" - If"; Ib' - If') and at constant α and varying $\underline{d}$ (series Ib" - Ib'; If''' and If'; IIIb''' - IIIb") indicates that the most efficient utilization of the charcoal in the adsorber, sent off for extraction from the first half of the bed, may be achieved by running the process at low values of α and $\underline{d}$, i.e., at values that lie within the region where experiment and theory are in satisfactory agreement (cf. diagram).

TABLE 5

Values of $\underline{N}$ and L_1 for Coriander Oil Charcoals 3 and 6

Specific rate of flow of solution, cm/min	Mean diameter of charcoal grains, cm: 0.1 (Charcoal No. 3)		0.1 (Charcoal No. 6)		0.16 (Charcoal No. 6)		0.28 (Charcoal No. 6)	
	N	L_1	N	L_1	N	L_1	N	L_1
1	1.0	6	1.2	6	1.75	30	3.55	100
2	1.0	12	–	–	–	–	–	–
3	1.2	20	–	–	–	–	5.3	150
4	3.65	80	–	–	–	–	–	–
5	–	–	–	–	5.0	150	6.0	250

As we see, choosing the proper values of α and $\underline{d}$ is an extremely important factor in the efficient utilization of charcoal in adsorbers.

If the adsorber is charged with charcoal, the diameter of which is less than 0.25 cm, the value of α may range up to 3 cm per minute without violating the conditions for the most efficient utilization of the charcoal; the calculation may be made from the asymptotic Equation (I), which does not involve allowing for the values of $\underline{N}$ and L_1, which vary with the grade of charcoal.

The use in the adsorber of dense charcoals, which usually possess high adsorption capacity, increases the operating period of the adsorber. In view of the fact that the extent of saturation of the first half of the bed decreases much faster for dense charcoals (Nos. 3 and 6) than for the less dense kinds (Nos. 2 and 4) as α and $\underline{d}$ are increased, the advisability of operating at low values of α and $\underline{d}$ even in these cases cannot be stressed too much.

We wish to express our indebtedness to Prof. A.A.Zhukhovitsky and Prof. A.P. Kondratsky for their advice and constant attention in this research.

SUMMARY

1. An analysis of experimental data on the basis of the dynamic theory of Zhukhovitsky and his associates has determined the range of values of α and $\underline{d}$ in which the experimental data are in good enough agreement with the theory, which makes it possible to employ this theory in calculating the operating time of adsorbers for coriander and eugenol essential oils at given values of α and $\underline{d}$.

2. The range of values of these parameters in which major deviations from the theory are observed, caused by the increasing part played by internal diffusion, has been determined.

Table 6

Characteristics of the Saturation of Beds of Charcoal with Coriander Oil at Various Operating Conditions for the Dynamic Tests

Charcoal	Series	Length of charcoal bed, cm.	Specific rate of flow of solution, cm/min	Diameter of charcoal grains, d, cm.	$\theta_{exp.}$ (min)	Adsorbed along the entire charcoal bed		Adsorption in equilibrium with C_o	Mean saturation of the 1st half of the charcoal bed		Mean saturation of the 2nd half of the charcoal bed	
						$C_o v^*$	% static saturation	a_o (g/g)	a (g/g)	% static saturation	a (g/g)	% static saturation
No. 2	Ia''	89	0.5	0.25	7248	4.07	84	0.23	0.225	98	0.16	70
	Ib''	89	1		3097	3.55	73		0.22	95	0.12	52
	Ib''	109	1		4057	4.67	78		0.225	98	0.17	72
	Ic''	89	2		1376	3.16	65		0.20	87	0.10	43
	Ic''	109	2		1878	4.31	73		0.22	95	0.11	48
No. 4	Id'''	89	3		622	2.15	52	0.20	0.16	80	0.05	25
	Ie''	89	4		366	1.68	41		0.13	65	0.035	17
	If'''	89	5		225	1.30	31		0.10	50	0.027	13
	Ib	109	1	0.325	2250	2.58	52	0.20	0.16	80	0.05	25
	Id'	109	3		370	1.28	26		0.065	31	0.02	10
	If'	109	5		121	0.69	14		0.045	22	0.013	6
	If'''	109	5	0.15	563	3.10	62		0.18	92	0.064	32
No. 6	IIIe''	50	1	0.25	5881	2.75	58	0.22	0.18	71	0.072	33
	IIIb'''	50	1	0.16	7422	3.50	74		0.21	95	0.10	45
	IIIb''''	50	1	0.10	8382	3.96	84		0.215	98	0.14	64
	IIIf''	50	5	0.25	347	0.82	17		0.06	27	0.015	7

*v denotes the volume of liquid flowing, in liters.

3. A semiempirical equation has been found for computing the period of protective action as a function of the length of the sorbent bed, based on the asymptotic equation of the theory. The experimental corrections introduced into the asymptotic equation are reflected in the magnitudes of the equation's constants, which increase as the part played by internal diffusion expands.

Computations of the period of protective action by means of our semiempirical equation exhibit deviations from the experimental data that lie within ± 5% as a rule.

4. Some conclusions are deduced concerning the most efficient utilization of charcoal in adsorbers for collecting essential oils from distillation water.

LITERATURE CITED

[1] A.N.Kharin and L.M.Voitko, J.Appl.Chem. 22, 8, 835 (1949).

[2] A.N.Kharin and L.M.Voitko, J.Appl.Chem. 22, 11, 1247 (1949).

[3] L.M.Voitko and A.N.Kharin, J.Appl.Chem. 22, 12, (1949).

[4] A.A.Zhukhovitsky, Ya.L.Zabezhinsky, and A.N.Tikhonov, J.Phys.Chem. 19, 253 (1945).

[5] A.N.Tikhonov, A.A.Zhukhovitsky, and Ya L.Zabezhinsky, J.Phys.Chem. 20, 1113 (1946).

[6] S.A.Voznesensky. Physicochemical Processes of Water Purification. United Scientific and Technical Press (1934).

[7] A.A.Zhukhovitsky, Ya. L. Zabezhinsky, and D.S.Sominsky, J.Phys.Chem. 13, 305 (1939).

[8] V.V.Markov. Trans. VIEMP, 3, (1937).

[9] I.V.Vinogradova and P.I.Kalugin. The Processing of Crude Essential Oils, 214 (1939).

[10] A.N.Obukhov and A.P.Kondratsky. The Technology of Essential Oil Manufacture. (1946).

Received August 7, 1950.

THE REDUCTION OF CARBON DIOXIDE WITH COKE MADE FROM MINED COAL

V. N. Ershov and V. V. Pomerantsev

Leningrad Polytechnic Institute

The reduction of carbon dioxide by coal is an extremely important reaction in furnaces as well as in gas producers. This reaction plays an exceptionally important role in metallurgy as well.

It has been investigated experimentally, under precise hydrodynamic conditions, only with electrode carbons, however [1]. And yet data on the reactivity of coke made from natural fuels, with allowances made for the hydrodynamics of the process, would be very useful in further research on processes that are of such importance in many branches of engineering.

The absence of research along these lines is due, on the one hand, to the difficulty of preparing geometrically regular samples of coke made from mined coal, and, on the other, to the presence of rather high percentages of ash in these coals. The latter factor affects the true course of the reaction considerably. This distorting effect of ash is due chiefly to the fact that a constantly spreading film of ash is formed on the surface of the coal as it burns, not to mention the possible catalytic action of the ash. The process must be carried out at comparatively low temperatures to eliminate the effect of ash film, the reaction rate being low at these temperatures and the effect of the ash film upon the progress of the reaction being negligible.

Another reason why investigating this process in the low-temperature region may furnish more dependable kinetic characteristics of a coal is that the reaction rate is limited only by the reactivity of the coal, the possible errors due to diffusion factors in the process being very slight under these conditions. But at low temperatures the determination of the amount of coal that has reacted from the data of volumetric gas analysis involves very large errors, inasmuch as the percentage of carbon dioxide in the reaction products drops very rapidly as the temperature is lowered.

It is obvious that these difficulties may be overcome in two ways: first, by employing new and more effective methods of gas analysis, and, second, by utilizing a gravimetric method for determining the amount of reacted coal.

Along the lines of the first, more general approach, we have developed a method of utilizing optical-acoustic gas analysis in the investigation of the oxidation (combustion) of coal and the reduction of carbon dioxide by coal. This problem will be dealt with in a separate paper.

The present paper sets forth an experimental method that provides an accurate hydrodynamic setup for the process and is free of the defects mentioned above, which have made it impossible to follow the progress of the reaction at temperatures below 900-950°C.

The endothermic nature of the reaction makes it comparatively easy to study. Moreover, the kinetic constants of coals in the reaction $C + CO_2 = 2CO$ can be employed in evaluating the characteristics of the $C + O_2 = CO_2$ reaction, which is extremely hard to investigate because of its exothermic nature.

EXPERIMENTAL

The experimental setup is shown diagrammatically in Fig. 1.

It consists of two Silit furnaces, one being used as a preheater for the reagent gas. The second furnace – the reactor – contains the sample under test. The sample consists of a coal surface, prepared by pressing pulverized coal into a special semicylindrical porcelain boat. The area of the coal surface ranged from 4 to 5.4 sq. cm; the sample weighed 1.5 to 1.7 grams; and the boat weighed 1.1 to 1.3 grams. The reactor tube was assembled so as to have the coal surface form one of the sides of a slitlike passage through which carbon dioxide was passed during the experiment. The reactor tube is shown diagrammatically in Fig. 2.

The temperature of the gas at the surface of the coal was measured with platinum – platinum-rhodium thermocouples with a $\underline{d}$ = 0.1 mm. The installation of the reactor tube and the arrangement of the thermocouples are shown in Fig. 2.

During the run the carbon dioxide was supplied from a tank; after being desiccated with calcium chloride, it entered the reactor tube, which consisted of the following units connected in series: the preheater, filled with broken porcelain; the supply unit, shaped like a slit 60-80 diameters long, designed to stabilize the flow; the reactor, in which the test sample

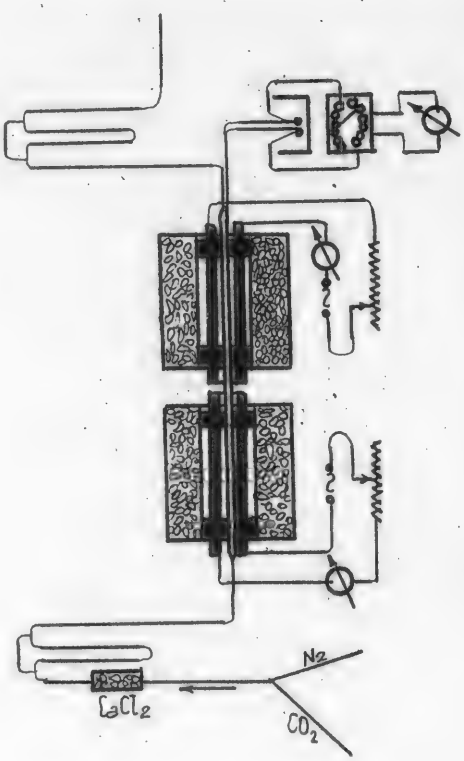

Fig. 1. Experimental layout.

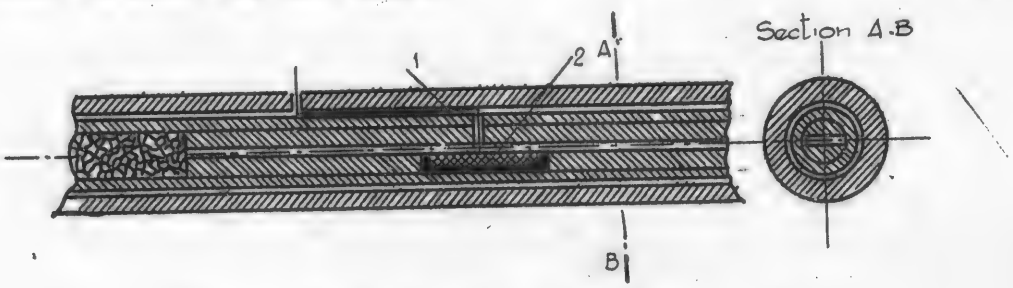

Fig. 2. Cross section of the reactor tube.

1-Thermocouple; 2-coal.

was placed; and the exhaust, with the same slit cross-sectional area.

The reactor tube could be disassembled easily, so that the boat could

be removed quickly for weighing.

The test samples of coal were prepared as follows. The mined coal was converted into coke by heating it to 850° C in a current of nitrogen until no more volatiles were given off. Then the coke was pulverized, the 70-80 μ fraction being used. The resultant powder was pressed into the boat and again roasted in a current of nitrogen at 900°C until its weight remained constant, after which its hydrodynamic stability was tested with respect to the carrying away of dust from the surface.

As soon as the run was over, the sample was immediately placed in a sealed ampoule to reduce adsorption phenomena to a minimum.

The tests were run as follows. The coal was slowly heated to the desired temperature, in the course of 1.5-2 hours, in a current of nitrogen; when the temperature was reached, the nitrogen was shut off and replaced by carbon dioxide. The temperature was kept constant during the run within ± 5°C. The run lasted from 15 minutes to 2 hours, depending upon the temperature.

The coal was also cooled off in a current of nitrogen, for 1.5 to 2 hours, after which the reactor tube was disassembled, and the coal was placed in an ampoule and weighed therein.

In our tests we measured: 1) the gas consumption before and after the reaction; 2) the temperature of the gas at the surface of the coal; and 3) the amount of coal that reacted.

The experiments covered the range 600-1000°C. The input of carbon dioxide amounted to 1.2 cc per sec. The cross-sectional area of the reactor slit was 0.15 sq. cm.

Coke made of Urals coal was tested, with a few electrode carbons for the sake of comparison. The experimental data were processed as follows:

The reaction rate Δg was computed from the loss of weight U_p:

$$U_p = \frac{\Delta g}{S\tau} \quad \frac{g}{cm^2 \cdot sec} \qquad (1)$$

referred to the unit of reacting surface of the coal, S, or:

$$U_p' = \frac{U_p}{12} \frac{g \cdot mole}{cm^2 \cdot sec} \qquad (1')$$

in moles of C or CO_2.

The apparent velocity constant $K_{app.}$ was calculated from the value of U_p' on the assumption that the reaction is of the first order, which is highly probable at temperatures above 650-700°C, [2]:

$$U_p' = K_{app} \cdot C_o = K_{app} \cdot \frac{P_o}{RT} \cdot \qquad (2)$$

Here C_o is the concentration of the reacting gas in the current; P_o is the partial pressure of the gas in the current; R is the gas constant; and T is the temperature of the reacting gas.

From Equation (2) we get

$$K_{app.} = \frac{U_p' RT}{P_o} \cdot \qquad (3)$$

In our tests, where the concentration of carbon dioxide in the gas flow is 100%, Equation (3) takes on the following form:

$$K_{app} = \frac{U_p' T}{0.141} \text{ cm/sec.} \qquad (3')$$

In establishing the true kinetic characteristics of the given kind of coal in the general case, we must distinguish between the kinetic and diffusion components of the overall process resistance

$$\frac{1}{K_{app.}} = \frac{1}{K_{true}} + \frac{1}{\alpha_{dif.}} . \qquad (4)$$

Here $K_{true} = K_o e^{-\frac{E}{RT}}$ is the velocity constant; E cal/mole is the activation energy; K_o cm/sec is the coefficient of the exponential term; and α_{dif} cm/sec. is the coefficient of material exchange.

The value of $\alpha_{dif.}$ is determined, by analogy with diffusion and heat emission, from the relationships between the criteria

$$Nu_{dif.} = \underline{f}(Re, Pr_{dif.}) \text{ or } Nu_{dif.} = \underline{f}(Pe_{dif.}).$$

In our calculations we employed the formula for laminar flow in a flat channel:

$$Nu_{dif.} = 13.2\, Pe_{dif}^{0.23} \left(\frac{e}{d}\right)^{-0.5} .$$

As calculations of the conditions used in the present research have shown, the $1/\alpha_{dif}$ term is negligibly small compared to the $1/K_{true}$ term, which indicates that the process takes place in the kinetic region. Hence, we may assume that $K_{app.} = K_{true}$ with a high degree of accuracy.

The principal data on part of the tests are listed in Tables 1 and 2, while the values of log K are plotted in Fig. 3 as a function of the temperature.

TABLE 1

Results of Tests of Chernogorsk Coal

T (°K)	τ (sec)	$\Delta g \cdot 10^4$ (g)	$U_p \cdot 10^6$ (g/cm² sec)	$K \cdot 10^4$ (cm/sec)	Re	$Pe_{dif.}$	$Nu_{dif.}$	α_{dif} (cm/sec)
880	4800	45	0.23	14.7	10.7	5.3	4.5	21.4
910	4800	75	0.37	23.3	10.7	5.3	4.5	22.7
915	4800	55	0.29	18.6	10.7	5.3	4.5	22.8
925	3600	82	0.50	32.3	10.5	5.3	4.5	23.0
960	2400	92	0.96	65.7	10.2	5.1	4.4	23.8
985	1800	96	1.33	92	10.2	5.1	4.4	24.7
1040	1800	210	2.92	216	10.1	5.1	4.4	26.7
1100	2400	960	9.3	660	9.8	4.9	4.4	29.0
1100	1800	620	7.5	532	9.8	4.9	4.4	29.0
1120	1800	685	8.9	631	9.7	4.9	4.4	29.9
1170	900	530	14.7	1240	9.6	4.8	4.4	31.6

The slope of the straight lines drawn through the experimental points for each coal yielded the values of the activation energy E and of K_o, the coefficient of the exponential term. The resultant kinetic characteristics are listed in Table 3.

The experimental data revealed that the values of the velocity constants for the different coals came closer together as the temperature was raised.

TABLE 2

Results of Tests of Coke Made from Bogoslovsky, Kizel, Chelyabinsk, and Bulanash Coals and of Electrode Carbon

	Bogoslovsky coke						Electrode carbon					
T, °K	875	945	995	1045	1115	1165	875	935	975	1040	1130	1175
$U_p \cdot 10^6$, g/cm²·sec	0.38	1.15	3.68	3.6	10.5	15.8	0.067	0.15	0.36	1.47	5.35	7.4
$K \cdot 10^4$ (cm/sec)	23.6	77	210	265	830	1315	4.16	10.0	24.8	109	430	615

	Kizel coal from the seam 164 meters deep						Kizel coal from the seam 174 meters deep					
T, °K	930	985	1060	1090	1165	1250	920	960	1000	1065	1100	1190
$U_p \cdot 10^6$, g/cm²·sec	0.064	0.16	0.52	1.62	3.18	8.45	0.07	0.17	0.38	1.37	1.85	5.9
$K \cdot 10^4$, cm/sec	3.96	11.1	39	125	262	750	4.56	11.2	27.3	103.3	145	496

	Chelyabinsk coke						Bulanash coke					
T, °K	890	925	975	1000	1100	1165	1235	1020	1075	1130	1165	1255
$U_p \cdot 10^6$, g/cm²·sec.	0.15	0.29	0.48	1.5	5.4	10.3	15.7	0.043	0.22	0.52	1.37	3.20
$K \cdot 10^4$ cm/sec	9.45	19.0	33	108	420	853	1370	3.1	16.7	41.5	113	284

The results of our tests are shown in Fig. 4, together with the functions secured by other authors.

As we see in Fig. 4, the straight lines $\log K = \underline{f}(1/T)$ for all the coals appear to originate at a common pole, with the coordinates $K_0 \cong 10^2$ cm/sec and $T \cong 2000°K$, in the temperature region below 2000°K.

This pole is not a point with the given coordinates, but rather a diffused region close to it, but for all practical purposes it is quite permissible to consider it to be a point with the coordinates cited.

We can then set up the following equation:

$$\log K_0 = 2 + 0.1095 \cdot 10^3 E, \qquad (5)$$

correlating the kinetic characteristics of the $C + CO_2 = 2CO$ reaction for coals of quite different structure at temperatures below 2000°K.

The values of the activation energies derived at the present time for various coals are listed in Table 4.

The differences in the activation energies for different coals are quite considerable. Since corrections were made for diffusion resistance and for the effect

TABLE 3

Kinetic Characteristics of Various Coals

Coal field	$E \cdot 10^3$ (cal/mole)	K_0 (cm/sec
Bulanash coal (coke, t 900°C)	51.0	$4.0 \cdot 10^7$
Kizel coal, seam 164-meters deep (coke, t 900° C)	43.2	$6.3 \cdot 10^6$
Kizel coal, seam 174 meters deep (coke, t 900° C)	41.4	$3.5 \cdot 10^6$
Electrode carbon	39.3	$2.0 \cdot 10^6$
Chelyabinsk coal (coke, t 900°C)	38.4	$1.26 \cdot 10^6$
Chernogorsk coal (coke, t 900°C)	35.3	$7.0 \cdot 10^5$
Bogoslovsky coal (coke, t 900°C)	33.0	$4.0 \cdot 10^{-5}$

TABLE 4

Values of the Activation Energies of Various Coals

Coal	Researcher	$E \cdot 10^3$ (cal/mole)	Literature
Anthracite	Clement et al	83	[4]
Anthracite	Kreisinger, Ovitz, Augustine	50 45	[3]
Bulanash coal (coke)	Ershov and Pomerantsev	51	
Bituminous coke	Clement et al	43.8	[4]
Kizel coal, 164 meters (coke)	Ershov and Pomarantsev	43.2	
Kizel coal, 174 meters (coke)	Ershov and Pomarantsev	41.4	
Charcoal	Clement et al	42.7	[4]
Electrode carbon	Ershov and Pomarantsev	39.3	
Bituminous coke	Sherman and Blizzard	38.5	[5]
Chelyabinsk coal (coke)	Ershov and Pomarantsev	38.4	
Chernogorsk coal (coke)	Ershov and Pomarantsev	35.3	
Peat coke	Klimov and Landn	33,85	[6,7]
Bogoslovsky coal (coke)	Ershov and Pomarantsev	33.0	

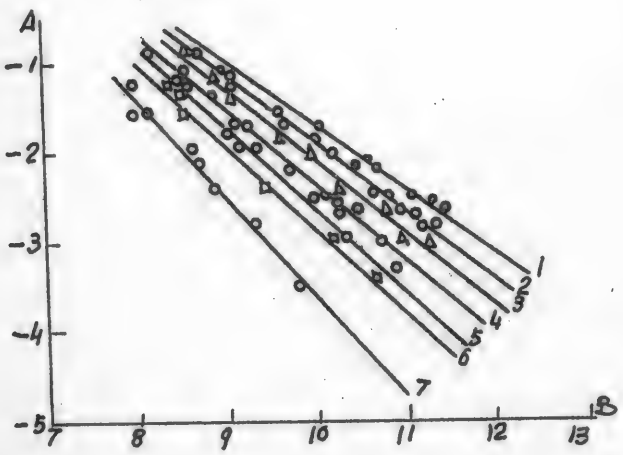

Fig. 3. Velocity constants as a function of temperature for coke made of Urals coals.

A-log K; B- $1/T \cdot 10^4$. 1) Bogoslovsky coal; 2) Chernogorsk coal; 3) Chelyabinsk coal; 4) electrode carbon; 5) Kizel coal; 6) Kizel coal; 7) Bulanash coal.

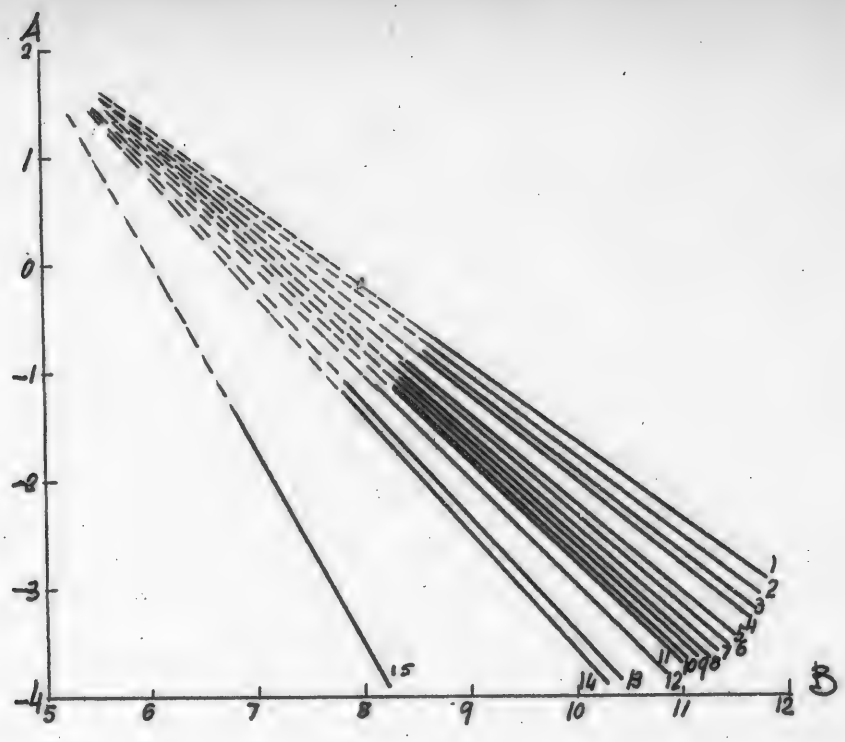

Fig. 4. Variation of the velocity constant with temperature for cokes of various coals.

A) Log K; B) $1/T \cdot 10^4$. 1) Bogoslovsky coal; 2) peat coke; 3) Chernogorsk coal; 4) shale coke; 5) Chelyabinsk coal and bituminous coke; 6) electrode carbon; 7) electrode carbon; 8) Kizel coal, seam 174 meters deep; 9) charcoal; 10) Kizel coal, seam 164 meters deep; 11) bituminous coke; 12) anthracite; 13) anthracite; 14) Bulanash coal; 15) anthracite.

of the reversible reaction in working up all the experimental material, these values of activation energies may be considered fairly reliable for temperatures below 2000°K.

It is highly significant that coke made from young coals has a much lower activation energy than coke made from hard coal and anthracite. If we ignore the single anthracite value from Clement's experiments, the values of the activation energy all fall within the range of $33 \cdot 10^3 - 51 \cdot 10^3$ cal per mole.

SUMMARY

1. A method has been developed that enables us to determine the kinetic characteristics of the $C + CO_2 = 2CO$ reaction for various coals at temperatures below 950° C. This method may be recommended as a way of determining the reactivity of coke made from mined coal.

2. The results of working up extensive experimental material, covering sixteen samples of coal, yield the following formula:

$$K = 10^2 e^{\frac{E}{R}\left(\frac{T}{2000} - 1\right)} \text{ cm/sec.}$$

for calculating the reaction rate in the temperature range from 900 to 2000° K.

3. The values of the activation energy may be taken to lie within the $33 \cdot 10^3$ - $51 \cdot 10^3$ cal/mole range, as shown in Table 4.

4. The overall (apparent) reaction rate should be determined from the equation:

$$\frac{1}{K_{app.}} = \frac{1}{K} + \frac{1}{\alpha_{dif.}} .$$

LITERATURE CITED

[1] Vulis and Vitmann, J.Tech.Phys., 11, 6 (1941).

[2] Semechkova and Frank-Kamenetsky, J.Phys.Chem. 1940, No. 3.

[3] Kreisinger, Ovitz, and Augustine, Bur. Mines Tech. 137 (1917).

[4] Clement, Adams, and Haskins, Bur. Mines Bull. 7 (1910).

[5] Sherman and Blizzard, Trans. Am. Inst. Mining and Met. Engrs., 69 (1923).

[6] Klimov and Lanin, Chemistry of Solid Fuels, 1 and 6 (1933).

[7] Klimov. New Methods for the Thermal Processing of Peat. United State Scientific and Technical Press (1939).

Received July 4, 1950.

THE TRANSITION OF A CATALYST INTO A HETEROGENEOUS STATE AND THE UNDERLYING CAUSES OF THIS PHENOMENON*

V. K. Tsyskovsky and N. A. Kiseleva

The assertion was made at an earlier date [1] that the physicochemical properties of a colloid quasiheterogeneous catalyst change during the initial period of oxidation, causing the catalyst to leave the reaction zone.

Our findings, which were not universal, naturally gave rise to further problems that called for solution. One of the factors that was unclear, in particular, was whether the physicochemical properties of the catalyst would change under different oxidation conditions (chiefly as the result of changes in the composition of the raw material and of the catalyst). Moreover, we had to discover the underlying reasons for the transition of the catalyst into a new physicochemical state.

The present paper does not aim at a profound study of the relationship between this phenomenon and changes in the chemical composition of the raw material, inasmuch as that problem is the subject of a separate investigation. We have run tests that have demonstrated the repeatability of the phenomenon no matter what the properties of the material to be oxidized are.

EXPERIMENTAL

In order to shed light on these problems we oxidized individual fractions of kerosene (that differed both in respect of their group composition and in their boiling points) with a catalyst – manganese binaphthenate – whose concentration remained constant throughout the tests (all the other conditions remaining the same). All the fractions were oxidized in such a manner as to enable the recording of the initial state of the catalyst photocolorimetrically, yielding a series of curves.

These tests indicated (Table 1 and Fig. 1) that the shift of the catalyst into a new physicochemical state is repeated independently of the group composition of the substrate or the latter's physical properties and that this is a regular behavior pattern.

Careful analysis of the data in Table 1 indicates that the duration of the initial period of the catalyst is a definite function of the physicochemical properties of the fractions to be oxidized.

In the oxidation, for example, of Fractions 1 and 2 (Table 1), which possess

*Report II of a series on the action of colloid quasiheterogeneous catalysds in the liquid-phase oxidation of kerosene fractions.

TABLE 1

Fraction No.	Fraction boiling range, °C	Group composition of fractions, wt.%			Duration of catalyst's initial state, minutes
		Aromatic hydrocarbons	Cyclanes	Alkanes	
1	220-240	15.0	30.0	55.0	3.0
2	240-260	14.0	27.0	59.0	11.0
3	240-260	16.63	12.51	70.86	13.5
4	240-260	21.93	11.8	66.3	15.15
5	240-260	25.2	5.98	68.3	21.0

similar group compositions but have different molecular weights, the initial periods were not commensurable, being shorter in the oxidation of fractions with lower molecular weight. This will be discussed later, since it proves to be closely related to the causes that underlie the changes taking place in the chemical composition of the catalyst.

The oxidation of fractions of similar molecular weight but different group composition indicated that the duration of the initial catalyst state depends solely upon the concentration of aromatic hydrocarbons: the higher the percentage of aromatic hydrocarbons in a given fraction, the slower was the change of the catalyst to a new physicochemical state (Fig. 1, Fractions 2, 3, 4, and 5).

This is not fortuitous, for we know that when some aromatic hydrocarbons are oxidized, they are converted into phenols, which are known to be powerful negative catalysts of oxidation reactions even in minute concentrations.

It may be assumed that the higher the concentration of aromatic hydrocarbons in the fraction and the higher the percentage of phenols in the substrate undergoing oxidation, the more will the oxidation reaction be retarded and the longer, therefore, will the period of the catalyst's initial state be.

As will be seen below, these phenomena are closely interrelated.

To eliminate any suspicion that the degeneration of the catalyst takes place only when manganese naphthenate is used, we explored oxidation reactions in which the naphthenates of other metals were employed as catalysts. The other conditions of the tests were the same as before, including the composition of the raw material.

We chose the naphthenic acids to form the catalyst radical only because they form salts with every metal that produce extremely stable colloid systems in hydrocarbons, as one of the present authors has shown [2]. That is why we did not consider the introduction into the tested

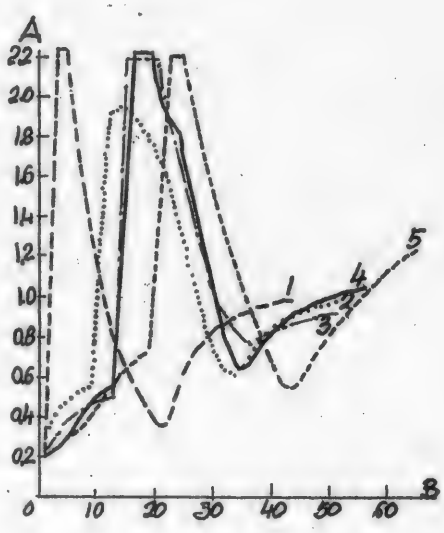

Fig. 1. Effect of the percentage of aromatic hydrocarbons in a kerosene fraction upon the duration of the catalyst's initial state.

A-Log i_0/i ; B-time, minutes. Temperature ranges of kerosene fractions, °C, and respective percentages of aromatic hydrocarbons: 1) 220-240; 15.0; 2) 240-480, 14.0; 3) 240-260, 16.43; 4) 240-260, 21.93; 5) 240-260, 25.2.

catalyst's radical of any other organic acid in our exploration of the effect of various cations. We were justified in supposing that the observed phenomenon would be repeated no matter what organic radical the catalyst contained.

Metals of Groups VII and VIII: Mn, CO, Fe, and Ni, were tested.

The naphthenates of these metals were added to the substrate to be oxidized in various concentrations of the metal contained in the naphthenates: in one set of tests the metal was added in equal parts by weight, and in the other in equimolar proportions.

We found that no matter how the cation in the catalysts was changed, the latter regularly passed through all the transformation stages involving the acquisition of new properties (Table 2).

TABLE 2

Cation entering into composition of catalyst	Duration of catalyst's initial stage, minutes	
	Catalyst concentration	
	By weight	Equimolar
Mn	16.0	16.0
Co	31.0	15.3
Fe	19.5	13.0
Ni	122.0	124.0

The only way to discover the reasons for the transition of the catalyst from one state to another was a thoroughgoing study of the substance that settled out of the solution. This was done by setting up an experiment on the oxidation of a substrate of constant composition with a neutral manganese naphthenate of arbitrary concentration. Oxidation was continued until the photocolorimeter recorded an appreciable drop in the ratio of the logarithms of the photocurrents, i.e., until the curve of acid numbers indicated a sharp rise.

Then oxidation was stopped, and the substrate was cooled and filtered through a colloid filter. After the precipitate had been carefully washed on the filter to remove the entrained substrate and then dried, it was found to be a light-yellow crystalline powder.

We found that after what we had previously called the catalyst was removed from the substrate, the latter no longer contained any organic derivatives of manganese. This was confirmed spectrographically, the manganese line being missing in the absorption spectrum.

Hence, we could assume that the catalyst had retained all the metal that it had contained at the start of oxidation, despite its qualitative changes. This was borne out by analysis of the substance recovered. The total manganese in the catalyst (based on the weight of the substrate) was the same as the weight of metal found in the precipitate.

Nevertheless, though the percentage of manganese in the original catalyst was 10.73% (of the naphthenate), its percentage in the resulting substance had risen to 18.7% (of the dry precipitate). This circumstance, plus chemical analysis of the crystalline precipitate extracted from the substrate after the latter had been oxidized, indicated that the chemical composition of the radical in the original manganese naphthenate had doubtless undergone some change.

Most of the substance recovered consisted of low-molecular organic salts of manganese that were soluble in cold water. The portion that was insoluble in water was decomposed by hydrochloric acid in order to isolate the organic acids that formed part of the radical in the free state.

The acids recovered bore little resemblance to the original naphthenic acids. They were hydroxy acids and tarry substances for the most part, and

Diagram and Results of Analysis of the Changed Catalyst

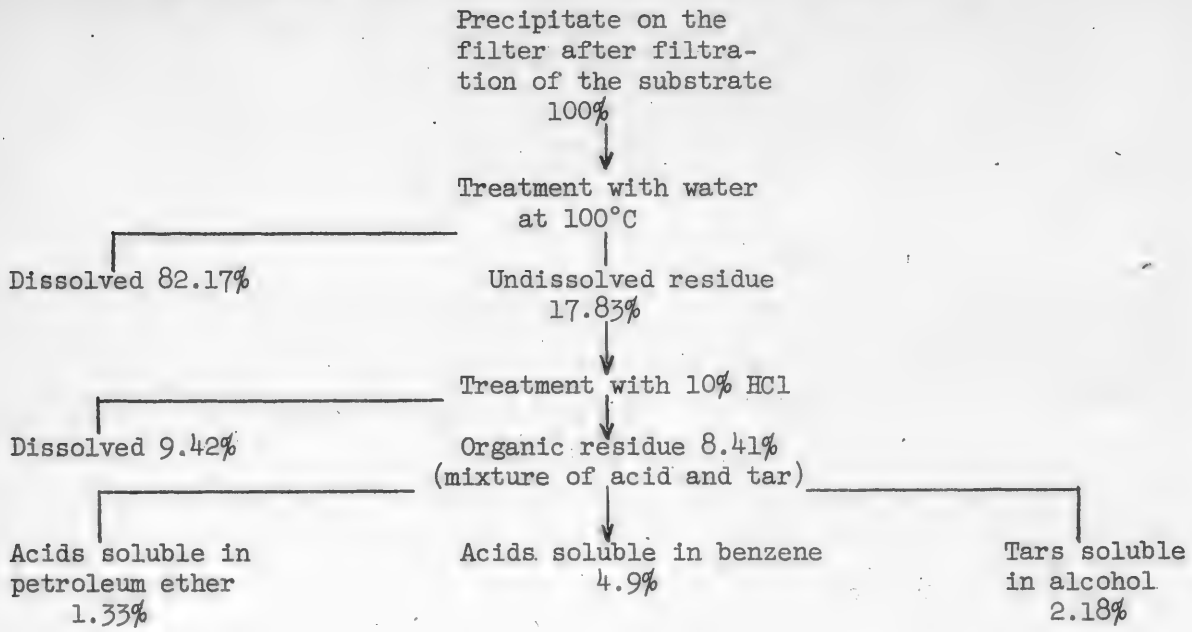
Precipitate on the filter after filtration of the substrate 100%
Treatment with water at 100°C
Dissolved 82.17%
Undissolved residue 17.83%
Treatment with 10% HCl
Dissolved 9.42%
Organic residue 8.41% (mixture of acid and tar)
Acids soluble in petroleum ether 1.33%
Acids soluble in benzene 4.9%
Tars soluble in alcohol 2.18%

contained almost no ordinary carboxylic acids, soluble in petroleum ether.

The mean acid number of the carboxylic acids recovered was only 165 mg KOH/gram, being somewhat lower than the acid number of the naphthenic-acid mixture that formed part of the radical of the original catalyst.

This change in the composition of the radical explains why the catalyst passed from a quasi-heterogeneous state to a heterogeneous one.

Let us consider the reasons for the marked change in the composition of the catalyst and for the appearance of water-soluble organic acids in it.

When the fresh substrate (before oxidation) is analyzed spectrographically with the neutral manganese naphthenate it contains, no carboxyl group is found in the infrared portion of the absorption spectrum.

The spectrogram (Fig. 2), recorded at the instant the catalyst degenerated (i.e., when crystalline particles visible in the field of a microscope appeared in the substrate), did exhibit a carboxyl group in that portion of the spectrum.

The spectrometric results indicate that the appearance of a carboxyl group coincides with a change of state of the catalyst; it is evident, therefore, that oxidation involves the formation of low-molecular acids that can react with the high-molecular radical of the catalyst.

The formation of low-molecular organic acids at the start of the reaction is no doubt also borne out by

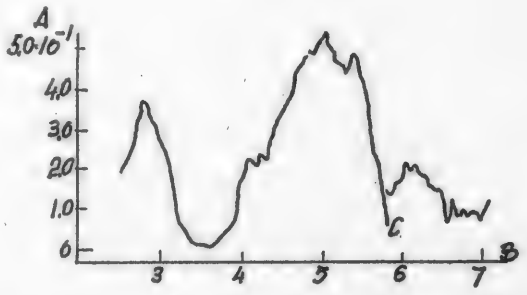

Fig. 2. Spectrogram of a solution of oxidized kerosene with a catalyst present, at the instant a sharp color change occurs.

A) Relative transmission of light II_0/II; B) Wavelength, μ; C) absorption spectrum maximum.

the presence of these acids in the organic radical of the changed catalyst.

This, too, is readily linked to the shortening of the period during which the catalyst is in its initial state as the molecular weight of the substrate is diminished (Fig. 1, Curves 1 and 2).

It has been shown previously [3] that the lower the molecular weight of the substrate, the more low-molecular, water-soluble acids will be formed during its oxidation and the faster will they be formed.

Thus, we now have a definite idea of how the catalyst degenerates. The oxidation reaction sets in as soon as the catalyst is introduced into the heated substrate, various quantities of low-molecular acids being accumulated, depending upon the oxidation conditions (temperature, group composition of the raw material, catalyst concentration, and the like).

The velocity of the reaction between these acids and the catalyst, present in a given concentration, will depend upon the amount of acids of this type produced, which naturally explains the variable time required for the appearance of the crystalline precipitate.

SUMMARY

1. It has been definitely established that high-molecular naphthenate catalysts are decomposed at the very start of oxidation, yielding low-molecular acids.

2. The organic salts (in a colloidal quasiheterogeneous state) exist in the substrate to be oxidized as positive catalysts that efficiently accelerate the oxidation reaction until they become heterogeneous as the result of interaction with the low-molecular acids.

LITERATURE CITED

[1] V.K.Tsyskovsky and N.A.Kiseleva, J.Appl.Chem. 1950, No. 9.

[2] V.K.Tsyskovsky. The Oxidation of Petrolatum and Paraffin. State Fuel Technology Press (1948).

[3] V.K.Tsyskovsky, J.Appl.Chem. 1948, No. 4.

Received March 17, 1950.

THE SYNTHESIS AND INVESTIGATION OF NOPENE

B. N. Rutkovsky and L. A. Alferova

Central Research Institute of Wood Chemistry

By condensing β-pinene with formaldehyde we have synthesized a new, optically-active, bicyclic primary alcohol, 6,6-dimethyl-2-ethylbicyclo-(1,1,3)-heptene-2, which we have named "nopol".

The dehydration of "nopol" to secure a vinylic compound had to be carried out under very mild conditions, since compounds of the terpene class have a pronounced tendency to undergo various kinds of isomeric transformations when acted upon by high temperature and various catalysts.

The use of acids and "acid" reagents in the dehydration of bicyclic terpene alcohols results, in most cases, in a profound change in the whole bicyclic system.

Only a few terpene alcohols are dehydrated by acids or "acid" reagents without exhibiting isomerization. When α-terpineol is dehydrated with potassium bisulfate, for example, a dipentene, terpinolene, is formed. The extreme ease with which terpenes are isomerized by acids and "acid" reagents makes all these methods very harsh and wholly unsuited to the dehydration of terpene alcohols.

There are no references in the literature to the isomerization of terpenes in an alkaline medium. It therefore seemed fitting to consider the possibility of using alkalies to dehydrate nopol. There is an interesting analogy here with the dehydration of β-phenyl ethyl alcohol [1], which has the same side chain arrangement as nopol. It is worthy of note that the primary and secondary phenyl ethyl alcohols behave altogether differently in dehydration. When α-phenyl ethyl alcohol is dehydrated to yield styrene, acid dehydrating agents are usually employed, such as phosphoric acid [2], sulfuric acid [3], potassium bisulfate [4], alumina [5], etc.; alkaline catalysts are no good for this dehydration.

β-Phenyl ethyl alcohol yields styrene only when alkaline agents are used, best being fused potassium hydroxide [1]; acids and "acid" reagents yield an ether.

The β-phenyl ethyl alcohol was dehydrated by an intermittent method as well as by a continuous method at a reaction temperature of 170-175° at standard pressure [1]. Terpene alcohols are dehydrated under extremely mild conditions by Chugaev's xanthogenate method, based upon the decomposition that some derivatives of xanthic acids suffer when they are heated to a comparatively low temperature for a short period. When this is done, none of the reactions requires the use of strong acid reagents, to begin with; secondly, xanthates are decomposed smoothly and readily at 160-180°. By using xanthates, Chugaev was able to secure bornylene instead of camphene when he dehydrated borneol [6], limonene instead of terpinene when dehydrating dihydrocarveol [7], and α-pinene when dehydrating pinocampheol [8].

EXPERIMENTAL

Dehydration of nopol in the vapor phase with Al_2O_3. The alumina, precipitated from aluminum nitrate with ammonia, was washed well and dehydrated at 300°. The nopol was dehydrated in a tube 1 cm in diameter, placed in a special furnace. The length of the Al_2O_3 bed was 40 cm. The furnace temperature was 180-300°C. The pressure in the system was 50 mm Hg. An alcohol fraction with the following constants: d_4^{20} 0.9630; n_D^{20} 1.4905; and α_D^{20} 23.12° (10 cm tube) was continuously fed to the evaporating flask. The alcohol vapors entered the dehydrating tube at a temperature of 190-200°. 10.0 g of the alcohol fraction passed through the tube per hour.

The distillate was the original alcohol:

d_4^{20} 0.9681; n_D^{20} 1.4907; α_D^{20} -23.25°.

Hence, the nopol was not dehydrated under these conditions.

Dehydration of nopol in the vapor phase with pumice. The pumice was washed and calcined in a muffle furnace. The alcohol was dehydrated in the same apparatus that served for the dehydration of the alcohol with Al_2O_3. The pumice bed was 40 cm long. The furnace temperature was 180-200°C. The pressure in the system was 50 mm Hg. The alcohol fraction with the following constants:

d_4^{20} 0.9677; n_D^{20} 1.4925; and α_D^{20} 24.35°,

was fed continuously into the evaporating flask. The alcohol vapors had a temperature of 190-200° upon entering the dehydrating tube. 10 ml of the alcohol fraction was passed through per hour. The distillate consisted of nopol with the following constants:

d_4^{20} 0.9676; n_D^{20} 1.4928; α_D^{20} 24.62,

i.e., the initial alcohol, so that nopol was not dehydrated in this test.

Dehydration of nopol in the vapor phase with potassium hydroxide (on pumice). The potassium hydroxide was applied to the pumice, which was then desiccated at 300°. The alcohol was dehydrated in the same apparatus that served for dehydrating the alcohol with Al_2O_3. The test conditions were the same as in the previous tests. The alcohol fraction, whose constants were: d_4^{20} 0.9677; n_D^{20} 1.4925; and α_D^{20} 24.35°, was fed continuously into the evaporating flask. The test was run with the alcohol entering the evaporating flask at the rates of 12.8 ml/hr, 15 ml/hr, and 23.5 ml/hr.

In no instance was the nopol dehydrated. In every case the distillate consisted of the original alcohol:

d_4^{20} 0.9680; n_D^{20} 1.4931; α_D^{20} 34.51°.

Dehydration of nopol in the liquid phase with anhydrous potassium hydroxide, by the intermittent method. In a flask fitted with a stirrer there was placed 0.75 g of potassium hydroxide (0.0134 mole) - Test 1; 2 g of potassium hydroxide (0.0357 mole) - Test 2; 6 g of potassium hydroxide (0.1071 mole) - Test 3, with 20 g of the alcohol fraction (0.1204 mole) added in each test.

The flask temperature was raised to 175° while the contents were stirred vigorously. No dehydration occurred at all in the first two tests. In Test 3, with a potassium hydroxide: alcohol molar ratio of 0.9:1 in the reaction mass, the mass within the flask gradually turned cloudy and more viscous. Stirring was stopped, and the pressure in the system was reduced to 30 mm Hg, but no distillate was driven off. The flask contained a thick, strongly foaming, light-brown mass.

Hence, the dehydration product of nopol displays a marked tendency toward

polymerization, so that it must be removed from the reaction zone as soon as it is formed; keeping it in the reaction mass results in its polymerization by high temperature and, apparently, by the catalytic action of the caustic potash. Therefore the intermittent method of dehydrating the alcohol cannot be employed.

Dehydrating nopol in the liquid phase by the continuous method with anhydrous potassium hydroxide. The potassium hydroxide was placed in a flask and nopol was added continuously at 180°. The test results are listed in Table 1, (see page 586).

We have found that when the dehydration product of the alcohol is kept in the flask, it covers the potassium hydroxide with a film of a polymer product, owing to its high susceptibility to polymerization, thus interfering with the further dehydration of the alcohol. It is seen in Table 1 that: 1) as the pressure in the system was lowered from 147 to 35 mm Hg, the condensate yield rose from 28.2% at 147 mm to 74.5% at 35 mm Hg, the temperature and the rate of alcohol feed remaining the same; 2) lowering the pressure in the system from 147 mm to 35 mm Hg caused the dehydration reaction to be more complete, being 73.8% at 35 mm as against 27.6% at 147 mm, based on the amount of water evolved; and 3) increasing the rate of feed of the alcohol, while keeping the other conditions the same, made the dehydration of the alcohol less complete. At an alcohol feed rate of 9.7 ml/hr, 73.8% was dehydrated, while 66% was dehydrated at 11 ml/hr.

The product of Operations 1-5 was fractionated in vacuum with hydroquinone (0.1%) into a tower 10 mm in diameter and 1.3 m high, filled with glass coils 3.5 mm in diameter, the diameter of the glass thread being 0.8 mm, the reflux ration being 12-15 (Tables 2 and 3).

TABLE 2

Fractionation of the Product of Operations 1-4. 62.5 g Used in Fractionation

Fraction No.	Boiling point, °C	Pressure, mm Hg	Weight, g	d_4^{20}	n_D^{20}	α_D^{20}	M
1	61.5-69.0	16	4.1	0.8759	1.4919	–	137.5
2	69 - 70	16	10.5	0.8863	1.5021	+ 7.60	140.0
3	70 - 71	16	13.7	0.8869	1.5040	+ 9.96	143.4
4	71 - 110	16	6.2	0.8924	1.5032	+ 8.00	155.4
5	110 - 110	16 - 10	7.8	0.9622	1.4921	-20.84	–
6	110-114	10	13.8	0.9685	1.4917	-22.04	–

The total recovered was 56.1 g. The residue was a thick tar.

The molecular weight was determined cryoscopically, by the Beckmann method, in benzene.

Molecular refraction of Fraction 3. MR_D Found: 49.41.
$C_{11}H_{16}$·2F. Computed: 47.664.
Exaltation of molecular refraction 1.75.

Analysis of Fraction 3.

3.896 mg substance: CO_2; 12.743 mg; H_2O 3.668 mg.
2.973 mg substance: CO_2 9.761 mg; H_2O 2.790 mg.
Found %: C 89.20, 89.39; H 10.54, 10.48.
$C_{11}H_{16}$. Computed %: C 89.19; H 10.81.

Table 1

Dehydration of Nopol in the Liquid Phase by the Continuous Method with Anhydrous Potassium Hydroxide

Test No.	Charge, grams		% alcohol in the fraction	Charge of 100% alcohol	Temperature of run °C	Pressure, mm Hg	Alcohol feed rate, g/hour	Charge of KOH, moles/mole of alcohol	Water evolved, (g)	Dehydration reaction (% of theoretical, based on water evolved	Hydrocarbon fraction collected, (g)	Fraction with a b.p. of 69-72° at 16 mm (g)	Analysis of fraction		Condensate yield, % of charge
	KOH	Alcohol fraction											d_4^{20}	n_D^{20}	
1	7.4	29.0	80.6	23.4	180-190	147	9.4	0.937	0.7	27.6	8.0		0.9441	1.4923	28.2
2	7.0	25.0	90.0	22.5	190-200	55	11.2	0.921	2.0	82.8	5.9	-30.4	0.9096	1.4970	25.6
3	7.0	25.0	90.0	22.5	190-200	47	12.3	0.921	1.7	69.7	9.5		0.9205	1.4959	40.8
4	7.0	64.9	86.6	56.2	195-200	35	9.7	0.369	4.5	73.8	45.8		0.9106	1.4980	74.5
5	14.0	213.6	82.6	176.5	190-200	30	11.0	0.235	12.7	66.0	136.9	-44.6	-	-	70.0

Table 6

Dehydration of nopol with $KHSO_4$

Test No.	Grams of alcohol fraction charge	% nopol	Grams of 100% alcohol charge	Grams of $KHSO_4$ charge	Test temperature, °C	Pressure, mm, Hg	Rate of alcohol charge, g/hour	Grams of water evolved	Dehydration reaction, % of theoretical	grams of hydrocarbon fraction recovered	Analysis		Practical yield, %
											n_D^{20}	d_4^{20}	
1	25.0	80.0	20.0	1.0	180-200	760	Per.	1.3	60.0	4.8	1.4973	0.9061	20.8
2	35.0	80.6	28.2	1.2	190-200	760	10.0	2.8	91.5	4.7	1.5003	0.9007	14.6
					Hydrogen fraction driven off from the residue in vacuum:								
					Fraction No. 1 up to 70° at 10 mm					1.2	1.5013	0.8947	
					Fraction No. 2 70-105° at 10 mm					1.8	1.4988	0.9638	
					Fraction No. 3 105-114° at 10 mm					6.6/14.3	1.4908	0.9702	30.1/44.7
3	41.0	80.6	33.0	1.6	190-200	60	9.0	2.3	71.9	18.8	-	-	52.1

TABLE 3

Fractionation of the Product of Operation 5. 124.6 g Used In Fractionation

Fraction No.	Boiling point, °C	Pressure, mm Hg	Weight, g	d_4^{20}	n_D^{20}	α_D^{20}
1	52 - 61.5	16	5.0	0.8661	1.4735	-
2	61.5 - 69.0	16	5.4	0.8791	1.4948	+ 0.64
3	69.0 - 69.5	16	8.2	0.8857	1.5033	+ 9.08
4	69.5 - 70.0	16	10.2	0.8870	1.5045	+10.94
5	70.0 - 70.5	16	9.2	0.8871	1.5048	+11.40
6	70.5 71.0	16	9.1	0.8872	1.5051	+13.5
7	71.0	16	7.9	0.8874	1.5053	+14.05
8	71 - 82	16	3.5	0.8893	1.5045	-
9	82 - 110	16-10	8.2	0.9514	1.4989	-22.26
10	110 - 112	10	16.9	0.9672	1.4930	-26.05
11	112 - 114	10	13.6	0.9691	1.4928	-25.77

The number of double bonds in the molecule was determined by oxidation with benzoyl hydrogen peroxide:

0.100 g of sample, active oxygen 0.0235 g.
0.107 g of sample, active oxygen 0.02447 g.

The number of double bonds found in the nopene molecule was: 2.1, 2.1.

The total recovered was 102.2 g; 44.6% of this total represented fractions boiling at 69-71° and 16 mm. Thus the yield of the dehydration product was 42.7%.

Analysis of Fraction 7 yielded the following results:

Molecular refraction MR_D found: 49.45.
$C_{11}H_{16}$·2F. Computed: 47.664.

The exaltation of molecular refraction, 1.79, indicated that conjugated double bonds were present.

Analysis of the fraction:

3.070 mg substance: CO_2 10.067 mg; H_2O 2.918 mg.
2.731 mg substance: CO_2 8.946 mg; H_2O 2.555 mg.
Found %: C 89.43, 89.34; H 10.51, 10.63.
$C_{11}H_{16}$. Computed %: C 89.19; H 10.81.

The double bonds were determined by oxidation with benzoyl hydrogen peroxide:

0.104 g sample; consumption of active oxygen: 0.0225 g;
0.629 g sample; consumption of active oxygen: 0.0293 g.

The number of double bonds found in the nopene molecule was; 2.0, 2.1.

Condensation of the hydrocarbon with maleic anhydride. 2.8 g of Fraction 6 (0.019 mole) was sealed into an ampoule with 2.2 g of maleic anhydride (0.022 mole) and heated for 1 hour over a boiling water bath. The contents of the ampoule were a thick yellow mass, which solidifed upon cooling. The excess maleic anhydride was separated by boiling with water. The unreacted hydrocarbon was separated by distillation with steam.

This yielded 4 g of an acid. The acid was recrystallized from benzene until it had a constant melting point of 168-169°. The acid number was found to be 418, 420; the number calculated for $C_{15}H_{20}O_4$ was 421.

Analysis: 4.000 mg substance: CO_2 9.931 mg; H_2O 2.998 mg.
4.225 mg substance: CO_2 10.492 mg; H_2O 3.186 mg.
Found %: C 67.71; 67.73; H 8.39, 8.38.
$C_{15}H_{20}O_4$. Computed %: C 67.67; H 8.27.

Oxidation of the hydrocarbon with a 4% $KMnO_4$ solution. 7.5 g of the hydrocarbon and 10 ml of acetone were placed in a flask fitted with a stirrer. While the mixture was chilled and stirred, a 4% acetone solution of $KMnO_4$ was added until the color of the solution remained pink. The $KMnO_4$ used totaled 22 g. The $KMnO_4$ was reduced rapidly. The manganese dioxide was suction-filtered out and boiled repeatedly with water; the aqueous extracts were concentrated, acidulated, and extracted with ether. The ether was driven off from the ether layer, and the residue was fractionated in vacuum.

This yielded only one fraction, which boiled at 184-186° at 4 mm of mercury, totalling 0.7 g. The acetone was driven off from the filtrate left after the MnO_2 had been filtered out, and the residue was fractionated in vacuum, two fractions with stable boiling points being collected:

1) B.p. 70-72° at 16 mm Hg: weight 1.0 g; d_4^{20} 0.8867; n_D^{20} 1.5037.

2) B.p. 135-140° at 4 mm Hg: weight 2.3 g; d_4^{20} 1.0727; n_D^{20} 1.5011.

The fraction that boiled at 70-72° and 16 mm was the original nopene.

Analysis of the fraction that boiled at 135-140° and 16 mm:

4.758 mg substance: CO_2 12.301 mg; H_2O 3.930 mg.
6.775 mg substance: CO_2 17.488 mg; H_2O 5.567 mg.
Found %: C 70.51, 70.40; H 9.24, 9.13.
$C_9H_{14}O_2$. Computed %: C 70.6; H 9.0.

Analysis of the fraction that boiled at 184-186° and 4 mm:

3.952 mg substance: CO_2 8.42 mg; H_2O 2.729 mg.
4.374 mg substance: CO_2 9.334 mg; H_2O 3.022 mg.
Found %: C58.11, 58.2069; H 7.60, 7.68.
$C_9H_{14}O_4$. Computed %: C 58.06; H 7.53.

Oxidation of the fraction that boiled at 135-140° at 16 mm Hg. The fraction was oxidized in acetone solution by a 4% acetone solution $KMnO_4$, with stirring and chilling. 1.5 g of the fraction was used for oxidation; 6.5 g of $KMnO_4$ was used up. The manganese dioxide was suction-filtered out and boiled with water. The water extracts were concentrated, acidulated, and extracted with ether. The ether was driven from the ether layer, and the residue was fractionated in vacuum.

This yielded only one fraction, totalling 0.8 g, which boiled at 184-186° and 4 mm Hg. Its acid number was found to be 600; the number computed for $C_9H_{14}O_4$ is 602.

Thus, the principal oxidation products were: a non-oxidized hydrocarbon, totaling 1 g; 2.3 g of an intermediate oxidation product, with the formula of $C_9H_{14}O_2$; and 0.7 g of the acid $C_9H_{14}O_4$ with a boiling point of 184-186° at 4 mm. The intermediate oxidation product was oxidized further with permanganate in acetone solution. The fraction that boiled at 184-186° and 4 mm was none other than pinic acid. The recovery of pinic acid proved that the initial hydrocarbon had a four-membered ring and a double bond at the 2-position in the ring [3].

The foregoing indicates that the dehydration product of nopol, which we have named "nopene", has the formula cited and thus is 6,6-dimethyl-2-vinyl-bicyclo-(1,1,3)-heptene-2.

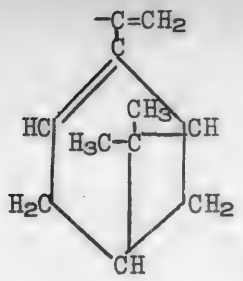

Dehydration of nopol in the liquid phases by the continuous method with anhydrous potassium hydroxide, using nitrogen. We ran tests using nitrogen in order to get the dehydration product out of the reaction zone as fast as possible. In every run 2.8 g of potassium hydroxide (0.05 mole) was placed in the flask (A in the figure), and at a temperature of 180-190° and a pressure of 50 mm of mercury the alcohol was continuously added to the flask from the dropping tube B through which nitrogen also entered the system. The tube through which the alcohol and nitrogen entered the system extended down to the bottom of the flask, its end being drawn out to a point. The constants of the initial alcohol were as follows: d_4^{20} 0.9680; n_D^{20} 1.4872.

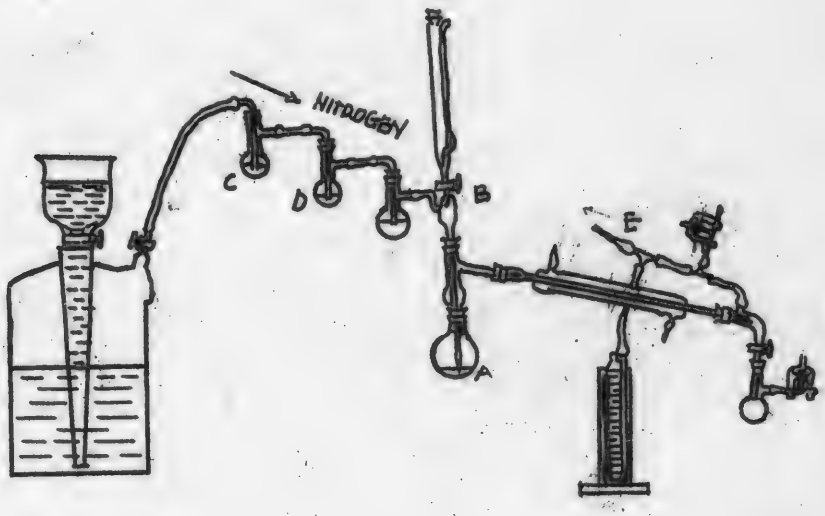

Layout of the apparatus for dehydrating nopol in the liquid phase by the continuous method.

A-Reaction flask; B-dropping tube; C-flask containing a $CuSO_4$ solution; D-flask containing H_2O; E-tube leading to vacuum pump.

The results of the tests are listed in Table 4.

TABLE 4

Dehydration of Nopol with Nitrogen

Test No.	Charge		Time required to add alcohol fraction, hr.	Grams of water evolved	Dehydration, % of theory	Grams of distillate secured	Distillate yield, % of the alcohol charge	Analysis of resulting distillate	
	Alcohol fraction (g)	100 % nopol, (g)						n_D^{20}	d_4^{20}
1	30	24	1.5	0.75	28	26.1	87	1.4915	0.9633
2	30	24	2.0	0.84	31	21.0	70	1.4904	0.9643
3	30	24	1.0	0.90	33	19.5	65	1.4910	0.9638

When less than 0.5 liter of nitrogen was used per hour, the polymer product formed clogged the capillary tube, and no more alcohol and nitrogen could enter the system. When 10.5 liters of nitrogen was used per hour, the distillate

contained the original alcohol.

When 4 liters of nitrogen was used in 1.5 hours, the distillate yield was as much as 87% of the alcohol charge and contained more nopene than in the tests in which 1-2 liters of nitrogen was used.

A brown polymer product was formed in the reaction flask in all the tests.

Dehydration of nopol by the intermittent method with $KHSO_4$. 25 g of the alcohol fraction, containing 80% of nopol, and 1 g of $KHSO_4$ (5% of the alcohol by weight) were heated in a flask, with vigorous stirring, to 180-200°. Under these conditions the dehydration reaction proceeded quickly, being practically complete within 2 hours.

The results of the test are listed in Table 6 (Test No. 1). The 17.7 g of residue left in the flask was a thick, light yellow resin with n_D^{20} 1.5269. The yield of distillate was only 20.8% of the alcohol charge in this test.

Dehydration of nopol by the continuous method with $KHSO_4$. This test was run at atmospheric pressure and in vacuum. In the former run, 1.2 g of $KHSO_4$ and 5 g of the alcohol fraction were charged into the flask. Another 30 g of the alcohol fraction was continuously added to the flask in the space of 3 hours, with vigorous stirring and a reaction mass temperature of 190-200°.

The results of the tests are given in Table 6 (Test No. 2). The residue left in the flask after the volatiles had been distilled off in vacuum was 19.2 g of a thick, tacky, light yellow resin with n_D^{20} 1.5313.

In the second test 1.6 g of $KHSO_4$ and 5 g of the alcohol fraction were placed in the flask. With the reaction mass kept at a temperature of 190-200° and with the pressure at 60 mm of mercury, 41 g of the alcohol fraction, containing 80.6% of nopol, was added to the flask continuously in the course of 4 hours.

The test results are shown in Table 6 (Test No. 3).

The residue in the flask was 18.7 g of a dark-yellow, tacky resin. The water was separated from the distillate; the distillate was desiccated and fractionated in vacuum with hydroquinone in a flask with a herringbone packing. The fractionation results are given in Table 5. 17.3 g were fractionated.

The total yield was 15.1 g, 2.3 g of which was a fraction with a b.p. of 69-71° at 16 mm Hg, which made the yield of the dehydration product 22%. The residue was a thick tar. The molecular weight was determined cryoscopically in benzene.

TABLE 5

Fractionation Results

Fraction No.	Boiling point, °C	Pressure, mm hg	Weight, g	n_D^{20}	d_4^{20}	M
1	60 - 69	16	4.4	0.8824	1.4987	139.3
2	69 - 71	16	2.3	0.8890	1.5013	142.9
3	71 - 75	16	1.4	0.9084	1.5005	150.4
4	75 - 108	16-10	1.5	0.9380	1.4949	164.4
5	108 - 144	10	5.5	0.9683	1.4900	-

The double bonds were determined by oxidation with benzoyl hydrogen peroxide:

0.0998 g sample; consumption of active oxygen 0.0196 g.
0.1176 g sample; consumption of active oxygen 0.0224 g.

The number of double bonds found in the nopene molecule was: 1.8.

Analysis of Fraction 2:

0.1206 g substance: H_2O 0.1160 g; CO_2 0.3910 g.
0.1478 g substance: H_2O 0.1414 g; CO_2 0.4822 g.
Found %: C 88.42, 88.98; H 10.46, 10.60.
$C_{11}H_{16}$. Computed %: C 88.19; H 10.81.

Securing the dehydration product of nopol by the Chugaev method, via the xanthate. 20 g of the nopol fraction, containing 93% of the alcohol, was poured into 20 g of anhydrous benzene, and then 2.6 g of finely pulverized metallic sodium was added a little at a time. The reaction flask was protected against atmospheric CO_2 by a tube filled with soda lime.

After the violent evolution of hydrogen had come to an end, the mixture was boiled over a water bath for 15 hours with a reflux condenser connected to the soda-lime tube. The solution gradually turned color, first turning yellow, then slowly changing to orange, and then to claret. The alcoholate solution was decanted from the unreacted metallic sodium (0.4 g) while still hot into a flask protected against atmospheric CO_2 and diluted with 150 ml of anhydrous benzene after it had cooled. Thus the reacted metallic sodium totaled 2.2 g, i.e., 15.9 g of 85.2% of the alcohol had reacted, and the sodium alcoholate totaled 18.00 g. The solution of sodium alcoholate was treated with 14 g of anhydrous carbon disulfide, or 190% of the theoretical. The carbon disulfide was added a little at a time from a dropping funnel while the solution was chilled with ice. The reaction product in the flask gradually took on a thick consistency as the xanthate was formed, and soon all the salt separated out as a solid yellow mass that was readily soluble in water, ether, and alcohol, and slightly soluble in benzene. The benzene solution of the xanthate was placed in a round-bottomed flask fitted with a reflux condenser, and 15 g of methyl iodide was added, a little at a time, from a dropping funnel. After all the methyl iodide had been added, the contents of the flask were heated over a water bath for 4 hours.

The reaction product was treated with water, and the upper layer was removed. The benzene was driven off over a water bath, the unreacted alcohol and the hydrocarbons being driven off with steam.

A heavy yellow oil, freely soluble in alcohol, was left in the distilling flask.

The xanthate was a thick, heavy, claret-colored oil. Its molecular weight, as determined cryoscopically in benzene, by the Beckmann method, was 230.9. The molecular weight calculated for $C_{13}H_{20}OS_2$ was 256.0.

Analysis of the xanthate:

0.153 g substance: 0.2677 g $BaSO_4$.
0.1010 g substance: 0.1751 g $BaSO_4$.
Found %: S 24.01, 23.82.
$C_{13}H_{20}OS_2$. Computed %: S 25.0.

The xanthate was subjected to dry distillation over an oil bath. The ester began to decompose when the temperature of the reaction mass was 200° at 50 mm Hg. The mercaptan was eliminated from the ester by shaking the latter four times with a 40% solution of sodium hydroxide; it was freed of the xanthate entrained by the decomposition products by distillation with steam. The dehydration product of nopol was desiccated and then distilled in vacuum. The boiling point of the product was 55-59° at 10 mm Hg.

The product yield was 2.6 g. The product had a yellowish tinge and a mercaptan odor. Its constants were:

n_D^{20} 1.5061; d_4^{20} 0.8894; molecular refraction found to be 49.48; computed for $C_{11}H_{16} \cdot 2F$; 47.664.

Analysis:

5.651 mg substance: CO_2 18.488 mg; H_2O 5.477 mg.
6.174 mg substance: CO_2 20.184 mg; H_2O 6.001 mg.
Found %: C 89.23, 89.16; H 10.77, 10.80.
$C_{11}H_{16}$. Computed %: C 89.19; H 10.81.

SUMMARY

1. A method for the dehydration of nopol has been worked out for the first time. The following methods have been tried out: a) dehydrating nopol in the vapor phase with alumina; b) with pumice; c) with potassium hydroxide on pumice; d) dehydration of nopol in the liquid phase with anhydrous potassium hydroxide by intermittent and continuous methods; e) dehydration with $KHSO_4$ by intermittent and continuous methods. f) dehydration of nopol by Chugaev's xanthogenic method. The best results were obtained in the dehydration of nopol in the liquid phase with anhydrous potassium hydroxide by the continuous method, the yield of hydrocarbons being 42.7% of theory.

2. The synthesized hydrocarbon 6,6-dimethyl-2-vinylbicyclo-(1,1,3)-heptene-2, which we have named "nopene", has the following constants:

Boiling point 71° C (at 16 mm); d_4^{20} 0.8874; n_D^{20} 1.5053; and a specific rotatory power $[\alpha]_D^{20}$ 15.24°.

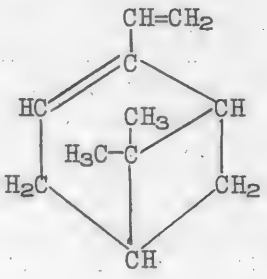

(I)

3. The structure of nopene was established as follows: a) the empirical fomula was established by ultimate analysis; b) the number of double bonds, determined by oxidation with benzoyl hydrogen peroxide, was found to be 2.0-2.1; c) the presence of a four-membered ring within the nopene molecule was proved by synthesizing pinic acid when nopene was oxidized by potassium permanganate; and d) the presence of conjugated double bonds in the nopene molecule was proved by synthesizing the dibasic acid $C_{15}H_{20}O_4$ when nopene was condensed with maleic anhydride; this is also proved by the magnitude of the exaltation of molecular refraction, which was 1.79. Thus, nopene may be attributed the following structure: (I).

LITERATURE CITED

[1] Sabetay, Bull. soc. chim. France, 45, 69 (1929); 43, 1601 (1928); 49, 3 (1931); 47, 614 (1930); Palfray, Sabetay, Sontag, Comptes rend., 193, 941, 1128, 1194 (1931).

[2] Vansheidt and Kan, J. Appl. Chem. 13, 1872 (1940); Klages, Allendorf, Ber., 31, 1003, 1298 (1898).

[3] Sanderens, Comptes rend., 182, 612 (1926); 188, 1073 (1929).

[4] Zalkind, Plastics, 1, 14 (1934).

[5] Zalkind and Vansheidt, J.Appl.Chem. 14, 521 (1941).

[6] Chugaev, J.Russ.Phys.Chem.Soc. 36, 1039 (1904).

[7] Chugaev, J.Russ.Phys.Chem.Soc. 31, 961 (1899).

[8] Chugaev and Esche, J.Russ.Phys.Chem.Soc. 39, 1330 (1907).

Received January 20, 1950.

BRIEF COMMUNICATIONS

THE KINETICS OF ABSORPTION DURING INTENSIVE STIRRING

M. Kh. Kishinevsky

Kishinev State University

In our preceding paper [1] we set forth the concepts that underlie our theory of absorption processes in systems with high turbulence in the reacting phases.

We define systems of high turbulence as those in which the turbulence does not die down near the phase boundary surface, so thatthe boundary surface is continuously being breached by turbulent currents. In such systems the transfer of a substance toward the phase boundary surface takes place largely as mass flow, in both the gaseous and liquid phases, inasmuch as the transfer of the substance by diffusion takes place immeasurably more slowly than its hydrodynamic transfer [2].

We introduced the notions of the period required for renewing the surface layer and the degree of neutralization of the surface layer in order to express the process rate quantitatively. The paper gave the derivations of kinetic absorption formulas for two limiting cases: low and high turbulence of the liquid phase, equivalent to the complete and negligible degrees of neutralization of the surface layer, respectively. The concepts of low and high turbulence are defined by the velocity of the chemical reaction as well as by the hydrodynamics of the liquid phase; when the reaction is rapid, the same hydrodynamic conditinns in the liquid phase may lead to the complete neutralization of the boundary surface, which we would therefore class as low turbulence, whereas, when the reaction is slow, the neutralization is negligible, and we would class it as high turbulence. In both cases, however, we presuppose the rupture of the boundary surface by turbulent currents.

The following formula was derived for complete neutralization of the surface layer:

$$\frac{d\omega}{\sigma \cdot d\tau} = \frac{mc + HP}{\frac{1}{V_n} + \frac{H}{P}} . \qquad (1)$$

With negligible neutralization of the surface layer, the formula for the absorption kinetics differs qualitatively from the first one:

$$\frac{d\omega}{\sigma \cdot d\tau} = \beta p \frac{KC + V_n}{KC + V_n + \beta/H} . \qquad (2)$$

In these formulas:

$\frac{d\omega}{\sigma \cdot d\tau}$ is the flow of the substance, in moles per unit boundary surface per

unit time; β is the hydrodynamic constant of the gas phase; V_n is the hydrodynamic constant of the liquid phase, equaling the linear velocity of mass flow normal to the boundary surface; C is the concentration of the chemically active component in the absorbent; P is the partial pressure of the gas being absorbed; H is the physical solubility of the gas being absorbed in the surface layer of the absorbent at a gas partial pressure of one atmosphere; m is the coefficient of the specified stoichiometric equation of the chemical reaction that accompanies the absorption process; and K is a constant that is proportional to the velocity constant of the chemical reaction.

These formulas agreed satisfactorily with the experimental data. Moreover, Formula (2) was used to determine the activation energy of the reaction between carbon dioxide and hydroxyl ions, the value of which coincided with those obtained by direct measurements.

The present paper deals with the derivation of a general equation for the kinetics of adsorption throughout the turbulence range, the boundary cases being those described by Formulas (1) and (2), provided, however, that the absorption processes involve reactions of the first order. This sort of reaction may take place whenever the solubility of the gas in the surface layer is practically independent of the extent of the latter's neutralization and, hence, remains unchanged throughout the period during which the surface layer is renewed.

The degree of turbulence of the liquid phase is characterized by the time $\Delta\tau$ required for renewing the surface layer. As turbulence increases, $\Delta\tau$ falls. The drop in $\Delta\tau$ entails a drop in the degree of neutralization of the surface layer.

Now let us consider the absorption process characterized by a renewal period $\Delta\tau$ for the surface layer and by a degree η of neutralization of this layer. The rate of absorption is then given by the equation

$$\frac{d\omega}{\sigma \cdot \sigma\tau} = V_n(m\eta C + C_i), \qquad (3)$$

where $m\eta C$ is the concentration of molecules of the absorbed gas bound to the surface layer: and C_i is the concentration of physically dissolved, free molecules in the surface layer.

The concentration of free molecules of the gas in the surface layer, C_i, is related to the partial pressure of the gas at the phase boundary, P_i, by the equation

$$C_i = HP_i. \qquad (4)$$

Since we have assumed that the reaction in the surface layer is of the first order, the degree of neutralization of the surface layer may be readily expressed in terms of the concentration of the chemically active component of the solution at the start of the reaction. For a first order reaction, we actually get the equation:

$$\ln \frac{C}{C - X} = K'\tau, \qquad (5)$$

where C is the initial concentration of the reactant – the chemically active component of the solution in the given case; $C - X$ is the concentration at the time τ; K' is the velocity constant for a first-order reaction, proportional to the practically unchanged concentration of free molecules of the gas in the surface layer. Since we are interested in the concentration of the chemically active component of the solution in the surface layer at the end of the period during which the latter is renewed, i.e., at the time $\Delta\tau$, τ must be substituted for $\Delta\tau$ in Equation (5). On the other hand,

$$C - X = (1 - \eta)C. \qquad (6)$$

Substituting (6) in (5) and solving for η, we get:

$$\eta = 1 - e^{-K'\Delta\tau}. \tag{7}$$

In accordance with what was stated above,

$$K' = K_c C_i, \tag{8}$$

where K_c is the velocity constant of a second-order reaction between the gas molecules and the molecules of the chemically active component of the solution.

After the necessary substitutions have been made in (3) the formula for the rate of absorption becomes:

$$\frac{d\omega}{\sigma \cdot d\tau} = V_n[m(1 - e^{-K_c C_i \Delta\tau}) \cdot C + C_i]. \tag{9}$$

Combining Equations (4) and (9) with the equation for mass transfer in the gas phase:

$$\frac{d\omega}{\sigma d\tau} = \beta(P - P_i), \tag{10}$$

we eliminate the variables P_i and C_i, which are hard to measure, and obtain the general equation relating the absorption rate to its fundamental parameters:

$$\frac{d\omega}{\sigma \cdot \Delta\tau} = \frac{mC\left[1 - e^{-\left(P - \frac{d\omega}{\sigma \cdot d\tau} \Big/ \beta\right) HK_C \Delta\tau}\right] + HP}{\frac{1}{V_n} + \frac{H}{\beta}}. \tag{11}$$

The equation is given in the implicit form, but it can be readily solved graphically, however. It holds good for any value of $\Delta\tau$ at values of η ranging from zero to unity.

Analysis of Equation (11) indicates that the formulas (1) and (2) derived by us in our preceding paper [1] cover the boundary case of absorption, with high turbulence in the liquid phase. Indeed, $\Delta\tau$ falls as the turbulence rises. When $\Delta\tau$ is small enough, we can resolve $e^{-\left(P - \frac{d\omega}{\sigma \cdot \Delta\tau} \Big/ B\right) HK_C \Delta\tau}$ into a series, and get the equation:

$$e^{-\left(P - \frac{d\omega}{\sigma \cdot d\tau} \Big/ \beta\right) HK_C \Delta\tau} = 1 - \left(P - \frac{d\omega}{\sigma\Delta\tau} \Big/ \beta\right) HK_C \Delta\tau.$$

if terms other than those of the first order are neglected.

Substituting in (11) and solving for $\frac{d\omega}{\sigma d\tau}$, we get:

$$\frac{d\omega}{\sigma\Delta\tau} = \beta P \frac{KC + V_n}{KC + V_n + \beta/H},$$

where $K = K_C m \Delta\tau V_n$.

This reciprocal transition may be explained easily enough. Equation (2) was derived on the assumption that when the turbulence is high, and hence $\Delta\tau$ is extremely small, both the concentration of the chemically active solution component in the surface layer and the concentration of the free gas molecules may be considered constant throughout the period of renewal of the surface layer. Equation (11) was derived on the assumption that only the concentration of the gas molecules

remains constant in the surface layer. But as the turbulence rises and $\Delta\tau$ falls, the change in the concentration of the chemically active component becomes practically infinitesimal, so that Equation (11) reduces to (2). It is obvious that Equation (11) holds good over a wider range than (2) does.

As the turbulence decreases in the liquid phase and $\Delta\tau$ increases,

$$-\left(P - \frac{d\omega}{\sigma \cdot d\tau}\ \beta\right)K_C \Delta\tau_H \underline{e} \longrightarrow 0,$$

the degree of neutralization of the surface layer approaches unity, and Equation (11) is reduced to (1).

Equation (11) gives the absorption rate as a function of all the parameters that affect the absorption process in one way or another. It shows that the variation of the process rate with any of the absorption factors changes with a change in the hydrodynamic conditions governing the process. For example, the partial pressure of the adsorbed gas, which has practically no effect upon the process rate at low turbulence, is one of the decisive factors at high turbulence. The concentration of the chemically active component of the absorbent, which is a major factor affecting the process rate at low turbulence, has a negligible effect on its rate at high turbulence.

This circumstance has been ignored in several research papers on the absorption process. Pozin's proportionality between the absorption rate and the concentration of the chemically active component in the solution and the fact that the absorption rate is independent of the partial pressure of the gas [3] are approximately true only at low turbulence, when the surface layer is completely neutralized.

Equation (11) may be solved graphically or resolved into an exponential series including the second-order term. It may be simplified in special cases.

Equation (11) is also of considerable value in determining the activation energies of some reactions that take place in solutions. It is more convenient for this purpose than (2), inasmuch as its use does not require the setting up of such high turbulence.

Research is now being carried out in the laboratory of physical chemistry of Kishinev State University on the kinetics of absorption processes under various hydrodynamic conditions. The results are in good agreement with the theory we have developed.

SUMMARY

The concept of the transfer of a substance by mass flow has been used to develop an equation for the kinetics of absorption that holds good for a wide range of turbulence in processes that involve first-order reactions.

LITERATURE CITED

[1] M.Kh.Kishinevsky and A.V.Pamfilov, J.Appl.Chem., 1949, No. 11, 1173.

[2] M.A.Velikanov. The Dynamics of River Currents. GIMIZ, Leningrad.

[3] M.E.Pozin, J.Appl. Chem. 20, No. 4, 353 (1947).

Received June 24, 1950.

THE PASSIVITY OF STAINLESS STEEL

G. P. Maitak and N. N. Gratsiansky

Institute of General and Inorganic Chemistry, Ukrainian Academy of Sciences

The researches of Akimov and his associates [1] have shown that the corrosion resistance of stainless steel is due to the formation on its surface of a protective oxide film, which also governs its electrode potential; hence, stainless steel can be passivated in an oxidizing medium with active cathodic depolarization, provided a protective oxide film is formed on its surface. The corrosion of stainless steel in sulfuric acid, for example, is diminished when ferric sulfate is present, though ferrous sulfate has no such effect [2]. The passivating action of the trivalent iron ions resembles the action of atmospheric oxygen and other oxidizing agents [3]. The corrosion of stainless steel is accelerated by the presence of ferric chloride [4], since the depolarizing action of the trivalent iron ions continues, while their passivating action is suppressed by the chlorine ions, in whose presence no protective film is formed.

The data set forth below, secured by us in an investigation of stainless steel as a material for use in making pickling tanks indicate that the relationship observed to exist between the effect of iron sulfates on the corrosion resistance and electrode potential of stainless steel in sulfuric acid is in agreement with the concepts set forth above.

EXPERIMENTAL

We measured the variations of the electrode potential with time and the corrosion of "18/8" stainless chrome nickel steel containing titanium in the following three solutions: 1) 20% H_2SO_4; 2) 5% $FeSO_4$ in 20% H_2SO_4; and 3) 5% and 10% $Fe_2(SO_4)_3$ in 20% H_2SO_4.

The steel we tested had the following percentage composition: Cr 17.10; Ni 8.35; Ti 0.26, and C 0.14.

We cut off plates 40 x 20 x 2 mm in size for our tests. The samples were quenched from 1100°C in water under industrial conditions. After quenching, the samples were cleaned up with a file and then with emery, after which they were wiped clean with filter paper dipped in alcohol and ether.

A preparation that contained no iron oxide was secured from a solution of chemically pure ferrous sulfate by precipitating it with alcohol. The test was run in the resulting solution as soon as it had been prepared. Hydrogen was blown through the 20% H_2SO_4 before the ferrous sulfate was dissolved in it. Potassium ferrocyanide gave no reaction for the trivalent iron ion in this solution of of ferrous sulfate in 20% H_2SO_4.

The third solution was prepared by dissolving the necessary quantity of chemically pure ferrous sulfate in 20% sulfuric acid and oxidizing the solution with hydrogen peroxide. Enough hydrogen peroxide was added to make potassium ferricyanide just give a reaction for the divalent iron ion. Then the solution

was boiled and cooled to 25° for measurements.

The potential of the steel sample was measured by a compensation method, determining the p.d. between the steel sample immersed in the test solution and a saturated calomel electrode that served as the reference electrode, and then recalculating the p.d. in terms of the standard hydrogen electrode.

The figure shows the hard-rubber frame (1) in which the test sample (2) was clamped before measurement. Electric contact with the sample was effected via a platinum wire (5), which passed through the hollow hard-rubber screw (4). The screw held the sample against the frame in such a way that the end of the platinum wire (5), wound into a flat spiral (6), was pressed against the sample [in the figure the screw (4) is not screwed tight]. To prevent the platinum wire from coming in contact with the solution, a rubber ring (3) was mounted at the end of the hard-rubber screw; when the screw (4) was tightened, this ring was pressed tight against the sample.

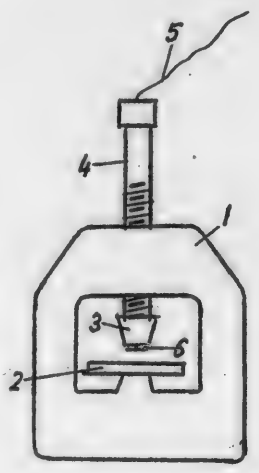

Diagram of the model for holding the sample of steel during measurement of the potential.

1)Hard rubber frame; 2)test sample; 3)rubber ring; 4)hard rubber screw; 5)platinum wire; 6)flat spiral of platinum wire.

A half-liter glass jar served as the test container, filled with 300 ml of the solution. The jar was closed by a rubber stopper, from which the frame and the sample were suspended in such a way as to have the sample in the middle of the solution; there were two tubes passing through the stopper: one for the connection via intermediate jars to the calomel electrode, and the other for the escaping hydrogen. The test run lasted 3 to 4 hours.

In our measurements we used a Rapps potentiometer and a mirror galvanometer. The jar containing the sample was placed in a thermostat at 25°C, together with the calomel electrode and the intermediate jars.

The test results indicate that there is a marked difference in the electrode potentials and in the latter's change with time between the corroded and passivated samples. The sign of the very first measurements and the way the potential was changing with time enabled us to say whether the sample was going to be passivated or corroded. Some of the samples were corroded in the first and second solutions, while others were passivated. All the samples were passivated in the third solution.

The passivated samples did not turn color during the test, nor did they lose any weight, while all their potential readings were positive with respect to the standard hydrogen electrode. The corroded samples changed color, grew darker, evolved hydrogen from the solution, and lost weight. On the five-point scale [5] their corrosion resistance was 4 – "slightly resistant," i.e., their loss in weight was 3 to 10 g per sq m per hour. All the values of the potential of the corroded samples were negative with respect to the standard hydrogen potential.

As soon as the corroded samples were immersed in the solution, their electrode potential increased (became more negative), attaining a maximum negative value (V_m) approximately at the same time as minute bubbles of hydrogen appeared on the surface of the sample. The time required for this maximum to be reached differed with the samples, ranging from a few minutes for most of the samples to

tens of minutes for some of them. Then the potential began to drop (became less negative), rapidly at first and then more slowly, to a value V_t, which varied hardly at all with time. The samples grew darker while this was going on, turning black by the end of the run.

In the samples that were passivated, the potential improved smoothly from the instant of their immersion in the solution until they reached the terminal value V_t.

The most typical values recorded for V_m and V_t are listed in the table.

Results of Measuring the Potentials V_m and V_t of Steel Samples

Composition of solution	Passivated samples			Corroded samples				
	No. of samples	value of + V_t		No. of samples	value of - V_t		value of V_t	
		of individual sample	mean		of individual sample	mean	of individual sample	mean
20 % H_2SO_4	5	0.23, 0.23, 0.24, 0.25 0.22	0.23	7	0.155, 0.150 0.150, 0.148 0.141, 0.146 0.147	0.148	0.105, 0.095, 0.110, 0.103 0.107, 0.103 0.100	0.103
5% solution of $FeSO_4$ and 20% H_2SO_4	5	0.50, 0.50, 0.55, 0.55 0.53	0.53	3	0.150, 0.153, 0.147	0.150	0.100, 0.102	0.101
5 and 10% solution of $Fe_2(SO_4)_3$ in 20% H_2SO_4	6	0.77, 0.76, 0.76, 0.78, 0.76, 0.76	0.76	All the samples tested with the third solution were passivated				

The effect of ferrous sulfate upon the corrosion of stainless steel in sulfuric acid is negligible. Some of the samples corroded in the second solution as well as in the first. We see from the table that the values of the potential (V_m and V_t) of the corroded samples were the same in the first and second solutions. In the passivated samples, the potential in the second solution was more positive than in the first.

In the presence of ferric sulfate, stainless steel is passivated in sulfuric acid. Even samples with scale spots that hadn't been cleaned off were passivated in the third solution, though they were always corroded in the first and second solutions. The positive potential of the sample, which is rapidly established in this solution, probably is the oxidative-reduction potential of ferric-ferrous oxide, the passivated steel acting as an indifferent electrode.

It should be added that electrolytic iron deposited on platinum plates and mild steel dissolve at the same potential, −0.23 volt, in the first and second solutions. In the third solution, after the iron dissolved, the potential changed abruptly to +0.77 volt, corresponding to the oxidative reduction potential of a ferric-ferrous oxide electrode.

LITERATURE CITED

[1] G.V.Akimov and G.B.Clark, Proc. Acad.Sci. USSR, 42, 76 (1944); G.V. Akimov and V.P.Batrakov, Ibid, 45, 124 (1944); G.V.Akimov and G.B.Clark, Ibid., 45, 399 (1944).

[2] J.G.Moneypenny. Stainless Iron and Steel. (Russ. Ed.). State Machinery Press, Moscow, 137 (1934).

[3] H.E.Skarle and R.Worthington, Int. Nickel Co., Inc., Tech. Inform. Bull. 3, 11 (1937); C. 1, 3954 (1939).

[4] N.D.Tomashov. The Corrosion of Metals with Oxygen Depolarization, 130, USSR Acad. Sci. Press, Moscow-Leningrad, 130 (1947).

[5] G.V.Akimov. Principles of Metal Corrosion and Protection, p. 300. Metallurgy Press, Moscow (1946).

Received July 25, 1950.

A LABORATORY APPARATUS FOR THE PRODUCTION OF KETENE ON A LARGE SCALE

D. D. Smolin, F. P. Kravtsov and A. P. Skoldinov
Research Laboratory of Experimental Chemotherapy, USSR Ministry of Health

Numerous devices have been described for the production of ketene by the pyrolysis of acetone on a laboratory scale (20-50 g of ketene per hour). The designs of these devices fall into two groups, depending on the method used to supply the heat required for pyrolysis. In the first type, pyrolysis is effected by passing acetone vapor through a tube that is heated externally in one fashion or another, [1]. The major feature of devices of the second type, the so-called "ketene lamp", is a metallic wire heated to incandescence by an electric current and placed in the acetone vapor [2]. The principal advantage of the first group is its simplicity of design. The second group of devices is somewhat more complicated, but they possess the advantages of compactness, a short warm-up period, and being always ready to start operating.

There is much less to be found in the literature on laboratory installations for the production of ketene on a large scale, with a capacity of several hundreds of grams of ketene per hour. Rather full details are available of only the Morey apparatus [3], which delivers 50-150 grams of ketene per hour, depending on how it is operated. It consists of a tube electrically heated from the outside, and hence is a representative of the first group of devices.

Increasing the size of the generator greatly impairs the even distribution of heat to the reaction zone through the tube wall; this complicates the design considerably. Copper tubing breaks down rapidly at the reaction temperature (700-750°), since the tube wall must be superheated considerably to transmit the heat, owing to the low coefficient of heat transfer under these conditions. Ferrous metals cannot be employed for the tube, because they cause a further decomposition of the pyrolysis products to elementary carbon, thus lowering the yield and clogging the reaction zone with coke.

The present paper describes an all-metal large-scale laboratory generator for the production of ketene, delivering from 200 to 400 grams of ketene per hour (depending upon the operating conditions). The acetone is pyrolyzed in the generator by open metallic helixes, which are heated to incandescence electrically and are located in the path of the acetone vapor. We adopted this design in order to retain in the large-scale all-metal generator the above-mentioned advantages inherent in the ordinary glass ketene lamps, compared to the devices designed as tubular generators.*

Arranging the heating elements in 4 horizontal planes perpendicular to the path of the acetone vapor makes it possible to shorten the time of contact between the acetone and the incandescent surface to the shortest time possible. Provision is also made for the rapid cooling of the heated gas after it emerges from the reaction zone.

Prolonged tests of the generator have shown that, besides its advantages of compactness and short start-up period, it also furnishes reproducible results, thus enabling us to measure out the ketene for reactions as required.

---

*A 100% metallic device, based on the same principle, has been described for the pyrolysis of turpentine to produce isoprene [4].

The yield of ketene from the acetone was 60-62% of the theoretical. This enables us to recommend the all-metal generator designed as indicated above for the laboratory generation of ketene on a large scale.

The operation of the generator will be analyzed in a subsequent report, which will also describe the results secured with various heating elements.

EXPERIMENTAL

Description of the generator. All parts of the generator (see Figure, page 621) in contact with the ketene are made of copper, except for minor parts such as valves, connecting pipes, and the like, which are made of brass. The individual parts of the generator were brazed together with copper or silver. The portion of the installation used to measure and absorb the ketene was made of glass, with rubber connections.

The evaporator 1 is a cylindrical vessel with a capacity of 7 liters, made of sheet copper 1.5 mm thick, fitted with a splash guard 2, a connection for the acetone inlet 3, a gauge glass 4, and a drain cock 5. At its neck 10 the evaporator is connected to the reaction chamber 6, which is equipped with a peephole glass 7.

The following are arranged in successive horizontal planes in the reaction chamber: a copper diffuser 11 to distribute the flow of acetone evenly, and four heating elements 8, arranged one above the other.

Each heating element consists of a flat ring of sheet copper (165 mm in diameter, ring width 12 mm, ring thickness 2 mm) to which 11 porcelain insulators (15 mm high) carefully freed of all glaze are attached by copper studs. The apparatus uses ordinary porcelain insulators – the small rollers employed in electrical engineering. The glaze must be removed because enamel becomes a fairly good conductor at the temperature used for pyrolysis. A coil of "Chromel A" wire (80% nickel, 20% chrome) 0.5 mm in diameter is suspended from the insulators by tiny hooks made of copper wire. The coil is made by tightly winding 4.5 meters of this wire, turn alongside turn, on a bar 4 mm in diameter, after which the coil is stretched out to an aggregate length of 90 cm and fastened to the insulators by copper wire. The heating elements are so arranged that the coils of two adjacent elements cross at 90°. The current is led in to the heating elements through the metallic walls of the generator by eight AE-180 sparkplug cores 9, with mica insulation, the cores being fitted with terminals top and bottom for the connecting wires [Fig. III (see Plate, page 621)]. The lead-ins are made airtight by a stuffing-box washer 12, which squeezes the mica collar of the plug against the housing of the generator.

The flange of the reaction chamber 6 is bolted to the reflux condenser 13, welded of 1.5-mm sheet copper. In addition to the outer cooling jacket 14, an internal coil of copper tubing 15 is used for cooling (total length 4.5 meters, tubing external diameter 1.6 cm, wall thickness 1 mm). The condensate is intercepted by the device 16. The condensate is returned to the evaporator via tube 17, the sight glass 18, the copper reservoir 19, with a capacity of 150 ml and a stopcock (to measure the returned acetone), and the siphon tube 31. The reflux condenser 13 is connected to the brine condenser 21 by a copper tube terminating in the unions 20. Brine cooling is effected by the parallel coils 22, made of copper tubing (tube diameter 1.6 cm, wall thickness 1 mm, total length of tubing in each coil 2.5 meters). All the coils terminated in the collector 23, with a capacity of 2 liters, fitted with a drain 24 to tap off the condensate and a tube for the exhaust gases.

The generator is connected to the open air through a column 26 packed with

calcium chloride. The system is equipped with a mercury safety valve 25, a safety bottle 27, and the 20-liter alkali-filled absorbing bottles 28 to calibrate the generator. The connections are made of glass tubing 1.4 cm in diameter with connecting sleeves of rubber tubing. The waste gases are burned after they pass through a safety valve 30, installed to prevent the backflash of the flame through the system. The valves 32 can be turned to deflect the current of gas into the reaction absorbing system – the reaction flasks 33.

The flange connection between the reaction chamber 6 and the reflux condenser 13, as well as the unions 20 are packed with graphited asbestos gaskets. The connections between the metallic parts of the apparatus and the glass tubes, such as the sight glasses 4 and 18, are effected simply and efficiently as follows: a rubber stopper is slipped over the connecting branch, with the glass tube passing through the stopper, after which the stopper is tightened by a coupling screw (Fig. IV; Plate, page 621). This procedure has proved its dependability whenever a device is operated at pressure (in the present instance the pressure was constituted by the resistance of the absorbing system). The couplings 3 and 5 are executed in the same way. The heating elements of the pyrolysis chamber are connected in parallel to 220-volt a-c network via the variable resistance 34, the ammeter 35, and the knife switch 36. Each heating element may be connected and adjusted independently (Fig. II; Plate, page 621). The evaporator is heated by an electric hot plate, the rating of which may be varied from 2 to 3 kw, which is likewise connected via a rheostat and an ammeter to the 220-volt network.

The evaporator 1 and the reaction chamber 6 are efficiently insulated on the outside by sheet asbestos.

Operational procedure. Anhydrous acetone is poured into the evaporator 1 and heated to boiling, with the reflux condenser 13 operating and the valve 37 open, until the condensate begins to be recycled, as is seen in the sight glass 18. Boiling is continued for 10 to 15 minutes to drive out all the air, after which the valve 37 is closed, and the current is turned on for the heating elements 8. The incandescence of the elements is checked through the sight glass 7, and the rheostats 34 are adjusted until all the heating elements are heated to about the same incandescence, corresponding to a wire temperature of 750-800° (dark-red glow). The upper heating elements, which are bathed by the already heated gas, need less current to maintain this temperature than the lower ones do. We have usually carried out pyrolysis at currents of 7, 7.5, 8, and 8 amps through the heating elements, from top to bottom, respectively. The sight glass is required only during the warming-up period of the generator, after which it is covered by a special screw-on cover. The current of ketene gas is passed, as desired, either through the calibrating system or into the reaction system. The latter consists of two 20-liter bottles 33, fitted with mercury-seal stirrers, connected together in series, and chilled externally by snow. Alcohols are acetylated with a small quantity (about 0.5% by weight) of concentrated sulfuric acid or benzenesulfonic acid. Amines may be acetylated in an organic solvent (benzene, acetone, chlorinated hydrocarbons, and the like), in aqueous solution, or in aqueous emulsion. If the acetylation product is a solid and is insoluble in the solvent used, the gas lines must be made of fairly large size (about 1.5 cm diameter) to prevent clogging the tubing with crystals, and they must be fitted with scouring devices 29. The gases that are not absorbed, consisting chiefly of methane plus carbon monoxide, ethylene, and the unreacted ketene, are burned at the exhaust vent. During the operation of the generator, the ammeters must be checked to ensure that pyrolysis is effected at a constant rate, the constant recycling of the condensate to the evaporator must be checked, and the amount of acetone in the evaporator must be checked through the sight glass 4.

As the condensate accumulates in the reservoir 23 of the brine condenser, it

must be drained off via the draincock 24. The generator is stopped by performing the following operations in the specified sequence: disconnecting the heating elements at the knife switches 36, disconnecting the evaporator hot plate, opening the valve 37 at the calcium-chloride column, and reversing the clamps 32.

Evalulation of Results

The capacity of the generator is determined by passing the gases coming from the pyrolysis chamber for 10 minutes through bubblers fitted with plates of porous glass into 30 liters of a 0.5 N solution of sodium hydroxide, contained in two absorption bottles 28 connected in series. To make sure that all the air has been driven out of the system, the generator should be operated in this fashion for 15 minutes before calibration is attempted.

Titration of the acid samples taken from both of the absorption bottles indicates the amount of acetic acid produced during the given period of generator operation.

The generator has been ordinarily operated as follows for synthesis purposes: the heating elements in the pyrolysis chamber were heated to incandescence by passing currents of 7, 7.5, 8, and 8 amps, respectively, through them; and the electric hot plate used to evaporate the acetone was run at 2.4 kw. Calibration has shown that the output of the generator is 250 grams of ketene per hour under these conditions.

Any slight change in the heating of the generator, whether in the pyrolysis chamber or for the evaporation of the acetone, affects the output considerably. If the power consumed by the electric hot plate is reduced to 2.2 kw, thus diminishing the supply of acetone to the pyrolysis chamber, while the ammeter readings for the heating-coil current are kept constant, for example, the output rises to 400 grams of ketene per hour. At this output, however, the capacity of the cooling system begins to be inadequate, and considerable acetone is lost. Raising the current in the pyrolysis coils has the same effect.

Increasing the acetone supply or decreasing the heating current in the pyrolysis coils, on the other hand, diminishes the generator output.

A material balance of the process was drawn up to determine the yield of ketene from the acetone. Four liters (3200 g) of acetone was placed in the evaporator. Operating the generator for an hour yielded 250 grams of ketene, while 2280 grams of acetone were left in the evaporator and 330 grams were recovered in the collector 23 in series with the brine condenser. Thus the generator consumed 590 grams of acetone per hour. The production of 250 grams of ketene requires 345 grams of acetone theoretically, so that the ketene yield was about 60% of the theoretical in the given run. The acetone losses comprise the vapor entrained with the gas current, plus the consumption of acetone in the side reaction involving the decomposition of ketene into carbon monoxide and ethylene.

The acetone left in the evaporator after the run contains some polymerization products of ketene, acetic acid, and acetic anhydride. The last two substances are produced mainly as the result of the reaction of ketene with water that may have entered the generator together with the acetone or as atmospheric moisture entering the generator after it has been assembled. We therefore employed a special column packed with calcium chloride to dry the air admitted to the generator. Acetic acid, acetic anhydride, and diketene are likewise found in the acetone condensate recovered after the brine condenser; some ketene is also found dissolved in the condensate, the percentage depending on the condensate temperature. After the condensate has been drained from the brine condenser, the ketene evaporates and polymerizes, thus causing the solution to darken and its temperature to rise spontaneously.

At the specified operating conditions the recycling of acetone from the water condenser to the evaporator, as measured by the device 19, is 7110 grams per hour; in other words, 7.7% of the acetone is pyrolyzed in a single pass through the chamber (based on the acetone consumed).

The method of installing the heating elements we employed eliminated overheating of the latter almost entirely. Nor was any corrosion of the metallic parts of the generator in contact with the gaseous reaction products observed, though a small incrustation of crystals of copper acetate was found on the walls of the evaporator.

SUMMARY

A large-scale all-metal laboratory generator for ketene is described, delivering 200 to 400 grams of ketene per hour, depending upon the operating conditions employed, and based upon the pyrolysis of acetone by open heating elements (coils) exposed to the acetone vapor.

LITERATURE CITED

[1] Schmidlin, Bergmann, Ber., 43, 2821 (1910); Hurd and associates, J. Am. Chem.Soc., 47, 1427 (1925); Synthesis of Organic Compounds, Vol. 1, p. 105, United State Chemical Technology Press (1932); V.D.Lyashenko, Symp. on the 25th Anniversary of the State Institute of Applied Chemistry, p. 73, State Chemical Press (1944).

[2] Synthesis of Organic Compounds, Vol. 5, p. 22. State Institute of Technology (1938); Williams, Hurd, J. Org. Chem., 5, 122 (1940); Dunban, Bolstad, J. Org. Chem., 9, 219 (1944).

[3] Morey, Ind. Eng. Chem., Ind. Ed., 31, 1129 (1939).

[4] I.I.Ostromyslensky. Rubber and Its Analogs, p. 268. Moscow, (1913).

Received December 20, 1949.

THE COMPOSITION OF RESINOUS DEPOSITS IN THE MANUFACTURE OF CELLULOSE

S. S. Malevskaya and E. I. Evropyeva *

Chair of Organic Chemistry, V. M. Molotov Institute of Technology, Leningrad

The composition of the physiological resin of spruce wood is extremely complicated, and many of its constituents break down when acted upon by chemical reagents. On the other hand, it undergoes strong chemical action in the processes of sulfite cooking, bleaching, and finishing: prolonged heating under pressure in an acid medium, and the action of solutions of bleaching powder, chlorine, and alkali. There is no doubt that this must affect the constituents of the resin substantially.

The present research has as its objective the investigation of the resinous deposits at various stages of the mannufacture of sulfite cellulose. We obtained samples from the Solikamsk and Priozero cellulose plants,** taken from the washing department at the sand boxes (Samples 1 and 2), i.e., immediately after cooking; from the bleaching room (after chlorination and bleaching (Samples 3 and 4); and after two-stage hypochlorite bleaching (Sample 5).

Samples 3 and 4 were bleached in three stages.

In the first stage they were treated with chlorine gas, and in the second and third they were bleached with calcium hypochlorite.

In some instances (Sample 4), they were washed with alkali (1.2% by weight of the fiber) at room temperature.

Sample 5 was bleached with calcium hypochlorite in two stages, the second stage being an after-bleach in an alkaline medium. Our investigation followed the outline set forth in an earlier paper [1]. All our findings are listed in the table.

We notice the gradual decrease in the percentage of neutral products and the increase in the percentage of acids in the resin.

The percentage of acids rises from 51% (Sample 1) to 80.4% (Sample 5). The percentage of neutral substances drops accordingly from 41.8% (Sample 1) to 15.1% (Sample 5) (see Figure).

Esters doubtless predominate in the neutral substances, being saponified by prolonged boiling under pressure in an alkaline medium (cooking) and by the action of the bleaching solutions and alkali. Since the neutral substances include fats,

---

*V. D. Anfinogenova and T. F. Pekina, students in the Faculty of Technology, assisted in the experimental portion of this research.

**We wish to express our gratitude to scientific associate E. Ya. Perelshtein for her assistance in collecting this material.

the fatty acids remain in the resin during saponification, while the glycerol is converted into an alkali. Some of the resin acids are likewise present in ester form.

The constituents of the resin are chlorinated by the action of chlorine and calcium hypochlorite.

In Tests 3, 4, and 5, the fatty acids, resin acids, and neutral products exhibited a positive qualitative reaction for chlorine: an intense green color of the flame with cupric oxide. In view of the interest attached to the composition of the chlorinated resin, this problem with be the topic of further research.

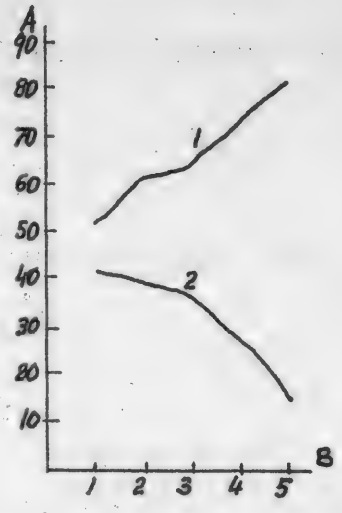

Relationship between percentages of acids and neutral substances.

A-Percentage; B-sample numbers; 1) acids; 2) neutral substances.

EXPERIMENTAL

The resin was freed of fiber by successive extraction with ether and alcohol in a Soxhlet.

The resin was separated into its constituents by the method outlined in our first report [1]. The ether extracts were treated with a 1% solution of NaOH in a separatory funnel. The neutral substances remained in the ether layer, while the acid salts dissolved in the aqueous solution, from which they were recovered by acidulation with acetic acid.

Precipitates usually settled out between the two layers, which were insoluble in alkali or in ether and were responsible for the losses during separation.

The neutral substances were saponified by heating with an alcoholic solution of KOH over a sand bath for 2 hours, with a reflux condenser. The amount of alkali used was based on the following calculation: 50 ml of 1 N KOH for every 10 g of substance.

After saponification was complete, the alcohol was driven off, and the residue was treated with water, a 1% aqueous solution of alkali, and ether. This method provided satisfactory separation into acid and neutral constituents, though a precipitate was thrown down between the aqueous and ethereal solutions that was soluble neither in alkali nor in ether. After the aqueous solution had been acidulated, the acids were extracted with ether.

After the acid mixture had been processed with methanol and H_2SO_4, the methyl esters of the fatty acids were distilled at reduced pressure.

Fraction 1 in all the tests and Fraction 2 in Tests 2 and 5 were pale-yellow liquids containing esters of unsaturated fatty acids. Fraction 2 (in Tests 1 and 3) was a solid containing traces of liquid esters. The residue was a dark, thick mass of esters of oxidized fatty acids.

In Tests 3, 4, and 5 the esters exhibited a positive qualitative reaction for chlorine.

The resin acids were processed with petroleum ether in the cold (Test 2). They were first dissolved in a small amount of ethyl ether, an excess of petroleum ether being added to the solution. A dark precipitate of the resin acids insoluble in petroleum ether settled out. The substances that were soluble in petroleum ether – the resin acids – constituted a yellow, tacky mass after the solvent had been driven off, which crystallized with difficulty upon standing.

Composition of Resinous deposits

Sample No.	Where collected	Ether extract (g)	A C I D S										Grams of methyl esters of fatty acids					Neutral substances										Source
			Total		Resin acids						fatty acids							Total		Volatile with steam	Precipitate	Ether-soluble substances, grams			g in alcoholic extract	g in ether and alcoholic extracts	% in alcoholic extracts	
							Soluble		Insoluble																		
							In petroleum ether																				
			(g)	(%)	(g)	(%)	(g)	(%)	(g)	(%)	(g)	(%)	Total, (g)	I	II	Residue	Losses	(g)	(%)	(g)	(g)	Total	Acids	Neutral substances				
1	Sand boxes of the washing department	40	20.4	51	6.2	15.5	5.4	13.5	0.8	2.0	13.3	33.3	14	10.3	1.2	1.5	1.0	16.7	41.8	-	-	16.7	10.3	6.4	0.6	40.6	1.5	Priozero cellulose plant
2	Sand boxes of the washing department	205.7	123.7	60.1	32.9	15.5	22.2	10.7	10.4	5.1	83.5	40.5	90.3	10.2	25.7	37.7	6.7	81.3	39.5	-	15.8	65.0	21.5	40.0	9.2	215.2	4.3	Solikamsk cellulose plant
3	Sorting screen of the bleaching department	58.4	36.9	63.5	13.5	23.1	4.0	6.8	7.4	12.6	21.0	36	23.5	3.6	3.1	13	3.5	21.2	36.3	-	-	21.2	7.4	12.4	3.7	62.1	5.9	Ditto
4	Recycled water collector in the bleaching department	73.0	53	72.6	29.1	39.8	3.4	4.6	25.5	34.9	21.2	29.1	23.5	6.1	-	14.2	3.2	19.6	26.9	0.1	2.6	14.6	5.0	9.1	6.8	79.8	8.5	Ditto
5	Alkali steep before the press	218.5	175.6	80.4	54.0	24.5	13.6	6.2	40.4	18.5	111.9	51.2	117.8	22.2	37.6	42.9	15.1	33.1	15.1	-	-	33.1	21.8	11.2	15.9	234.4	6.8	Priozero cellulose plant

In Tests 1, 3, 4, and 5 the processing with petroleum ether involved heating for 30 minutes over a water bath. After the mixture had cooled, the solution containing the resin acids soluble in petroleum ether was separated out, the solvent was driven off, and the deposits were weighed.

SUMMARY

1. The neutral products of spruce resin contain esters, including those of the fatty acids. After cooking, the resin contains 39.5-41.8% neutral substances and 51-60.1% acids.

2. The esters are not cleaved appreciably during bleaching with chlorine and calcium hypochlorite, provided no alkali is present. The neutral substances total 36.3%, and the acids 63.5%.

3. The saponification of the esters continues during the two-stage bleaching with hypochlorite and washing with alkali. The percentage of neutral acids drops to 26.9%. When bleaching was done with alkali present, the neutral substances left totaled only 15.1%, while the percentage of acids rose to 80.4%.

LITERATURE CITED

[1] J. Appl. Chem., 22, 1310 (1949).

Received June 12, 1950.

THE PRODUCTION OF A CORKLIKE MATERIAL FROM POLYVINYL CHLORIDE PLASTICS*

M. V. Alekseyev

A porous corklike structure is imparted to polyvinyl chloride plastics by adding various pore-forming agents, which decompose and expand during the plastication of the material, producing minute closed pores throughout the mass. Azodiethyldicarboxylic acid, which decomposes readily at 100°C, is a strong pore-forming agent.

Important requirements in pore formation are the production of uniform small pores and their uniform distribution throughout the mass. The pore structure is governed by the following factors:

1. The elasticity of the plastics when heated.

2. Gas formation and the nature of the gas.

3. The methods used for the heat treatment of the mass: temperature, pressure, and duration of treatment.

The amount of pore-forming agent added depends upon the desired degree of expansion of the material and the volume of the gas evolved.

In the usual procedure, involving free gas formation, the pores are interconnected; they can be squeezed and they absorb water, like a sponge. Material of this sort is unsuited to outdoor exposed heat insulation. To secure a material with closed pores, a method is used in which the gases evolved in the plastication of the material do not expand, but, on the contrary, are compressed several hundred percent and remain compressed within the material as it cools under pressure. The swelling – expansion – of the material takes place in the second stage, during its heating in the heating chamber, at first under pressure, for a long time, so that the gases overcome the resistance to their expansion and increase the initial volume of the molded parts several hundred percent.

The addition of a mixture of lead selenite and soda, totaling no more than 1% of the aggregate weight of the composition, in addition to the pore-forming agent, ensures uniformity. The thermodynamic state of the gas in the porous material is governed by the temperature and the pressure, while the velocity of the gas molecules and their number in a given volume yield a microstructure. The reaction velocity is measured by the amount of pore-forming agent decomposed per unit time and depends upon the following factors: the concentration, the temperature, the catalyst, and the pressure. Lowering the pressure disturbs the constancy of these relationships, and if the pressure is lowered suddenly, say from 5 atm to 2 atm, the gas is liberated in minute bubbles, and the liquid seems to boil.

---

*Certificate of authorship No. 75397, issued in 1949 and No. 82177, issued in 1950.

The physical and mechanical properties of polyvinyl chloride films depend upon the nature of the material: as the temperature is raised, the material's elasticity increases considerably, while its tensile strength drops. When a molded sample of polyvinyl chloride is quickly cooled under the press after having been heated, a phenomenon is observed that is extremely important in the technology of expanding the material: the rapid cooling converts the mass, which flows under the combined effects of temperature and pressure, into a solid, in which all the molecules remain in the random state they occupied at the instant of cooling. A system of this sort endeavors to expand when heated with all the load removed, and to establish molecular order, i.e., crystallize during slow cooling. The portion of the solid that is not crystallizable imparts a certain elasticity to the material.

The thickness of films of the corklike material diminishes according to a definite pattern after the critical size of 5-10 μ has been attained, after which rupture occurs, and the hitherto isolated pores are united under the internal pressure of the gas they contain; their volume increases, thus producing a large-pore material.

The use of plasticizers and copolymers greatly promotes the attaining of porosity in the material; less of the pore-forming agent is required and the steam-treatment of the material need not be so long.

But when the percentage of plasticizer is high, thus softening the material considerably, the material swells up at first and then subsides, since the gases overcome the resistance of the films, rupture the cells, and escape from the material. The evolution of hydrochloric acid is often observed during the heat treatment of the material; the acid reacts with some pore-forming agents, raising the temperature and carbonizing the material. This may be prevented by using stabilizers and mixed pore-forming agents. Calcium stearates and glyptals protect polyvinyl chloride against decomposition at 155-165°C.

Principal Properties of the Material

Volumetric weight	80 to 200 kg per m^3
Tensile strength	30 to 40 kg per cm^2
Bending strength	over 80 kg per cm^2
Resilience	over 10 kg per cm^2
Thermal conductivity	0.035 to 0.033 cal/m^2/hour
Sound absorption	0.7 to 0.8.

The material is softened by boiling in water, but does not absorb any water. It does not dissolve in acids, alkalies, or alcohols, resists attacks by living organisms, and possesses protective anti-rodent properties. The corklike material is easily worked with a knife or file and can be glued or nailed.

Received August 5, 1950.

THE SYNTHESIS OF ASYMMETRICAL AZO COMPOUNDS

B. M. Bogoslovsky and Z. S. Kazakova

Laboratory of Dye Chemistry, Moscow Textile Institute

In our earlier reports [1,2,3] we were able to demonstrate that altering the conditions of the well-known Sandmeyer reaction, which results in the formation of symmetrical diaryls and their substituted derivatives, makes it possible to obtain very high yields of various symmetrical azo compounds, many of which are extremely hard to prepare by ordinary methods of synthesis. We also put forward, as a first approximation, an explanation of the mechanism involved in this transformation, proved that this reaction could be employed for the benzene, naphthalene, and anthraquinone series, and set forth some empirical rules that we had observed, such as, that positive substituents promote the formation of azo compounds, while negative substituents, especially those at the ortho position to the amino group to be diazotized, lead to the formation of the corresponding diaryl derivatives.

In our desire to extend this reaction to the asymmetrical azo compounds, the synthesis of which is even more complicated than that of symmetrical azo compounds, as a rule, we tried to synthesize these compounds by using an equimolar mixture of the diazo compounds of two different amines in the reaction (while retaining, on the whole, the method we had adopted) [2]. The following combinations were employed in our previous investigation: 3-toluidine and 4-toluidine; 3-toluidine and 3-aminophenol; 4-toluidine and 4-aminophenol; and a few others. All of these experiments exhibited the pattern of selective reaction of the diazo compounds, resulting in the preparation of a mixture of two different symmetrical azo compounds. The yield of the asymmetrical azo product was extremely low. It was also found that the yield of the azo product is a maximum whenever the excess mineral acid in the diazo solution added to the ammoniacal cuprous oxide is eliminated by adding sodium acetate. The higher the acidity of the diazo solution, the lower will be the yield of the azo compound and the higher will be the percentage of the halogen derivative. When the reaction is carried out so as to produce a diaryl compound, the yield of the latter rises with the acidity of the medium. Using neutral solutions tends to promote the formation of tarry products.

We took two combinations of diazo compounds to explore the feasibility of producing asymmetrical azo compounds: 1) anthranilic acid and 4-toluidine; and 2) anthranilic acid and N-aceto-1,4-phenylenediamine.* In each of these combinations one of the diazo compounds contained a negative substituent, while the other contained a positive one.

It is readily seen that, in the light of the empirical rules stated above, each of these two cases could, theoretically speaking, yield three compounds,

* Using diazo compounds of sulfanilic and 4-aminobenzoic acids results in the formation of a mixture of products that are hard to separate; we were unable to isolate individual products from such a mixture.

one of them being a symmetrical azo compound, another an asymmetrical diazo compound, and the third the respective diaryl (diphenyl) derivative.

In the first case, therefore, we expected to secure: a) diphenic acid; b) 4,4'-azotoluene; and c) 2-carboxy-4'-methylazobenzene; and in the second: a) diphenic acid; b) 4,4'-bis-(acetamino)-azobenzene; and c) 2-carboxy-4'-acetaminoazobenzene.

Our expectations were borne out by experiment, all the compounds listed being recovered from the reaction mass, and the sought-for asymmetric azo compounds being produced in appreciable quantities.

The experiments described in the present report on the synthesis of symmetrical and asymmetrical azo compounds is merely of a preliminary nature and cannot claim to be a complete explanation of the mechanism involved in the reaction of diazo compounds with the cuprous salt.

EXPERIMENTAL

Preparation of the copper catalyst solution. 57.0 g (0.2 mole) of copper sulfate was dissolved in 200 ml of hot water, and 60 ml of 25% ammonia solution was added. 14 g (0.2 mole) of hydroxylamine hydrochloride, dissolved in 40 ml of water, was added to the resulting blue solution while it was still hot. The resulting cuprous salt was employed in each of the tests described below, on the basis of 0.2 mole of the amine mixture.

Preparation of the diazo solutions. a) 13.7 g (0.1 mole) of anthanilic acid was mixed with 100 ml of 5 N hydrochloric acid, chilled to 3-5°, and diazotized with a solution of 7 g of sodium nitrite in 20 ml of water. The resulting diazo solution was diluted to one liter volume with ice water and then filtered.

b) 11 g (0.1 mole) of 4-toluidine was mixed with 100 ml of 5 N hydrochloric acid, chilled to 3°, and diazotized with a solution of 7 g of the nitrite in 20 ml of water. The resulting solution was diluted to one liter volume with ice water and then filtered.

c) 15 g (0.1 mole) of N-aceto-1,4-phenylenediamine was placed in 100 ml of 5 N hydrochloric acid, chilled to 3°, and diazotized with 7 g of the nitrite dissolved in 20 ml of water. The diazo solution was diluted with ice water to one liter volume and then filtered.

Synthesis of Asymmetrical Azo Compounds

a) Synthesis of 2-carboxy-4'-methylazobenzene. A mixture of the chilled solutions of 0.1 mole of diazoanthranilic acid and 0.1 mole of diazo-4-toluidine was added, with stirring, in the course of 10 minutes to the ammoniacal cuprous oxide (vigorous foaming was observed). After the mixture had been stirred for an hour, the yellow precipitate was filtered out and washed successively with hot water, 10% hydrochloric acid, and again water, and then dried. The resultant product weighed 16.5 g. The dry product was heated with 10% soda solution and the portion that did not dissolve in the soda solution (4.8 g) was filtered out. Crystallization of this insoluble portion from alcohol yielded a product in the form of minute yellow needles with a m.p. of 142°, which is the melting point given in the literature for 4,4'-azotoluene.

When the soda solution was acidulated, a yellow precipitate was thrown down (about 8 g), which consisted of minute yellow needles with a m.p. of 110° after crystallization from 50% aqueous alcohol. Analysis indicated that this product was 2-carboxy-4'-methylazobenzene.

Determination of nitrogen by the Dumas method:

4.800 mg substance: 0.501 ml N_2 (746 mm, 23°C).
$C_{14}H_{12}N_2O_2$. Computed %: N_2 11.66.
Found %: N_2 11.82.

Reducing the 2-carboxy-4'-methylazobenzene by heating it with hydrosulfite in alkali resulted in the formation of the corresponding hydrazo compound, with a m.p. of 126°; colorless leaflets, freely soluble in alcohol, hot water, and an alkali solution. It turns yellow rapidly if exposed to the air when wet.

Determination of nitrogen by the Dumas method:

3.756 mg substance: 0.385 ml N_2 (744 mm, 21°C).
$C_{14}H_{14}N_2O_2$. Computed %: N_2 11.57.
Found %: N_2 11.65.

Heating the hydrazo compound with 10% hydrochloric acid yielded a grayish product, soluble in acids and alkalies and diazotizable. The free base had a m.p. of 140°. It may be assumed that this substance, which we did not investigate any further, was a product of the rearrangement of the hydrazo compound, viz.: 2,4'-diamino-5-methyl-3'-carboxydiphenyl.

Diphenic acid (0.8 g) was recovered from the evaporated filtrate secured after filtration of the principal mixture of reaction products.

b) Synthesis of 2-carboxy-4'-acetaminoazobenzene. A solution of 0.1 mole of diazoanthranilic acid was mixed with a solution of 0.1 mole of diazo-N-aceto-1,4-phenylenediamine, and the resulting mixture was poured, with constant stirring, in the course of 10 minutes into a chilled solution of the copper catalyst (this was accompanied by vigorous foaming). After the mixture had been stirred for an hour, the yellow-brown precipitate was filtered out, washed on the filter successively with water, hydrochloric acid, and water, and dried. Yield: 18.7 g.

The precipitate was heated with a 10% soda solution, the portion that was insoluble in the soda (7 g) being filtered out, and the soda filtrate being acidulated with hydrochloric acid. The precipitated yellow 2-carboxy-4'-acetaminoazobenzene was crystallized from alcohol, yielding the product as extremely small orange needles with a m.p. of 250°. The yield was 8.7 g, or 46% of the theoretical.

Determination of nitrogen by the Dumas method:

4.853 mg substance: 0.627 ml N_2 (748 mm, 21°C).
$C_{15}H_{13}N_3O_3$. Computed %: N_2 14.84.
Found %: N_2 14.77.

The properties of the synthesized 2-carboxy-4'-acetaminoazobenzene were as follows. Heating it with a 20% solution of sulfuric acid or with a 10% solution of sodium hydroxide saponified the acetyl group, yielding 2-carboxy-4'-aminoazobenzene, which is slightly soluble in water, somewhat more soluble in hot alcohol, and very freely soluble in aqueous alkali. It fuses at 232° after crystallization from alcohol. Reduction of the aminoazo product with hydrosulfite in an alkaline medium yields 1,4-phenylene diamine and anthranilic acid. It should also be noted that 2-carboxy-4'-aminoazobenzene may be used as an indicator in acidimetry: it is bright yellow in an acid medium, orange in a neutral one, and light-yellow in an alkaline one.

The product obtained as a residue (7 g) after the initial precipitate had been treated with the soda solution, was recovered as small yellow needles with a m.p. of 277° after crystallization from alcohol; the properties of this product are those of 4,4'-bis-(acetamino)-azobenzene.

Diphenic acid (1.0 g) was recovered by evaporating the filtrate secured in filtrating the principal mixture of reaction products.

LITERATURE CITED

[1] B.M.Bogoslovsky, J.Gen.Chem. 16, 2, 193 (1946).

[2] B.M.Bogoslovsky, Trans. Moscow Textile Inst. 11, (1948).

[3] B.M.Bogoslovsky and Z.S.Kazakova, Trans. Moscow Textile Inst. 12 (1950).

Received January 20, 1950.

A HIGHLY DISPERSED PREPARATION OF SULFATHIAZOLE SILVER*

K. A. Libman

All-Union Research Laboratory for Dispersed Medicinals

The objective of the present research has been the production of a highly dispersed preparation of sulfathiazole silver for local application.

According to the literature, a colloidal dispersion of sulfathiazole silver is used successfully in urology and otolaryngology. The preparation does not irritate the mucous membrane of the nose, eyes, bladder, etc. There is very little information in the literature, however, on the method of producing a colloidal dispersion of sulfathiazole silver. In view of the fact that the methods described in the literature for the preparation of a colloidal dispersion of sulfathiazole silver are complicated, we have tried to produce it by easier methods. This can be done in either of two ways: condensation or dispersion. Producing a colloidal dispersion by the first method, however, requires a suitable solvent for the sulfathiazole silver, since it is insoluble in water or organic solvents. We therefore confined our efforts to the dispersion method, using acoustical irradiation of the silver salt in a magnetostriction generator.

EXPERIMENTAL

Sulfathiazole silver is produced by reacting aqueous solutions of sulfathiazole sodium with silver nitrate. The reagents are used in molar proportions. The reaction is as follows:

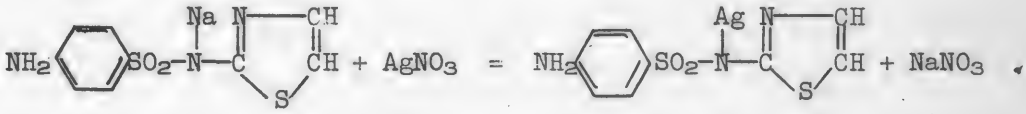

The sulfathiazole silver prepared with mechanical stirring is a coarse dispersion and hence, is an unstable disperse system.

To increase the degree of dispersion of the sulfathiazole silver we modified the method of its synthesis so as to pour the silver nitrate solution into the solution of sulfathiazole sodium: 1) with accoustical irradiation; 2) in the presence of a protective colloid; and 3) with acoustical irradiation and a protective colloid.

Microscopic observations have indicated that the degree of dispersion of sulfathiazole silver was increased only when it was irradiated acoustically in the presence of a protective colloid. The liquid was freed of the sodium nitrate formed in the double decomposition reaction by filtering after irradiation and washing the pastelike precipitate with water.

To increase the degree of dispersion, the washed paste was irradiated acoustically for 1, 2, 3, and 6 more hours. It was found that the percentage of

* Report I of a series on this topic.

particles below 1.5 μ in size increased 2.4% after 6 hours of irradiation over the percentage secured with a single hour of irradiation, so that acoustic irradiation was performed thenceforth for only one hour.

In our tests we used 0.5% of pectin, inasmuch as 1% increased the viscosity to such an extent as to cause difficulty in handling. Adding 0.5% of pectin yielded satisfactory results in respect of the stability and degree of dispersion of the preparation.

We used sedimentary analysis to determine the degree of dispersion of the medium, using the Figurovsky microbalance. The particle dimensions were likewise measured microscopically, the preparation being diluted 1:5 with water for this purpose.

We ran the following tests during the preparation of the sulfathiazole silver to settle the problem of whether acoustic irradiation was required in both stages - the silver salt and the paste: 1) irradiating both stages; 2) mixing with a stirrer in the first stage and irradiating the second; and 3) mixing with a stirrer in both stages.

In the first test, the particles below 0.7 μ in size totaled 42.4% of the total; in the second 17.9%, and in the third 10.7%. This indicated that irradiation of both stages yields a dispersion with a higher percentage of small particles than when only the second stage is irradiated, while irradiation of the second stage yields more small particles than when both stages are stirred with a mechanical stirrer (Table 1).

TABLE 1

Effect of the Method Used in Preparing Sulfathiazole Silver Upon The Degree of Dispersion

Dispersal method		Per cent of particles of various sizes				
Silver salt	Paste	Particle dimensions, μ				
		Up to 0.7	0.7-1.5	1.5-4.5	4.5-7.5	7.5 and over
Acoustic irradiation	Acoustic irradiation	42.4	17.1	21	7.5	12
Mechanical stirring	Acoustic irradiation	17.9	14.5	44.5	11.8	11.3
Mechanical stirring	Mechanical stirring	10.7	13.8	47.0	10.5	18

The data in Table 1 were borne out microscopically. When both stages were irradiated acoustically, the whole field was filled with particles up to 1.5 μ in size, particles larger than 12 μ in size being rare. When the second stage was irradiated and the first stage was stirred, the field was partially filled with particles up to 35 μ in size, while when both stages were stirred mechanically, part of the field was filled with 75 μ particles.

The dispersions produced by acoustically irradiating both stages contained 12 to 18% of particles larger than 7.5 μ in size, however, which could not fail to affect their stability. Tests indicated that 50% of the large particles could be gotten rid of by allowing the dispersions to settle for 10 days (Table 2).

The best results were obtained by centrifuging. Centrifuging a dispersion of sulfathiazole silver at 3000 rpm for 7 hours yielded an almost transparent liquid, in which there were no particles larger than 0.5 μ.

TABLE 2

Results of Sedimentary Analysis Before and After Settling

Test No.	Settling time, days	Per cent of particles of various sizes			
		Particle dimensions, μ			
		Up to 1.5	1.5-4.5	4.5-7.5	7.5 and over
4	-	35.4	39.9	6.7	18
5	10	52	31	5	12

TABLE 3

Results of Sedimentary Analysis Before and After Drying

Test No.	Time	Per cent of particles of various sizes			
		Particle dimensions, μ			
		Up to 1.5	1.5-4.5	4.5-7.5	7.5 and over
6	Before drying	20	24.5	16.6	38.9
	After drying	61.4	25.9	5.0	7.7
7	Before drying	35.5	38.4	9.4	16.7
	After drying	58.7	17.8	8.5	15

In our search for methods of keeping the preparation for a long time, we dried it in various ways: 1) at room temperature; 2) with gentle heating in vacuum; and 3) in the frozen state, by desiccating the labile substances. The only preparation to retain its initial degree of dispersion was the one dried by the last method; this was borne out by the results of sedimentary analysis before and after drying.

The preparation must be dried in the frozen state, since at a higher temperature the pectin apparently loses its protective properties, resulting in aggregation of the particles. In several tests we were able to observe the growth of the smaller fraction after drying (Table 3). As we see, the disaggregation of the particles is paralleled by a partial dehydration of the pectin.

On the basis of our findings, we have worked out the following method of producing the preparation. A solution of silver nitrate is gradually added, in molar proportions, to an aqueous solution of sulfathiazole sodium containing pectin as a protective colloid, while the whole is irradiated acoustically in a magnetostriction generator. After all the sodium nitrate has been added, the liquid is filtered on a Buchner funnel under vacuum, and the sodium nitrate is washed out of the resultant precipitate, a paste, with water. The paste of sulfathiazole silver is diluted with water until it contains 15% of the salt, after which it is acoustically irradiated with the same protective colloid. A preservative is added to the preparation. The resulting highly dispersed preparation of sulfathiazole silver is a viscous white or pinkish liquid, depending upon the color of the pectin.

SUMMARY

1. A highly dispersed preparation of sulfathiazole silver has been produced by acoustical irradiation in a magnetostriction generator with a protective colloid – pectin.

2. Acoustical irradiation yields a more highly dispersed preparation than does mechanical stirring.

3. The preparation retains its initial dispersion after being desiccated in the frozen state.

Received March 29, 1950.

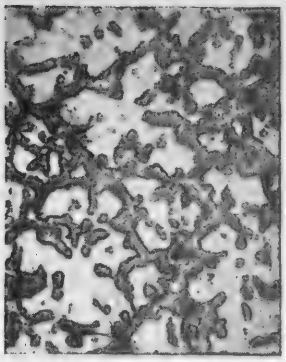

Fig. 10. Microstructure of the alloy MC-4. 100 x magnification.

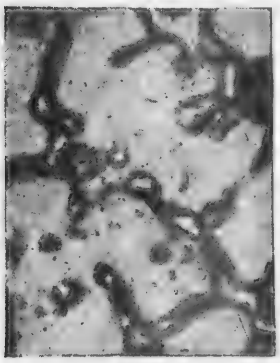

Fig. 11. Microstructure of the alloy MC-4. 300 x magnification.

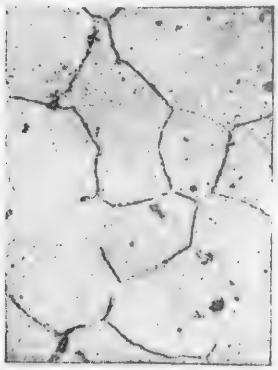

Fig. 12. Microstructure of the alloy MC-4 after heating to 420° for 16 hours. 100x magnification.

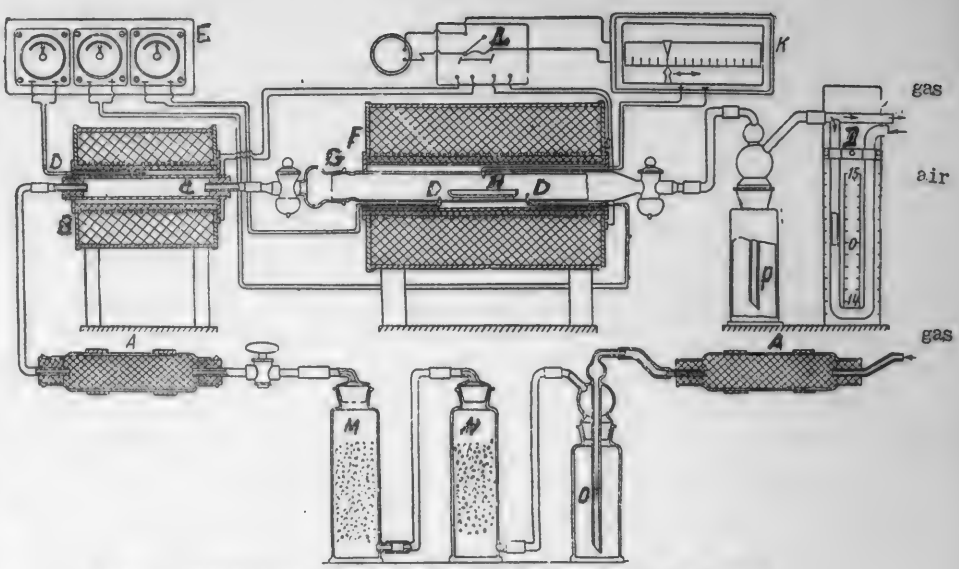

Fig. 1. Apparatus Layout for Investigating the gaseous corrosion of magnesium alloys.

A-Tube filled with glass wool, B-electric furnace; C-porcelain tube; D-chrmel-alumel thermocouples; E-galvanometers; F-furnace containing samples; G-glass tube with ground-glass ends; H-Pt-Pt/Rh thermocouple; I-rheometer; K-potentiometer; L-magnetic starter; M-bottle containing soda lime; N-bottle containing $CaCl_2$; O-bottle containing sulfuric acid; P-jar containing sulfuric acid.

A Laboratory Apparatus for the Production of Ketene on a Large Scale p 601

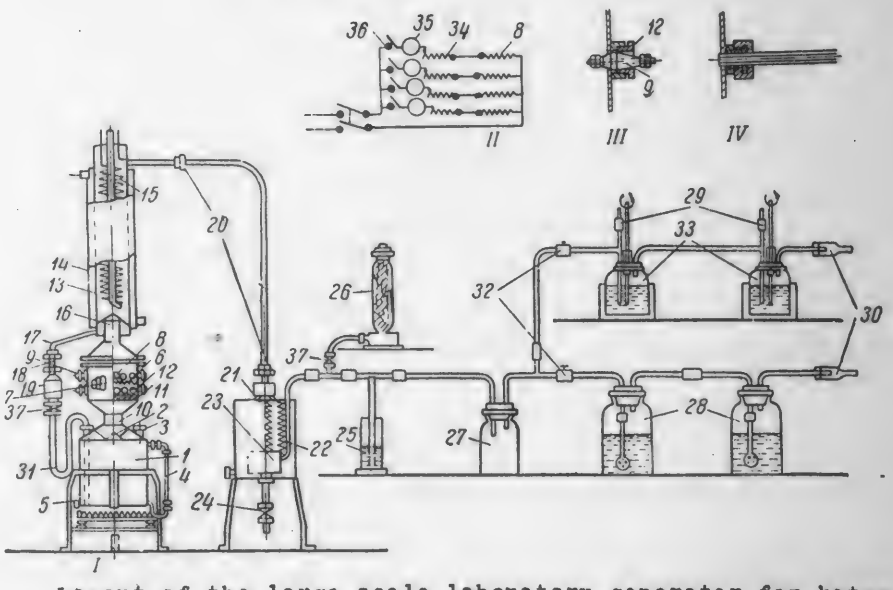

Layout of the large scale laboratory generator for ketene

I-General layout of the equipment; II-coil circuits; III-current lead-in into reaction chamber; IV-glass-metal connection. See text for numbered notation.